

WSRC-RD-91-21

**CHARACTERIZATION OF THE GEOLOGY, GEOCHEMISTRY, HYDROLOGY
AND MICROBIOLOGY OF THE IN-SITU AIR STRIPPING DEMONSTRATION SITE
AT THE SAVANNAH RIVER SITE (U)**

C. A. Eddy, B. B. Looney, J. M. Dougherty, T. C. Hazen, and D. S. Kaback

May 1, 1991

**WESTINGHOUSE SAVANNAH RIVER COMPANY
SAVANNAH RIVER SITE
Aiken, South Carolina 29808**

DISTRIBUTION OF THIS DOCUMENT IS UNLIMITED

DISCLAIMER

This report was prepared by Westinghouse Savannah River Company (WSRC) for the United States Department of Energy under Contract No. DE-AC09-89SR18035 and is an account of work performed under that contract. Neither the United States Department of Energy, nor WSRC, nor any of their employees makes any warranty, expressed or implied, or assumes any legal liability or responsibility for the accuracy, completeness, or usefulness, of any information, apparatus, or product or process disclosed herein or represents that its use will not infringe privately owned rights. Reference herein to any specific commercial product, process, or service by trademark, name, manufacturer or otherwise does not necessarily constitute or imply endorsement, recommendation, or favoring of same by WSRC or by the United States Government or any agency thereof. The views and opinions of the authors expressed herein do not necessarily state or reflect those of the United States Government or any agency thereof.

WSRC-RD--91-21

Derivative Classifier _____
D.B. Moore, Section Manager
Authorized Derivative Classifier

DE92 011055

Characterization of the Geology, Geochemistry, Hydrology and Microbiology of the In-situ Air
Stripping Demonstration Site at the Savannah River Site (U)

C. A. Eddy, B. B. Looney, J. M. Dougherty, T. C. Hazen, and D. S. Kaback

May 1, 1991

Authentication: _____

Approved by: _____
D.B. Moore, Manager
Environmental Sciences Section
Savannah River Laboratory

APPROVED

WESTINGHOUSE SAVANNAH RIVER COMPANY
SAVANNAH RIVER SITE
Aiken, South Carolina 29808

Prepared for the U.S. Department of Energy under Contact No. DE-AC09-89R180035

MASTER

DISTRIBUTION OF THIS DOCUMENT IS UNLIMITED

4/2

Characterization of the Geology, Geochemistry, Hydrology and Microbiology of the In-situ Air Stripping Demonstration Site at the Savannah River Site (U)

Table of Contents

Table of Contents.....	i
List of Tables	iii
List of Figures.....	v
List of Appendices	vii
Abstract.....	ix
1.0 Objective.....	1
2.0 Introduction and Background.....	3
3.0 General Site Description	5
Stratigraphy	5
Congaree Formation	5
Santee Formation.....	5
Barnwell Group.....	5
Clinchfield Formation.....	5
Dry Branch Formation.....	6
Tobacco Road Sand.....	6
"Upland Unit"	6
Geologic Cross Sections	6
Wells and Borings.....	7
3-D mapping	8
4.0 Hydrology.....	17
Conceptual Description of SRS Groundwater System.....	17
Hydrology of the Field Demonstration Site	17
Aquifer Characteristics.....	18
5.0 Sampling.....	37
Water Sampling Techniques	37
Groundwater from Monitoring Wells	37
HydroPunch.....	37
Sediment Sampling Techniques	37
6.0 Analytical Techniques.....	39
Analysis of VOC in Sediment and Groundwater	39
Microbiological Analytical Techniques	39
Acridine Orange Direct Counts (AODC)	39
Enumeration by Plate Count (Spread Plate)	39
Community Diversity.....	39
Phospholipid Fatty Acid Analysis	39
Fluorescent Antibody Analysis.....	40
Nucleic Acid Analysis.....	40
7.0 Results	41
Groundwater.....	41
Groundwater from Wells	41
HydroPunch.....	41
Sediments	41
3D Modeling.....	41
Comparison of Water and Sediment Data	42
Microbiology.....	44

8.0	Summary	115
	Groundwater.....	115
	Sediments	115
	Microbiology.....	116
9.0	References Cited.....	117

List of Tables

Table 3.1	Elevation of Geological Picks.....	9
Table 3.2	Monitoring Well Completion Details.....	10
Table 4.1	Summary of Initial Water Level Measurements.....	21
Table 4.2	Summary of Aquifer Tests Performed Near the Study Area.....	22
Table 4.3	Summary of Aquifer Parameters Estimated By Model Calibration.....	23
Table 4.4	Summary of Aquifer Parameters For Clay Zones Estimated By Laboratory Measurements on "Undisturbed" Core Samples.....	24
Table 4.5	Summary of Sieve Analysis of MHT Well Cores.....	25
Table 7.1	Bulk Parameters of Groundwater	46
Table 7.2	TCE and PCE Results for Groundwater in the MHT Wells.....	47
Table 7.3	Average of Duplicate Analysis of TCE and PCE Results from HydroPunch Samples.....	48
Table 7.4	Maximum Values of TCE and PCE Measured in MHT and MHV Sediment Samples.....	49
Table 7.5	Density of Bacteria in Sediment from MHT-1C	50
Table 7.6	Density of Bacteria in Sediment from MHT-2C	51
Table 7.7	Density of Bacteria in Sediment from MHT-3C	52
Table 7.8	Density of Bacteria in Sediment from MHT-4C	53
Table 7.9	Density of Bacteria in Sediment from MHT-5C	54
Table 7.10	Density of Bacteria in Sediment from MHT-6C	55
Table 7.11	Density of Bacteria in Sediment from MHT-7C	56
Table 7.12	Density of Bacteria in Sediment from MHT-8C	57
Table 7.13	Density of Bacteria in Sediment from MHT-9C	58
Table 7.14	Density of Bacteria in Sediment from MHT-10C.....	59
Table 7.15	Viable vs. Direct Counts of Bacteria in MHT-2C Sediment.....	60
Table 7.16	Viable vs. Direct Counts of Bacteria in MHT-3C Sediment.....	61
Table 7.17	Viable vs. Direct Counts of Bacteria in MHT-5C Sediment.....	62
Table 7.18	Viable vs. Direct Counts of Bacteria in MHT-7C Sediment.....	63
Table 7.19	Viable vs. Direct Counts of Bacteria in MHT-9C Sediment.....	64
Table 7.20	Phospholipid Fatty Acid Analysis of Sediment from MHT-2C by Depth	65
Table 7.21	Phospholipid Fatty Acid Analysis of Sediment from MHT-4C by Depth	66
Table 7.22	Phospholipid Fatty Acid Analysis of Sediment from MHT-7C by Depth	67
Table 7.23	DNA Analysis of Sediment Samples by Depth	68

List of Figures

Figure 2.1	Map showing the location of the Savannah River Site.....	4
Figure 3.1	Stratigraphic Column	12
Figure 3.2	Schematic Diagram showing Relationship between Clay Layers and Hydrologic Features.....	13
Figure 3.3	Location Map for the MHT C Wells	14
Figure 3.4	Location Map for the MHT D Wells	15
Figure 3.5	Location Map for the MHV Boring Locations	16
Figure 4.1.	Potentiometric Map for Aquifer IA.....	30
Figure 4.2.	Potentiometric Map for Aquifer IB.....	31
Figure 4.3.	Potentiometric Map for Confined Zones of Aquifer System II	32
Figure 4.4.	Potentiometric Map for the Water Table Zone	33
Figure 4.5.	Potentiometric Map for the Semiconfined Zone	34
Figure 4.6.	Vertical Gradients Measured at Well Clusters.....	35
Figure 7.1	Map of Pretest TCE Contamination in the MHT C Wells	69
Figure 7.2	Map of Pretest PCE Contamination in the MHT C Wells	70
Figure 7.3	Map of Pretest TCE Contamination in the MHT D Wells	71
Figure 7.4	Map of Pretest PCE Contamination in the MHT D Wells	72
Figure 7.5	Plot of TCE Concentration vs. Depth in Sediment for MHT1C	73
Figure 7.6	Plot of TCE Concentration vs. Depth in Sediment for MHT2C	74
Figure 7.7	Plot of TCE Concentration vs. Depth in Sediment for MHT3C	75
Figure 7.8	Plot of TCE Concentration vs. Depth in Sediment for MHT4C	76
Figure 7.9	Plot of TCE Concentration vs. Depth in Sediment for MHT5C	77
Figure 7.10	Plot of TCE Concentration vs. Depth in Sediment for MHT6C	78
Figure 7.11	Plot of TCE Concentration vs. Depth in Sediment for MHT7C	79
Figure 7.12	Plot of TCE Concentration vs. Depth in Sediment for MHT8C	80
Figure 7.13	Plot of TCE Concentration vs. Depth in Sediment for MHT9C	81
Figure 7.14	Plot of TCE Concentration vs. Depth in Sediment for MHT10C.....	82
Figure 7.15	Plot of PCE Concentration vs. Depth in Sediment for MHT1C	83
Figure 7.16	Plot of PCE Concentration vs. Depth in Sediment for MHT2C	84
Figure 7.17	Plot of PCE Concentration vs. Depth in Sediment for MHT3C	85
Figure 7.18	Plot of PCE Concentration vs. Depth in Sediment for MHT4C	86
Figure 7.19	Plot of PCE Concentration vs. Depth in Sediment for MHT5C	87
Figure 7.20	Plot of PCE Concentration vs. Depth in Sediment for MHT6C	88
Figure 7.21	Plot of PCE Concentration vs. Depth in Sediment for MHT7C	89
Figure 7.22	Plot of PCE Concentration vs. Depth in Sediment for MHT8C	90
Figure 7.23	Plot of PCE Concentration vs. Depth in Sediment for MHT9C	91
Figure 7.24	Plot of PCE Concentration vs. Depth in Sediment for MHT10C.....	92
Figure 7.25	Three Dimensional Model of Pretest TCE (Z=1).....	93
Figure 7.26	Three Dimensional Model of Pretest TCE (Z=0.1).....	94
Figure 7.27	Three Dimensional Model of Pretest TCE (Z=0.001).....	95
Figure 7.28	Three Dimensional Model of Pretest TCE (Z=0.1, Antilog).....	96
Figure 7.29	Three Dimensional Model of Pretest TCE (Z=0.001, Antilog).....	97
Figure 7.30	Block Diagram of Pretest TCE (Z=0.001, Antilog).....	98
Figure 7.31	Plot of HydroPunch Concentrations vs. Bulk Sediment Concentrations.....	99
Figure 7.32	Plot of Field Estimated Kd Values vs. Bulk Sediment Concentrations	100
Figure 7.33	Depth Profile of HydroPunch Concentrations and Well Water Concentrations From MHT 4C.....	101
Figure 7.34	Changes in Direct Count by Depth	102
Figure 7.35	Changes in MHT-2C Plate Count by Depth.....	103
Figure 7.36	Changes in MHT-8C Plate Count by Depth.....	104

Figure 7.37	Changes in Average 1% PTYG by Depth	105
Figure 7.38	Bacteria (Drilling Fluid vs. Sediment).....	106
Figure 7.39	Comparison of MHT-5C Direct and Plate Counts.....	107
Figure 7.40	Ratio of MHT-5C Direct Counts to Plate Counts.....	108
Figure 7.41	MHT-3C Bacterial Diversity by Depth (1% PTYG)	109
Figure 7.42	MHT-3C Bacterial Diversity by Depth (PTYG).....	110
Figure 7.43	MHT-3C Bacterial Diversity by Depth Comparison	111
Figure 7.44	Allocation Species from 1% PTYG to Community by Depth for MHT-3C ..	112
Figure 7.45	Allocation Species from PTYG to Community by Depth for MHT-3C.....	113

List of Appendices

- Appendix I Geophysical Logs from the MHT-C Well Series**
- Appendix II Results from VOC Analysis of MHT and MHV Samples**

Abstract

The Savannah River Site is the location of an Integrated Demonstration Project designed to evaluate innovative remediation technologies for environmental restoration at sites contaminated with volatile organic contaminants. This demonstration utilizes directionally drilled horizontal wells to deliver gases and extract contaminants from the subsurface. Phase I of the Integrated Demonstration focused on the application and development of in-situ air stripping technologies to remediate soils and sediments above and below the water table as well as groundwater contaminated with volatile organic contaminants.

The objective of this report is to provide baseline information on the geology, geochemistry, hydrology, and microbiology of the demonstration site prior to the test. The distribution of contaminants in soils and sediments in the unsaturated zone and groundwater is emphasized. These data will be combined with data collected after the demonstration in order to evaluate the effectiveness of in-situ air stripping. New technologies for environmental characterization that were evaluated include depth discrete groundwater sampling (HydroPunch) and three-dimensional modeling of contaminant data.

The sediments studied at the Integrated Demonstration Site are composed of layers of sand, clay, and gravel deposited in shallow marine, lagoonal, or fluvial environments. The hydrology of the subsurface is characterized by an approximately 135 foot thick vadose zone, a relatively thin water table, an underlying semiconfined zone, and is bounded at the base by the top of a confined aquifer. The clay layers are generally relatively thin or discontinuous with the exception of clay layers at an elevation of approximately 200 feet and a thicker zone of interlayered clay and sand found at an elevation of approximated 270 feet.

Concentrations of volatile organic contaminants in the groundwater and sediments vary vertically and horizontally beneath the site: concentrations measured in groundwater collected from wells range from approximately 400 to 1800 ppb trichlorethylene TCE and 20 to less than 200 ppb tetrachloroethylene PCE; concentrations measured with a HydroPunch sampler range from less than detection to 13,000 ppb TCE and less than detection to 280 ppb PCE; and concentrations measured in sediment samples range from less than detection to 16 ppm TCE and from less than detection to 5 ppm PCE. Generally, the highest levels of contamination were found slightly above and within the clay rich zones. Three dimensional modeling shows that most of the contamination at the site is associated with the clay zone at and below the 270 foot elevation. Shallow clay zones on the west side of the site near the process sewer line at 325 feet and 300 feet elevation are also contaminated.

Comparison of the analytical results from the HydroPunch data with the sediment data indicates that significant quantities of TCE and PCE have been lost from the sediments sampled in the saturated zone. The results suggest that loss of volatile organics during sediment sampling may be more significant for the sandier samples. Since sampling and analytical protocols used to collect sediments samples were carefully designed to minimize loss of volatiles, the data suggest that loss of volatiles from the core may result from core drainage or infiltration of the core by uncontaminated drilling fluid.

Overall, the total number of organisms present at various depths at the site appear approximately equivalent to the number of organisms found in the subsurface at other parts of this country. However, the number of organisms culturable from the vadose zone is lower than that generally reported elsewhere. Microbiological diversity in this system is also relatively low. It appears that the vadose zone microbial community at this site is under severe stress. This can probably be

attributed to nutrient deprivation. Phospholipid fatty acid analyses show that indeed the organisms present are in stationary growth phase or in various stages of starvation survival. Both the fluorescent antibody analyses and the nucleic acid probe analyses suggest that microorganisms capable of degrading TCE/PCE are naturally present throughout the sediment column. TCE-degraders that utilize methane are also present throughout the sediment at the site.

1.0 Objective

The Integrated Demonstration Project at SRS is designed to evaluate innovative remediation technologies for the restoration of sites contaminated with volatile organic contaminants. Phase I of the Integrated Demonstration focused on the application and development of in-situ air stripping technologies to remediate soils and sediments above and below the water table as well as groundwater contaminated with volatile organic contaminants. The objective of this report is to document the baseline characteristics of the Integrated Demonstration Site.

An extensive network of characterization boreholes was installed as part of Phase I of the Integrated Demonstration Project. These boreholes were used for a variety of purposes including: (1) to characterize the lithology, stratigraphy, microbiology and hydrology of the site; (2) to determine the distribution of contamination prior to the field test; (3) to monitor the pressures and concentrations of dissolved constituents in the groundwater; (4) to monitor the pressure and concentration of gases in the vadose zone; (5) to facilitate geophysical measurements.

Several types of information are presented and discussed in this report, including: a general site description, stratigraphy, hydrology, type and location of borings, sampling and analysis techniques for groundwater and sediments, distribution of contaminants, and structural and functional characterization of the subsurface microbiological community. The pretest data presented in this report will be compared with data collected during and after the full scale field demonstration to provide a detailed measure of the effects of the in-situ air stripping process.

2.0 Introduction and Background

The Savannah River Site is a 300-square mile facility owned by the U.S. Department of Energy near Aiken, South Carolina (Figure 2.1). A priority of the environmental restoration research program at the Savannah River Site (SRS) is to investigate new technologies for in situ remediation of groundwater and soils. Technologies such as vapor extraction, vitrification, deep soil mixing, air stripping, and biotechnology, are currently being developed to remediate contaminated soils and groundwater in the subsurface.

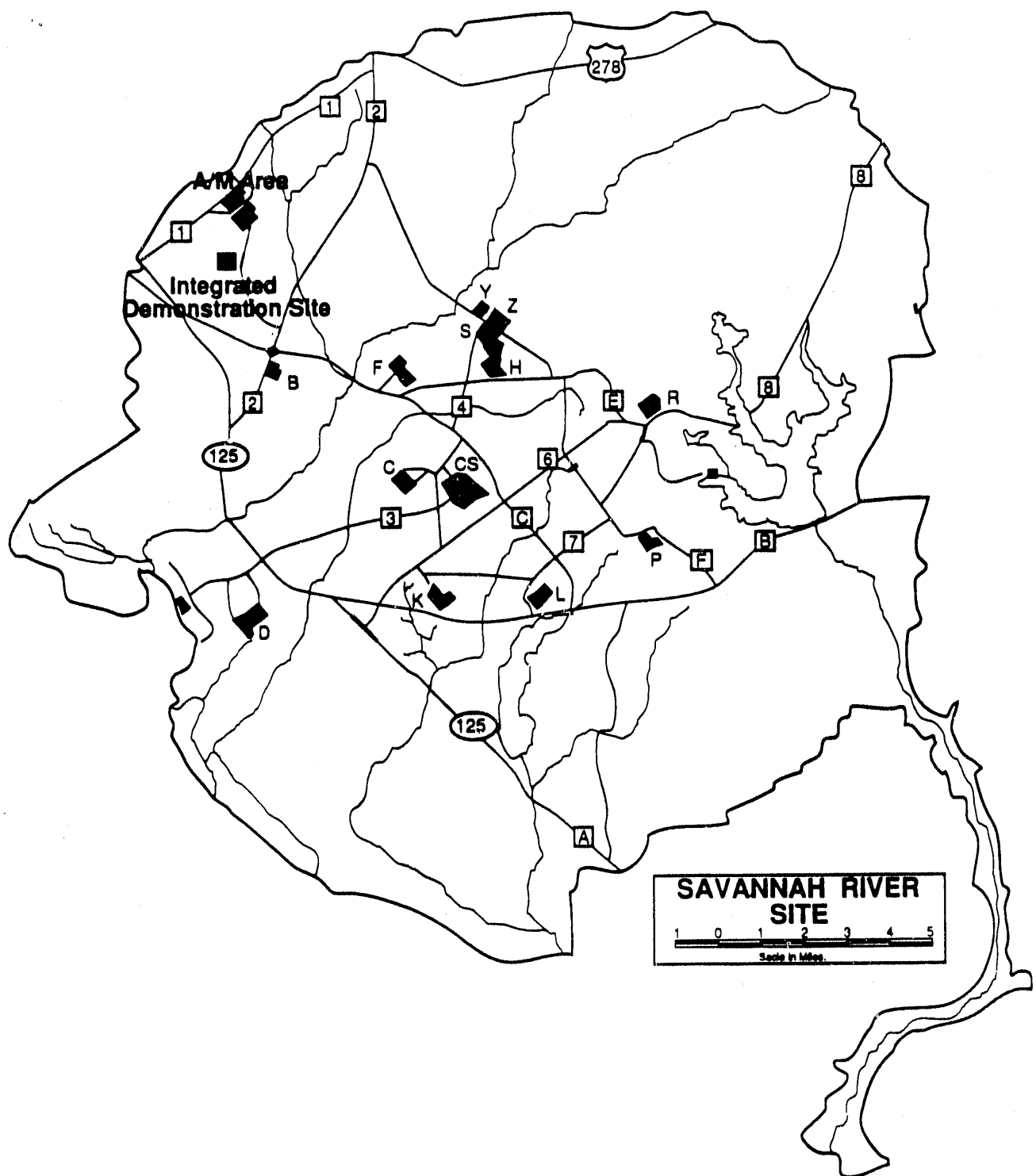
Subsurface contamination with volatile organic contaminants is a common problem across the United States. These solvent materials have been used as metal degreasers at numerous industrial facilities for a number of years. Contamination of groundwater with these solvents has created large plumes that migrate both vertically and laterally. Traditional methods of remediation involve pumping combined with above-ground treatment for groundwater, and excavation and removal or treatment of soils. In situ methods are preferred as they offer the potential to substantially reduce costs and time, as well as to improve the effectiveness and efficiency of remediation.

At the Savannah River Site trichlorethylene (TCE) and tetrachloroethylene (PCE) were used as metal degreasing solvents since 1952. A groundwater plume containing elevated levels of these compounds exists over in an area greater than one square mile. A standard groundwater extraction and treatment system has been in operation since 1984 and has removed approximately 230,000 pounds of solvents from the groundwater. Residual solvents continue to leach into the groundwater from the vadose zone.

The theoretical basis for most traditional remediation systems is that these volatile organic compounds will partition preferentially into the vapor phase from the aqueous phase. The in situ air stripping process brings the vapor phase into contact with the aqueous phase in the ground rather than above the ground.

The demonstration site was selected along an abandoned process sewer line that carried wastes to a seepage basin operated between 1958 and 1985. The sewer line acted as a source of contamination as it is known to have leaked at numerous locations along its length. Because the source of contamination was linear at this particular location within the overall plume, horizontal wells were selected as the injection and extraction system (Kaback et al., 1989).

Figure 2.1 Map showing the location of the Savannah River Site.



3.0 General Site Description

Stratigraphy

The Savannah River Site is located on the Atlantic Coastal Plain which consists of a wedge of unconsolidated and semiconsolidated sediments that increases in thickness from zero at the contact with Paleozoic and preCambrian basement rocks to the west of SRS to 4000 feet at the South Carolina coastline. The Coastal Plain sediments are approximately 1000 feet thick at SRS, range in age from Late Cretaceous to Recent, and consist of stratified clay, sand, gravel and variable amounts of limestone. In general these sediments dip gently to the southeast.

The sediments within 200 feet of the surface are of interest to this study. They consist of sands, sandy clays, clayey sands, and clays deposited from the Middle to Upper Eocene in shallow marine, lagoonal, or fluvial environments. As a result, the sequence lacks the lateral continuity typically found in sediments formed in deep marine environments. A stratigraphic column for the site region is given in Figure 3.1 and general descriptions of the geologic formations are described below. The stratigraphic units described are present in the study area, however, exact correlations were not made as additional paleontological studies would be required to complete the correlations.

Congaree Formation

The early Middle Eocene Congaree Formation consists of yellow, orange, tan, gray and greenish gray, well-sorted, fine-to-coarse-grained quartz sands. Thin clay laminae occur throughout the section, and pebbly layers, clay clasts, and glauconite are present. The unit formed in a shallow marine environment. The Congaree is about 60 feet thick at the northwestern boundary of the SRS and about 85 feet thick near the southeastern boundary. Most of the characterization boreholes penetrate into the sandy the upper portions of the Congaree Formation.

Santee Formation

The upper Middle Eocene Santee Formation consists of carbonates, calcareous quartz sands, and glauconitic sands and clays. Both the fine-grained, often glauconitic sands of the Warley Hill Member, and the green clay beds of the Caw Caw member occur at or near the base of the Santee Formation and comprise the "green clay" referred to informally in many previous SRS reports. The calcareous components of the McBean Member are absent in the study area. The formation is approximately 40 feet thick at the northwestern boundary of the SRS and thickens to more than 80 feet near the southeastern boundary. The top of the "green clay" is reached at an elevation of approximately 200 feet in the study area and is 3 to 8 feet thick.

Barnwell Group

Clinchfield Formation

The sediments of the Barnwell Group (Upper Eocene) lie unconformably on the Santee Limestone. The group includes from oldest to youngest: the Clinchfield Formation, Dry Branch Formation, and the Tobacco Road Sand (Figure 3.1). The Clinchfield Formation is sandy and contains some clay and siliceous sponge spicules. It cannot be identified in the study area and generally can only be unequivocally identified at SRS where it is found between the carbonates of the Griffins Landing Member of the Dry Branch Formation and the McBean Member of the Santee Limestone. It has been estimated to be a maximum of 25 feet thick within the SRS.

Dry Branch Formation

The Dry Branch Formation includes the Twiggs Clay Member, the Irwinton Sand Member, and the Griffins Landing Member. The Twiggs Clay Member and the Irwinton Sand Member are present in the study area. The Twiggs Clay Member, which is tan, light gray, and brown, is up to 12 feet thick in wells at the SRS and is not continuous over distances up to several miles. It has been informally referred to as the "tan clay" in previous SRS reports and the top of this unit is located at an elevation of approximately 270 feet in the study area. The Griffins Landing carbonate member of the Dry Branch ranges from 0 to 45 feet in thickness in the southeastern part of the SRS but was not observed in the study area. The Dry Branch Formation is about 50 feet thick near the northwestern boundary of the site and about 80 feet thick near the southeastern boundary.

Tobacco Road Sand

The Tobacco Road Sand conformably overlies the Dry Branch Formation. The formation consists of moderately to poorly sorted, red, brown, tan, purple, and orange quartz sands; and pebble layers are fairly common. The Tobacco Road Sand was deposited in a shallow marine deposit. The formation is widely exposed at the SRS and varies in thickness because the top of the unit is an erosional surface. The unit is at least 50 feet thick locally at SRS.

"Upland Unit"

The "Upland unit" is an informal stratigraphic term applied to deposits that locally unconformably overlie the Tobacco Road sands at higher elevations in the southwestern South Carolina Coastal Plain. The most common lithology of the "Upland unit" is highly cross-bedded, fine- to very coarse-grained sand. The sand generally consists of angular to subangular quartz and large mica flakes in a matrix of kaolinitic clay. White, kaolinitic clay balls are also common. The "Upland unit" was deposited in high-energy, highly variable fluvial to estuarine depositional environments.

Geologic Cross Sections

Cross sections were prepared using gamma ray (natural) and 16" and 64" resistivity geophysical logs and core logs (Plate 1). Clay layers are typically characterized by relatively low resistivities and high gamma ray intensities. The clay layers in the study area were correlated on the basis of increases in gamma ray intensity together with decreases in resistivity and grain size but the distinct increases in gamma ray intensity did not correlate exactly with location of the clay layers. This can be explained by the observation that the gravel-rich units in the study area are also characterized by high gamma intensities. Several of the strongest correlations across the study site resulted where a clay rich layer is overlain or underlain by a gravel-rich bed (10-15% gravel); for example, the large increase in gamma ray intensity found where a foot thick gravel overlies a clay at a depth of 40 feet in MHT1C (Plate 1).

A longitudinal cross section through wells MHT1C, MHT4C, MHT6C, MHT8C, and MHT10C is included in this report (Plate 1). A major focus in the preparation of the cross section was to document the lateral continuity and thickness of clay zones in the study area. The continuity of the clay layers is critical to the interpretation of contaminant migration as the clay layers often serve as aquitards, and therefore can control contaminant distribution. The cross section illustrates that four of the clay layers were determined to be significant to the hydrology and contaminant distribution at the site: two of the layers are continuous across the site and two are discontinuous. The elevations of the tops of these clay layers are located at 325 ft elevation (depth of approximately 30 to 53 feet), 300 ft elevation (depth of 58 to 71 feet), 270 ft elevation (depth of 90 to 100 feet), and 200 ft elevation (depths of 160 to 170 feet) (Table 3.1). In this study, these clays will be referred to informally as the 325 ft clay, 300 ft. clay, the "tan clay zone", and the "green clay". A schematic

diagram showing the relationship between the clay layers and the hydrologic features at the site is shown in Figure 3.2. The 325 ft clay is only present wells MHT 1, 2, 3, 4, 5, 6. It is not present in the northeastern half of the study area. The 300 ft clay is found in MHT 1, 2, 3, 4, 6, and 8. This clay is discontinuous in the study area and is not present on the northeast side of study area. The top of the "tan clay zone" is continuous across the site and is identifiable in all of the MHT wells. In the study area, the tan clay zone is not present as a single continuous clay layer but as a variable thickness of interlayered sand and clay beds. The top of the "tan clay zone" zone is found at an elevation of 270 feet and the thickness of this zone that consists of discontinuous clayey and sandy layers is approximately 65 to 75 feet. The "green clay" (elevation 200 ft) is present in all wells with the exception of MHT 10. This clay bed is also an identifiable stratigraphic marker in most wells at SRS. This clay layer is the confining unit that separates the semi-confined from the confined unit in the study area.

Wells and Borings

Several series of borings and well clusters were completed to provide access to the subsurface including: a series of borings designated by the prefix MHT completed as well clusters; a series of borings designated by the prefix MHV completed as vadose zone piezometers; and a series of borings designated by the prefix MHM completed for geophysical monitoring. Additional borings were done to collect depth-discrete water samples with the HydroPunch sampler.

Continuous cores were collected to a depth of approximately 200 feet from one borehole in each of the ten MHT clusters. Above the water table, samples were collected using a split spoon sampler with a hollow stem auger. Below the water table, a punch core was used in conjunction with mud rotary drilling to collect the core samples. Geophysical logging of the MHT boreholes included natural gamma ray, sp, resistivity (16" and 64"), density, and neutron logs. Copies of the gamma ray and resistivity logs are included in Appendix I. The MHT and MHV cores were logged in the field: samples were collected at 5 foot intervals and major lithology changes for VOC analysis; and samples for microbiological analysis were collected every 10 feet. The MHT cores were microscopically examined in the SRL core-logging laboratory. Sand (grains 2 mm - 0.0625 mm), gravel (grains > 2 mm), clay (grains < 0.0625 mm), and carbonate percentages were determined, as were the muscovite, lignite, glauconite and sulfide content of the cores. Selected samples were sieved for grain size analysis. Sandy layers range in thickness from a centimeter to several meters. The clay from the study area is commonly banded or mottled, and varies in color from yellow, orange, and tan, to lavender, blue, gray, purple, and green. The clay layers range in thickness from a centimeter to several meters. Generally the thicker layers have a significant component of sand or consist of finely interlayered clay and sand.

Ten two-well clusters designated by the prefix MHT were installed. Locations of the well clusters are shown in Figure 3.3 and 3.4. Two of the MHT well clusters were located northwest of the injection well (MHT1, MHT2), four well clusters were located between the injection and the extraction wells (MHT4, MHT6, MHT8, MHT10), and four well clusters were located to the southeast of the extraction well (MHT3, MHT5, MHT7, MHT9). The MHT clusters were completed as four inch monitoring wells and consist of a well screened in the water table (designated with the suffix D) and a well screened with five foot screens in the underlying semiconfined aquifer at elevations ranging from 204 to 214 feet (designated with a suffix C). Ideally, the water table wells were to be screened with twenty foot screens with 5 feet of the screen above the water table and 15 feet below the water table. Since the water table zone is approximately 5 to 10 feet thick, the twenty foot screens were installed with more than 5 feet of the screen above the water table to avoid screening into the underlying semiconfined aquifer. Specific well construction details are given in Table 3.2.

At the start of the vacuum extraction, water samples from the MHT wells were analyzed for volatile organic constituents, pH, temperature, conductivity, dissolved oxygen, Eh, and microbial populations.

Five borings (designated by the prefix MHV) were cored in order to install piezometer clusters in the vadose zone. MHV4 is located west of the injection and extraction wells, MHV1, MHV3 and MHV5 are located between the vapor extraction and injection wells, and MHV2 is located east the injection and extraction wells (Figure 3.5). These borings were drilled with 6-1/4 inch hollow stem auger and sampled with a split spoon sampler to at least 120 feet. Continuous sediment cores were collected and sampled for VOC analysis. Each of the MHV holes was completed as a multiple piezometer cluster. Three piezometer tubes were installed in each hole: each tube was completed with a one inch tee, one inch ball valve, an access port, and a five foot screen. Specific well construction details are given in Table 3.2.

A HydroPunch sampler was used to collect groundwater samples at discrete depths . Samples collected with the HydroPunch are designated with the prefix MHP and were collected adjacent to the well clusters at MHT2, MHT3, MHT4, MHT5, MHT7, MHT8, MHT9, and MHT10. Each sample was analyzed for VOC content and baseline microbial characteristics.

All collection methods were designed to minimize microbial contamination of cores from adjacent depths and drilling fluids. Barrels were steam cleaned between collections.

3-D mapping

A three dimensional geologic model of the study area will be prepared at a later date.

Table 3.1 Elevation of Geological Picks

Well I. D.	Elevation of Top(feet)	Elevation of Bottom (feet)	Thickness (feet)
325 ft. clay	MHT-1C	332.3	326.3
	MHT-2C	330.7	323.7
	MHT-3C	320.2	315.2
	MHT-4C	327.2	318.2
	MHT-5C	314.6	312.6
	MHT-6C	316.3	310.3
	MHT-7C	absent	absent
	MHT-8C	absent	absent
	MHT-9C	absent	absent
	MHT-10C	absent	absent
300 ft. Clay	MHT-1C	304.3	301.3
	MHT-2C	304.7	303.7
	MHT-3C	299.2	294.2
	MHT-4C	299.2	292.2
	MHT-5C	absent	absent
	MHT-6C	293.3	290.3
	MHT-7C	absent	absent
	MHT-8C	297.8	294.8
	MHT-9C	absent	absent
	MHT-10C	absent	absent
270 ft Clay Zone "Tan Clay Zone"	MHT-1C	271.3	198.3
	MHT-2C	275.7	199.7
	MHT-3C	272.2	197.2
	MHT-4C	272.2	202.2
	MHT-5C	269.6	204.6
	MHT-6C	265.3	201.3
	MHT-7C	273.5	204.5
	MHT-8C	269.8	199.8
	MHT-9C	267.3	205.3
	MHT-10C	273.4	
200 ft Clay "Green Clay"	MHT-1C	198.3	195.3
	MHT-2C	199.7	196.7
	MHT-3C	197.2	189.2
	MHT-4C	202.2	194.2
	MHT-5C	204.6	197.6
	MHT-6C	201.3	194.3
	MHT-7C	204.5	202.5
	MHT-8C	199.8	196.8
	MHT-9C	205.3	201.3
	MHT-10C	absent	absent

Table 3.2 Monitoring Well Completion Details

MHT Wells

Well ID	SRS East (ft)	SRS North (ft)	Ground Elev (ft)	TOC Elev (ft)	Riser Elev* (ft)	Pad Elev (ft)	Top of Screen (ft)	Bottom Screen (ft)	Top of Filter (ft)	Bottom Pack (ft)
MHT-1C	48765.60	102706.80	362.3	364.99	365.17	362.8	209.3	204.3	211.2	200.3
MHT-1D	48760.21	102697.34	362.0	364.47	NA	362.5	237.5	217.5	241.0	216.0
MHT-2C	48780.28	102747.08	363.7	366.28	366.46	364.2	211.7	206.7	215.1	203.7
MHT-2D	48784.24	102756.60	363.9	367.28	367.46	364.4	240.1	219.5	242.7	218.6
MHT-3C	48861.11	102704.33	362.2	364.92	365.09	362.7	209.2	204.2	212.5	200.2
MHT-3D	48856.75	102694.60	361.7	364.36	364.70	362.2	236.7	216.7	240.1	215.3
MHT-4C	48863.53	102778.90	367.2	369.62	369.79	367.5	213.2	208.2	216.3	203.2
MHT-4D	48857.11	102772.12	366.6	368.94	NA	366.9	241.6	221.6	244.9	219.6
MHT-5C	48905.88	102725.11	363.6	366.28	366.45	364.2	209.6	204.6	214.9	201.1
MHT-5D	48893.54	102721.66	363.5	366.05	366.36	364.0	240.0	219.9	218.6	218.5
MHT-6C	48900.03	102810.82	369.3	371.79	371.97	369.6	212.3	207.3	215.3	201.3
MHT-6D	48891.01	102808.16	369.1	371.36	NA	369.5	244.1	224.1	247.0	222.1
MHT-7C	48977.48	102788.85	367.5	370.10	370.30	368.0	211.5	206.5	216.4	200.5
MHT-7D	48967.28	102786.76	367.4	370.09	NA	367.9	239.4	219.4	246.0	219.4
MHT-8C	48970.24	102880.69	368.8	371.64	371.80	369.3	211.8	206.8	214.5	201.8
MHT-8D	48960.71	102875.76	369.1	371.77	NA	369.6	240.1	220.1	243.5	219.1
MHT-9C	49015.58	102814.40	367.3	369.71	369.88	367.8	214.3	209.3	215.7	205.8
MHT-9D	49018.07	102805.14	367.2	369.85	370.02	367.7	242.2	222.2	246.6	220.8
MHT-10C	49011.57	102892.30	368.4	370.82	371.11	368.9	211.4	206.4	213.4	203.4
MHT-10D	49001.21	102890.12	368.5	371.04	NA	369.0	239.5	219.5	242.9	217.5

* = Elevation of the top of the water level monitoring access tube; some water table wells do not have these tubes.

Table 3.2 Monitoring Well Completion Details (Continued)

MHV Wells

Well I.D.	SRS East (ft)	SRS North (ft)	Ground Elev (ft)	TOC Elev (ft)	Pad Elev (ft)	Top of Screen Elev (ft)	Bottom of Screen Elev (ft)	Top of Filter Pack Elev (ft)	Bottom of Filter Pack Elev (ft)
'MHV-1A '	48841.98	102749.34	365.3	367.72	365.7	321.30	316.09	322.00	316.20
'MHV-1B '	48841.98	102749.34	365.3	367.72	365.7	295.30	290.09	298.80	285.90
'MHV-1C '	48841.98	102749.34	365.3	367.71	365.7	270.30	265.09	276.85	262.80
'MHV-2A '	48903.22	102755.87	366.0	368.33	366.5	322.00	316.79	324.10	315.30
'MHV-2B '	48903.22	102755.87	366.0	368.31	366.5	296.00	290.79	297.90	288.40
'MHV-2C '	48903.22	102755.87	366.0	368.32	366.5	271.00	265.79	273.40	262.10
'MHV-3A '	48874.06	102774.69	367.9	370.36	368.3	322.90	317.69	324.90	316.70
'MHV-3B '	48874.06	102774.69	367.9	370.36	368.3	298.55	293.34	303.60	292.60
'MHV-3C '	48874.06	102774.69	367.9	370.35	368.3	272.90	267.69	275.00	262.60
'MHV-4A '	48842.53	102841.68	365.7	368.73	368.3	323.20	317.99	325.70	317.20
'MHV-4B '	48842.53	102841.68	365.7	368.64	368.3	295.70	290.49	297.90	289.30
'MHV-4C '	48842.53	102841.68	365.7	368.79	368.3	271.70	266.49	274.40	265.30
'MHV-5A '	48917.46	102878.82	368.9	371.69	369.3	323.90	318.69	326.50	316.20
'MHV-5B '	48917.46	102878.82	368.9	371.62	369.3	300.90	295.69	304.70	295.50
'MHV-5C '	48917.46	102878.82	368.9	371.67	369.3	283.90	278.69	285.90	275.80

Figure 3.1 Stratigraphic Column

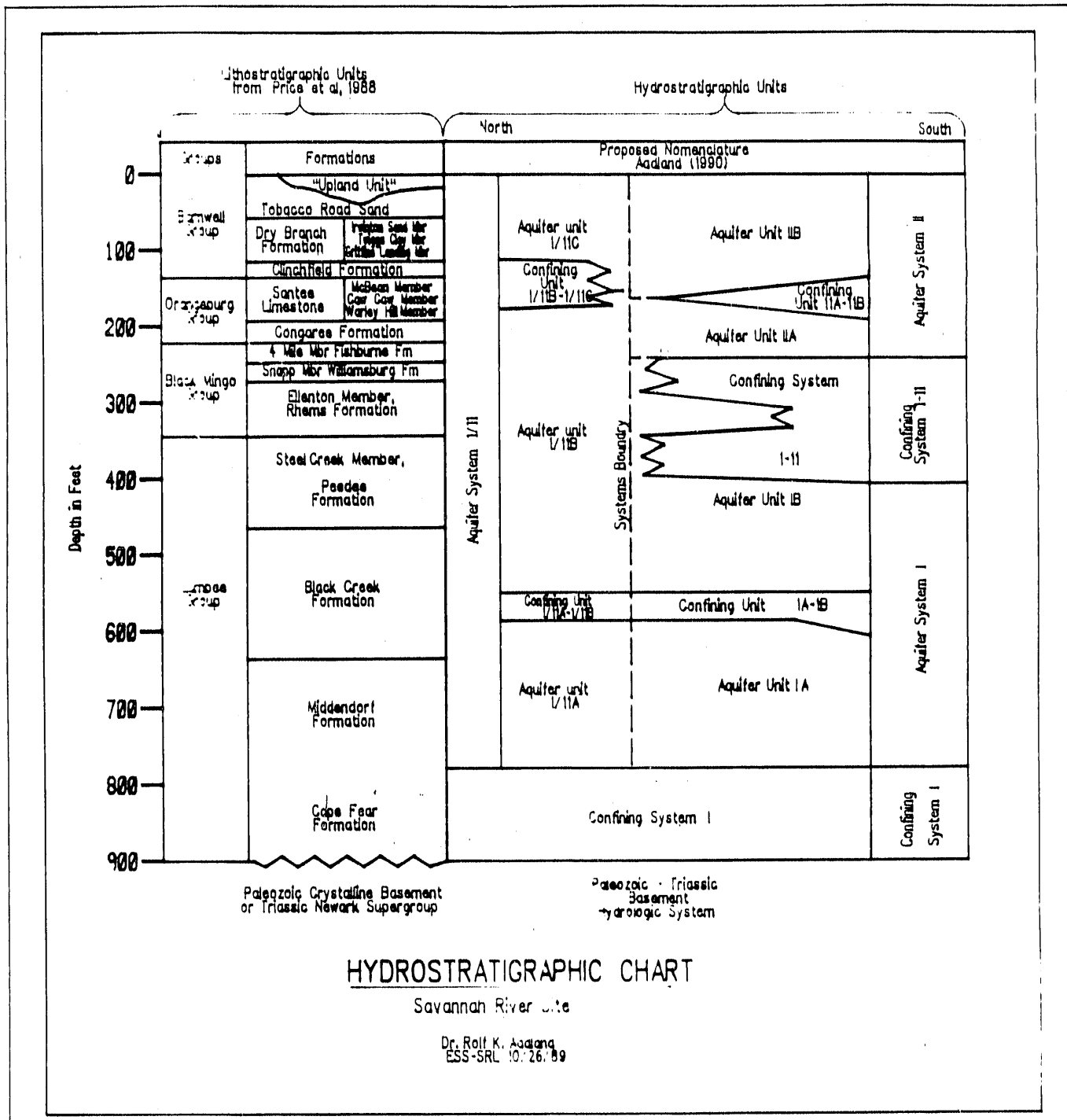


Figure 3.2 Schematic Diagram showing Relationship between Clay Layers and Hydrologic Features

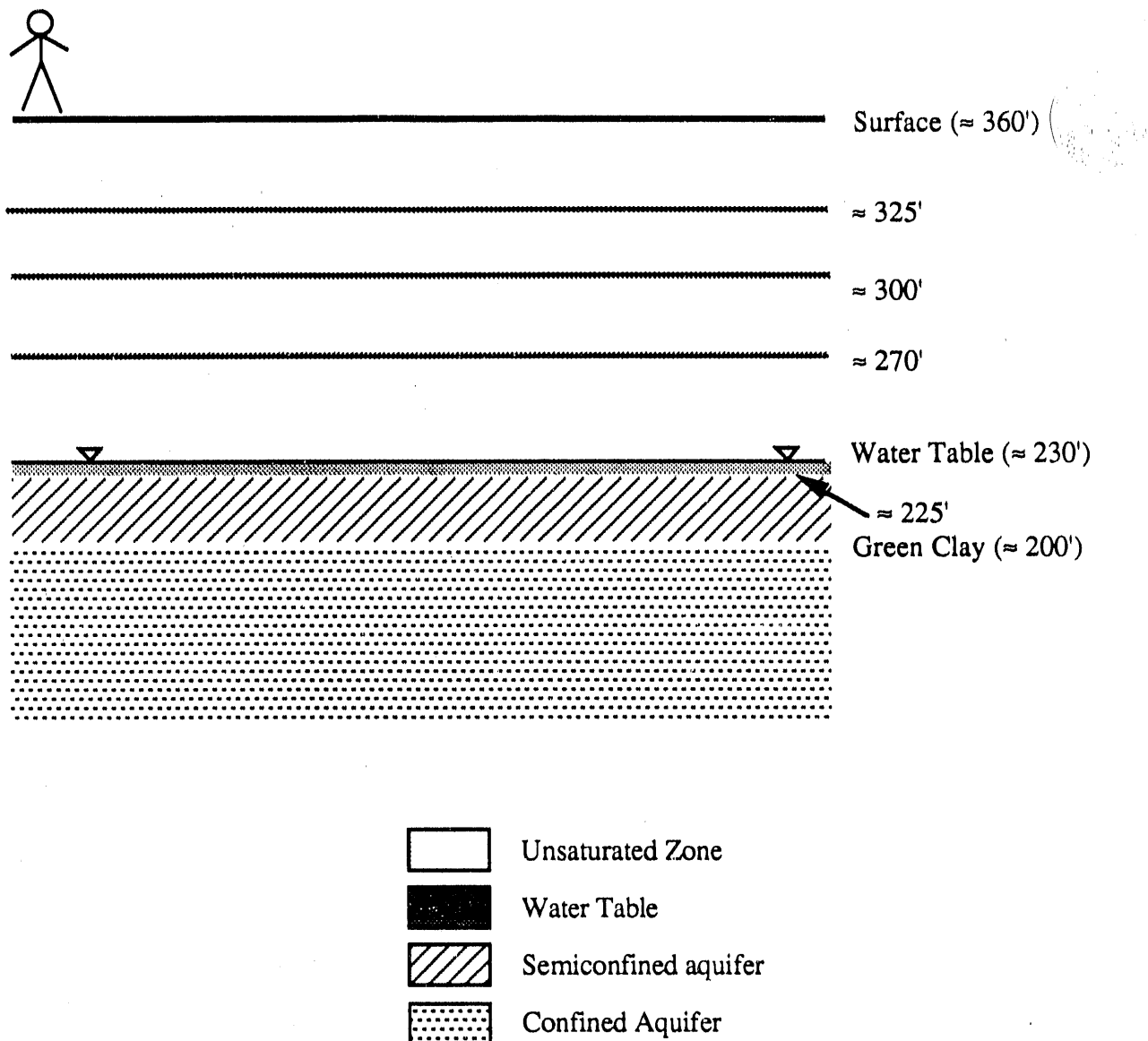


Figure 3.3 Location Map for the MHT C Wells

Base Map – Semiconfined Zone Monitoring Wells

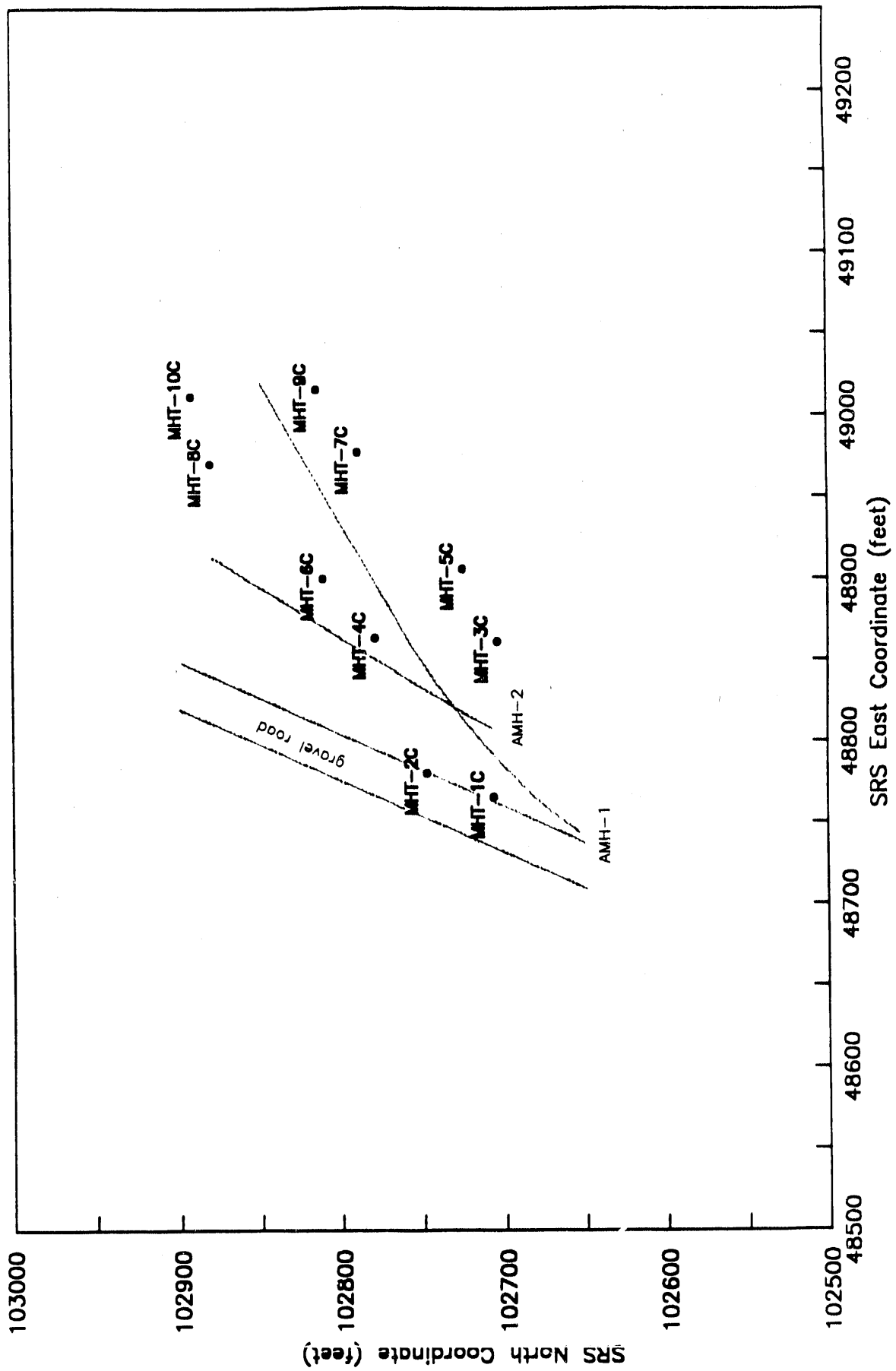


Figure 3.4 Location Map for the MHT D Wells

Base Map – Water Table Monitoring Wells

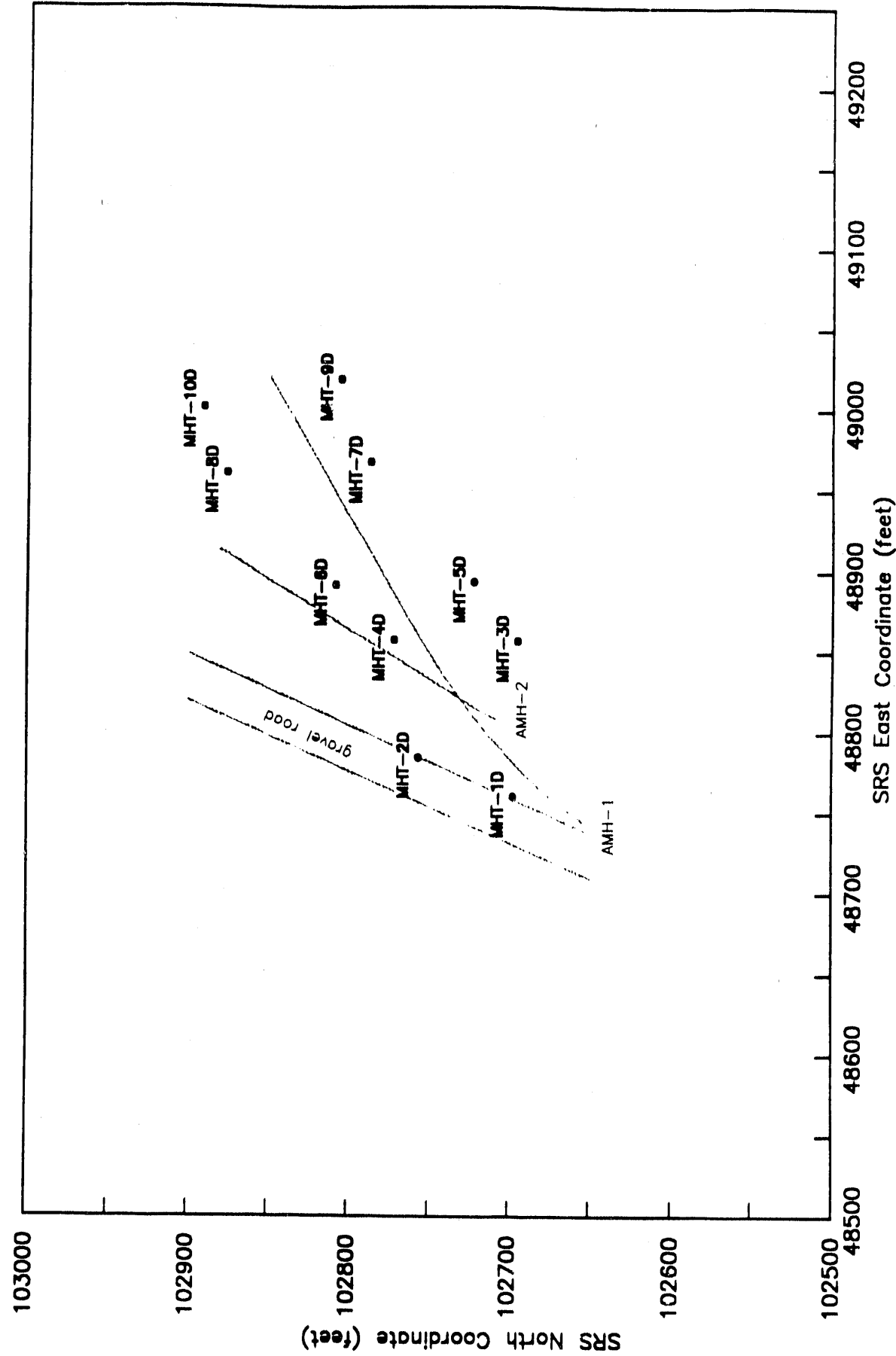
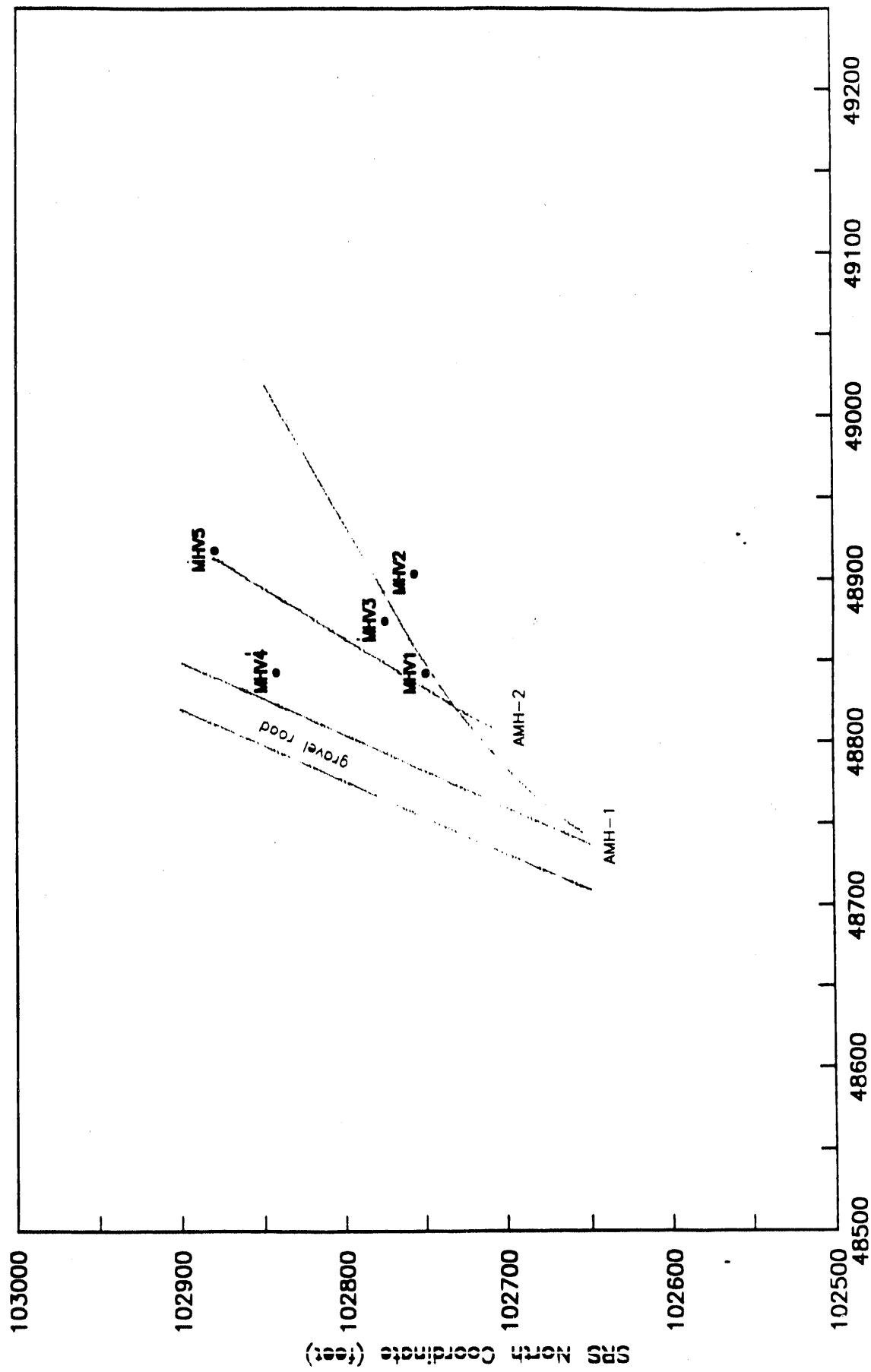


Figure 3.5 Location Map for the MHV Boring Locations

Base Map – Vadose Zone Monitoring Clusters



4.0 Hydrology

The demonstration site is underlain by interbedded sand, silt, and clay. This lithological pattern provides the framework that governs the flow of fluids in the subsurface (for both gases and liquids). The water table is at a depth of approximately 130 to 140 feet below grade at the demonstration site. The sitewide and local hydrostratigraphy, subsurface hydrologic properties, initial hydrologic conditions, and vadose zone properties are addressed in the following sections.

Conceptual Description of SRS Groundwater System

The direction and rate of flow in a groundwater system is governed by the hydrologic boundaries (i.e., where water enters and leaves the system) and the nature of the subsurface materials (e.g., hydraulic conductivity, heterogeneity, etc.). The resulting hydraulic heads and hydraulic gradients indicate flow direction. Characterization of the subsurface materials and mathematical modeling allow estimation of flow rates and the potential for contaminant transport. A conceptual description of the groundwater system underlying SRS, on a sitewide scale, based on water level measurements made in 1988 is provided below to assist in understanding the detailed hydrogeology at the demonstration site (Looney et al., 1990).

There are several water bearing zones beneath SRS that are separated by less permeable aquitards. Site streams and the Savannah River incise the various layers and serve as hydrologic boundaries. Water enters the site system through recharge and flow from upgradient and flows downward and laterally toward local streams in the shallow zones and toward the Savannah River in the deeper zones. The fact that each layer may be governed by a different hydrologic boundary results in different flow directions in the various zones. The nomenclature for the hydrostratigraphy underlying SRS has evolved and changed over the last several decades. On a sitewide scale, the hydrostratigraphy can be roughly described in terms of two aquifer systems. The deeper system (Aquifer System I) is comprised of two zones (Aquifer IA and IB), consisting primarily of sediments of Cretaceous Age, flowing toward the Savannah River (Figures 4.1 and 4.2). A relatively thick sequence of interbedded clays (primarily associated with the Ellenton Formation) forms an aquitard between the shallow and deep aquifer systems. The shallow system (Aquifer System II) is located primarily in sediments of Tertiary Age and generally consists of several water bearing zones (one or more confined or semiconfined zones and a water table zone). Flow in the confined water bearing zones in this upper system is generally toward Upper Three Runs Creek or the Savannah River (Figure 4.3). The potentiometric surfaces for the semiconfined and water table zones are complex due to the recharge-discharge relationships to the various site streams and the significant vertical component of flow in several of the zones.

Hydrology of the Field Demonstration Site

The contaminants at the field demonstration site and zone of influence of the in situ air stripping system are located in the upper aquifer system. This system consists of three water bearing zones separated by less permeable aquitards. The water table is located at an elevation of approximately 230 feet above msl in relatively fine grained and highly variable sediments. The water table is separated from a semiconfined zone by a thin-somewhat discontinuous aquitard that occurs at an elevation of approximately 225 feet. The semiconfined zone is separated from a confined zone by the green clay at an elevation of approximately 200 feet. The bottom of the confined zone is defined by clays of the Ellenton Formation at an elevation of approximately 150 feet above msl. The horizontal injection well is completed in the semiconfined zone near the wellhead and dips into the confined zone near the distal end of the horizontal perforated section. The confined water bearing zone is associated with sands of the Congaree Formation, and the semiconfined and water table zones are generally associated with the Santee Formation and the lower sections of the Barnwell Group. The remainder of the section is generally unsaturated with perched water identified at some locations or associated with significant recharge events.

Water level data collected at the beginning of the demonstration test are listed on Table 4.1. Pretest potentiometric surfaces for the water table and semiconfined zone are shown in Figures 4.4 and 4.5. As discussed above, monitoring wells at the field demonstration site are completed in the water table and semiconfined zones only (the zones that encompass and overlie the injection horizontal well). Vertical gradients are plotted on Figure 4.6. These data are typical of the monitoring wells installed to monitor the area-wide groundwater flow, contaminant transport and remediation system progress (Dupont, 1986). In A/M area, water enters the subsurface through precipitation and recharge; flow in the water table is primarily vertical (downward) into the semiconfined zone. In this zone, flow is both horizontal and vertical (downward). Once water reaches the confined zone, flow is primarily horizontal toward discharges in Upper Three Runs Creek, which serves as a hydrologic boundary/drain. Note that the water table wells show almost no horizontal gradient with the exception of the water level in well MHT-9D. This well is approximately 10 feet higher than the other water table wells. This phenomenon occurred over a long period and was measured by several individuals, using independent measuring devices. This well appears to be measuring a zone with relatively significant quantities of perched water that are not found in the rest of the demonstration site. This observation will be studied further in the post test characterization and in future work at the site.

Aquifer Characteristics

A large number of pump tests, sieve analyses and other characterization studies have been performed to provide characterization of the water bearing zones in the vicinity of the field demonstration site. Hydrogeologic properties of the saturated zone have primarily been evaluated through the performance of aquifer tests. These tests have been performed for all of the aquifers in the Coastal Plain section (Dupont, 1986; Dupont, 1983). Table 4.2 summarizes data for the upper water bearing zones of interest at the demonstration site. The table provides summary data for studies from across SRS and provides more detailed results for those tests closest to the demonstration site. The data derived from well designed fully penetrating pump tests indicate that the composite saturated hydraulic conductivity of the upper water bearing zones is approximately 0.009 to 0.012 cm/sec. As expected, values obtained at monitoring wells (slug tests that are impacted by short screens and inefficient design) yielded lower values.

Several groundwater flow and transport models have been developed to support the groundwater corrective action program in the A/M Area of SRS where the field demonstration site is located (Dupont, 1986; Beaudoin et al., 1991). Calibration of these models is based on matching water levels, as well as data in recharge and streamflow in the model area. Thus, the calibrated models provide one more means to determine aquifer parameters; these parameter estimates represent the consolidation of several types of data based on fundamental hydrologic relationships and mathematical algorithms. Table 4.3 lists aquifer parameters resulting from model calibration in the vicinity of the demonstration site. The composite horizontal hydraulic conductivity of the upper zones (calculated as the depth weighted mean - Freeze and Cherry, 1979) is 0.013; this value compares favorably with the pump test results presented above.

Sitewide values of several bulk subsurface parameters determined primarily from laboratory tests are documented in Looney et al. (1987). The range of total porosity reported for SRS sediments is approximately 0.3 to 0.6 (cm³ of water/cm³). Total porosities in clay zones are in the upper part of this range (\approx 0.4 to 0.6), while more permeable sand zones are in the lower part of this range (\approx 0.3 to 0.5). The effective porosities measured at SRS range from 0.1 to 0.3. Bulk densities in a variety of studies generally range from 1.4 g/cm³ to 1.7 g/cm³. As a result of relatively higher average porosity and relatively lower specific gravity of the solids, the clay zones tend to have slightly lower bulk densities than sandy zones. Borehole geophysical logs (gamma-gamma density and neutron) to estimate density and porosity were performed on all of the well clusters at the

demonstration site. The magnitude of the measured data and the pattern with respect to lithology are consistent with sitewide values. Porosity values were estimated based on neutron probe response calibrated for porous sediments containing water. The resulting porosities below the water table were in the range of 0.2 to 0.5 with most of the values between 0.3 and 0.4. Peaks in the porosity below the water table corresponded to clay zones identified by gamma logs, resistivity logs, and core examination. The neutron logs above the water table are responding primarily to changes in moisture content - the conversion to porosity is not accurate because the formation is not saturated with water. The density logs (based on a generic calibration for "sandstone" containing water) yield somewhat higher values than expected (based on other studies at SRS). Most of the estimated density values from the logs are in the range of 1.6 to 2.1 g/cm³. As expected, the clay zones tended to have slightly lower bulk densities than the sand zones. These higher values should be used with caution since the appropriateness of the calibration to SRS has not been verified.

"Undisturbed" core samples of significant clay zones have been collected in several drilling studies at SRS (Bledsoe, 1984; Bledsoe, 1986; Bledsoe, 1988). Results for samples that are relevant to the depth of interest at the demonstration site (many of the samples were collected from significantly deeper zones) are tabulated on Table 4.4. As expected, the saturated hydraulic conductivities for the clay zones are much lower than the more transmissive water bearing zones. Values for the "tan clay" zone are in the range of 10⁻⁷ to 10⁻⁶ cm/sec and values for the green clay zone are in the range of 10⁻⁸ to 10⁻⁵ cm/sec. Values for total porosity were in the expected range for clay samples with most values ranging between 0.35 and 0.6.

Many investigators have shown that the hydrologic properties of subsurface materials are related to the textural properties (as influenced by depositional factors). For example, hydraulic conductivity has often been related to the grain size distribution for unconsolidated sediments such as those at the field demonstration site. Detailed grain size distribution measurements were made on closely spaced intervals in several of wells cored at the demonstration site (MHT 1, MHT 5, MHT 7, and MHT 9). The data have been summarized on Table 4.5. Several parameters are presented in the table. Except as noted, all values are in ϕ units where, $\phi = -\log_2 d$ (d in millimeters). The following key indicates significance of the various reported values (Folk, 1980):

Mean and Median - higher numbers represent finer grained sediments.

Standard Deviation -

< 0.50	well sorted
0.50 to 0.71	moderately well sorted
0.71 to 1.0	moderately sorted
1.0 to 2.0	poorly sorted
> 2.0	very poorly sorted

Skewness -

+1.0 to +0.3	very fine skewed
+0.3 to +0.1	fine skewed
+0.1 to -0.1	symmetrical
-0.1 to -0.3	coarse skewed
-0.3 to -1.0	very coarse skewed

Kurtosis -

< 0.9	platykurtic
0.9 to 1.11	mesokurtic
1.11 to 1.5	leptokurtic
> 1.5	very leptokurtic

Sorting -

< 0.30	well sorted
0.30 to 0.5	moderately sorted
> 0.5	poorly sorted

The semiquantitative methods documented in the literature (e.g., Beard and Weyl, 1973) to relate the textural characteristics to numerical predictions of hydraulic conductivity have not been entirely satisfactory, yielding estimates that are 2 to 10 times higher than pump tests and modeling results. For example, sieve estimated hydraulic conductivities for sandy intervals (< 20 % clay) range from \approx 20 to \approx 80 darcies (0.02 to 0.08 cm/sec) with the values centering near 50 darcies (0.05 cm/sec). Samples with somewhat greater clay contents (20% to 40%) yielded sieve estimated hydraulic conductivities of \approx 5 to \approx 20 darcies (0.005 to 0.02 cm/sec). Sieve based estimates of hydraulic conductivity can not be determined using the Beard and Weyl (1973) nomogram for samples that contain more than 40% clay. A selection of alternate approaches for estimating hydraulic conductivity from sieve data [e.g., the methods of Hazen, Fair and Hatch (see Freeze and Cherry, 1979) or Masch and Denny, 1966] yield values that are similar to or greater than Beard and Weyl (1973). Differences between hydraulic conductivities determined by pump tests/model calibrations and sieve data estimation methods may result from the relatively low hydraulic conductivities of the materials at the Integrated Demonstration Site (they are at the low end of the calibrations) and differences in the shape and packing of natural Coastal Plain sediments compared to the laboratory sand columns constructed for developing the calibrations. Nonetheless, the detailed textural information provides a clear picture of the expected pattern of hydraulic conductivity variation as a function of depth at the site. More appropriate relationships are being developed to allow better estimates of hydraulic conductivity from the data. These will be presented in a separate report.

A vertical vacuum extraction test was performed at the demonstration site in 1987. Vacuum (drawdown) data in the vadose zone piezometers were modeled. The resulting permeabilities for the transmissive zones were consistent with those reported for the saturated zone (\approx 10 darcies). Permeability-moisture curves are not available at this time, however, undisturbed vadose zone samples are being collected for these measurements during the post test characterization.

Table 4.1 Summary of Initial Water Level Measurements

Well I.D.	Depth to Water	Elevation	Depth to Water	Elevation	Midpoint of Screen
	(feet)	(feet)	(feet)	(feet above msl)	
Well I.D.	20-Jul-91	20-Jul-91	6-Aug-91	6-Aug-91	
'MHT-1C '	136.35	228.82	136.47	228.70	206.8
'MHT-1D '	135.40	229.07	135.65	228.82	227.5
'MHT-2C '	137.70	228.76	137.78	228.68	209.2
'MHT-2D '	138.45	229.01	138.60	228.86	229.8
'MHT-3C '	136.25	228.84	136.22	228.87	206.7
'MHT-3D '	135.50	229.2	135.65	229.05	226.7
'MHT-4C '	140.90	228.89	141.00	228.79	210.7
'MHT-4D '	139.65	229.29	139.95	228.99	231.6
'MHT-5C '	137.40	229.05	137.50	228.95	207.1
'MHT-5D '	137.20	229.16	137.30	229.06	230.0
'MHT-6C '	143.10	228.87	143.12	228.85	209.8
'MHT-6D '	142.10	229.26	142.30	229.06	234.1
'MHT-7C '	141.25	229.05	141.42	228.88	209.0
'MHT-7D '	140.00	230.09	140.36	229.73	229.4
'MHT-8C '	142.90	228.9	143.05	228.75	209.3
'MHT-8D '	142.50	229.27	142.65	229.12	230.1
'MHT-9C '	141.20	228.68	141.30	228.58	211.8
'MHT-9D '	130.55	239.47	130.47	239.55	232.2
'MHT-10C '	142.10	229.01	142.18	228.93	208.9
'MHT-10D '	141.50	229.54	141.80	229.24	229.5

Table 4.2 Summary of Aquifer Tests Performed Near the Study Area.

A/M Area "Uppermost Aquifer"*

(includes water table, semiconfined, and confined zones as defined in this report)

RMW8/RMW10 hydraulic conductivity \approx 34 ft/day = 12.4 darcies = 0.012 cm/sec
storage coefficient \approx 0.0009

RWM6/RWM7 hydraulic conductivity \approx 29 ft/day = 10.6 darcies = 0.010 cm/sec
storage coefficient \approx 0.0006

RWM7/RWM6 hydraulic conductivity \approx 25 ft/day = 9.1 darcies = 0.009 cm/sec
storage coefficient \approx 0.0006

range of values in study:

minimum	hydraulic conductivity \approx 1 ft/day = 0.4 darcies = 0.0003 cm/sec
median	hydraulic conductivity \approx 25 ft/day = 9.1 darcies = 0.009 cm/sec
maximum	hydraulic conductivity \approx 59 ft/day = 21.5 darcies = 0.021 cm/sec

SRS wide Values **

water table/semiconfined zones

minimum	hydraulic conductivity \approx 0.5 ft/day = 0.2 darcies = 0.0002 cm/sec
average	hydraulic conductivity \approx 5 ft/day = 1.8 darcies = 0.002 cm/sec
maximum	hydraulic conductivity \approx 32 ft/day = 11.7 darcies = 0.012 cm/sec

confined zone

minimum	hydraulic conductivity \approx 1 ft/day = 0.4 darcies = 0.0003 cm/sec
average	hydraulic conductivity \approx 6 ft/day = 2.2 darcies = 0.002 cm/sec
maximum	hydraulic conductivity \approx 96 ft/day = 35 darcies = 0.034 cm/sec

* Dupont 1986 - Specific data from fully penetrating well pairs that are less than 200 feet from the demonstration site are provided. The range of values is based on all fully penetrating pairs located within 4000 feet of the demonstration site and data from partially penetrating monitoring wells. All reported values assume an average screened interval of approximately 100 feet

** Christensen and Gordon, 1983 - Data summarized from slug tests near the center of SRS. Data from short screen zones in monitoring wells. Poor well efficiency in such wells would tend to result in low (underestimates of) hydraulic conductivity.

Table 4.3 Summary of Aquifer Parameters Estimated By Model Calibration

A/M Area Modeling Calibration Results *

water table/semiconfined zone

 hydraulic conductivity \approx 7 ft/day = 2.6 darcies = 0.0025 cm/sec

confined zone (upper section)

 hydraulic conductivity \approx 58 ft/day = 21.1 darcies = 0.020 cm/sec

confined zone (lower section)

 hydraulic conductivity \approx 44 ft/day = 16.0 darcies = 0.016 cm/sec

weighted average for this study

 hydraulic conductivity \approx 37 ft/day = 13.5 darcies = 0.013 cm/sec

* Dupont, 1986 and Beaudoin et al., 1991 - Water table in model consists of the water table and semiconfined zones as defined in this report. The confined zone in the model is divided into two subzones. The reported values assume the following interval thicknesses: water table / semiconfined \approx 25 feet, upper confined \approx 30 feet, and lower confined \approx 20 feet.

Table 4.4 Summary of Aquifer Parameters For Clay Zones Estimated By Laboratory Measurements on "Undisturbed" Core Samples.
"Tan Clay"

Well P-20 (210-211)	vertical hydraulic conductivity = 4.7×10^{-7} cm/sec horizontal hydraulic conductivity = 5.2×10^{-7} cm/sec total porosity = 0.627
Well P-30 (105-108)	vertical hydraulic conductivity = 8.1×10^{-7} cm/sec horizontal hydraulic conductivity = 6.8×10^{-7} cm/sec total porosity = 0.529
"Green Clay"	
Well P-13 (237-239.5)	vertical hydraulic conductivity = 5.6×10^{-5} cm/sec horizontal hydraulic conductivity = 5.3×10^{-5} cm/sec total porosity = 0.364 to 0.371
Well P-14 (168-170)	vertical hydraulic conductivity = 4.5×10^{-5} cm/sec horizontal hydraulic conductivity = 2.4×10^{-7} cm/sec total porosity = 0.365 to 0.375
Well P-15 (171)	vertical hydraulic conductivity = 4.1×10^{-7} cm/sec horizontal hydraulic conductivity = 1.7×10^{-6} cm/sec total porosity = 0.421 to 0.465
Well P-18 (180-182)	vertical hydraulic conductivity = 2.7×10^{-8} cm/sec horizontal hydraulic conductivity = 2.0×10^{-8} cm/sec total porosity = 0.408
Well P-19 (210-211)	vertical hydraulic conductivity = 1.2×10^{-8} cm/sec horizontal hydraulic conductivity = 2.8×10^{-6} cm/sec total porosity = 0.388
Well P-20 (210-211)	vertical hydraulic conductivity = 9.1×10^{-7} cm/sec horizontal hydraulic conductivity = 1.1×10^{-6} cm/sec total porosity = 0.445
Well P-20 (210-211)	vertical hydraulic conductivity = 9.1×10^{-7} cm/sec horizontal hydraulic conductivity = 1.1×10^{-6} cm/sec total porosity = 0.445
Well P-28 (132-134)	vertical hydraulic conductivity = 2.0×10^{-7} cm/sec horizontal hydraulic conductivity = 1.9×10^{-7} cm/sec total porosity = 0.510

Bledsoe, 1984; Bledsoe, 1986; Bledsoe, 1988 - hydraulic conductivity measured using falling head test.

Table 4.5 Summary of Sieve Analysis of MHT Well Cores.

Well	Depth	Mean	Std Dev	Skewness	Kurtosis	Median	Sorting
MHT1C	66.0	1.40	0.78	0.15	1.18	1.34	0.47
MHT1C	68.0	1.32	0.60	0.08	1.25	1.32	0.35
MHT1C	70.0	1.30	0.60	0.02	1.33	1.30	0.33
MHT1C	72.0	1.35	0.68	0.07	1.24	1.34	0.40
MHT1C	74.0	1.49	0.80	0.15	1.20	1.41	0.46
MHT1C	76.0	1.55	0.90	0.23	1.39	1.45	0.48
MHT1C	80.0	1.23	0.91	0.06	1.17	1.21	0.56
MHT1C	82.0	1.25	0.76	-0.02	1.09	1.26	0.50
MHT1C	84.0	1.24	0.74	-0.02	1.07	1.24	0.49
MHT1C	86.0	1.47	0.97	-0.11	1.20	1.53	0.59
MHT1C	138.0	0.98	1.00	0.13	1.06	0.94	0.66
MHT1C	138.5	1.27	1.07	-0.08	0.78	1.33	0.87
MHT1C	143.0	1.00	1.03	0.10	1.08	0.98	0.68
MHT1C	152.0	1.20	0.76	0.18	1.24	1.15	0.46
MHT1C	153.0	1.27	0.81	0.02	1.24	1.29	0.50
MHT1C	155.0	2.97	0.59	-0.19	1.23	3.03	0.36
MHT1C	157.0	1.27	1.04	0.34	1.27	1.05	0.57
MHT1C	159.0	1.93	1.22	-0.11	1.01	2.04	0.82
MHT1C	161.0	1.97	1.45	0.16	0.85	1.74	1.09
MHT1C	170.0	1.86	0.58	0.12	1.13	1.83	0.36
MHT1C	175.0	1.74	0.56	0.03	1.13	1.73	0.34
MHT1C	180.0	2.51	0.51	-0.09	1.37	2.57	0.30
MHT1C	184.0	1.79	0.62	-0.01	1.16	1.79	0.38
MHT-5C	71	3.00	2.55	0.52	2.72	2.17	0.73
MHT-5C	73	1.56	0.86	0.05	1.01	1.52	0.58

Table 4.5 Summary of Sieve Analysis of MHT Well Cores (continued)

Well	Depth	Mean	Std Dev	Skewness	Kurtosis	Median	Sorting
MHT-5C	75	1.48	0.86	0.07	1.14	1.43	0.53
MHT-5C	77	1.28	0.59	0.00	1.25	1.28	0.34
MHT-5C	79	1.23	0.65	0.03	1.20	1.23	0.39
MHT-5C	81	1.26	0.77	0.05	1.08	1.25	0.51
MHT-5C	83	1.20	0.73	-0.01	1.05	1.20	0.49
MHT-5C	85	1.24	0.76	-0.02	1.07	1.25	0.50
MHT-5C	87	1.11	0.84	0.01	1.10	1.11	0.53
MHT-5C	89	1.02	0.75	0.06	1.21	1.00	0.44
MHT-5C	91A	0.97	0.71	-0.17	1.17	1.08	0.43
MHT-5C	91B	1.04	0.75	-0.06	1.21	1.09	0.44
MHT-5C	93	1.93	2.02	0.45	2.29	1.67	0.78
MHT-5C	95	2.21	2.52	0.58	2.14	1.43	0.90
MHT-5C	97	2.03	1.60	0.42	3.30	1.92	0.48
MHT-5C	100	2.04	1.32	0.29	3.18	2.06	0.41
MHT-5C	103	2.02	1.50	0.29	3.27	2.03	0.46
MHT-5C	105	1.92	1.45	0.10	2.54	2.04	0.54
MHT-5C	110	5.66	4.61	0.57	0.58	3.51	4.52
MHT-5C	120	9.50	3.84	-0.49	0.96	10.83	2.49
MHT-5C	126	6.07	4.35	0.55	0.63	4.06	4.06
MHT-5C	150	0.99	1.31	0.06	1.16	0.96	0.81
MHT-5C	152	1.52	0.93	0.19	1.49	1.46	0.48
MHT-5C	155	1.04	1.18	0.00	0.97	1.04	0.82
MHT-5C	158	2.03	1.93	0.28	1.85	1.94	0.90
MHT-5C	161	1.44	0.88	0.17	1.05	1.35	0.57
MHT-7C	73	3.00	2.73	0.58	2.96	2.37	0.79

Table 4.5 Summary of Sieve Analysis of MHT Well Cores (continued).

Well	Depth	Mean	Std Dev	Skewness	Kurtosis	Median	Sorting
MHT-7C	75	1.18	0.56	-0.07	1.08	1.19	0.35
MHT-7C	77	1.17	0.69	-0.02	1.16	1.19	0.43
MHT-7C	79	1.59	0.83	0.08	1.03	1.53	0.55
MHT-7C	81	1.19	0.75	0.04	1.02	1.17	0.51
MHT-7C	83	1.42	1.07	0.22	1.33	1.32	0.61
MHT-7C	85	1.21	0.74	0.00	1.06	1.20	0.49
MHT-7C	87	0.94	0.74	-0.03	1.12	0.95	0.45
MHT-7C	87	1.15	0.84	0.07	1.16	1.13	0.52
MHT-7C	89	1.10	0.83	0.04	1.15	1.09	0.50
MHT-7C	91	1.02	0.77	-0.01	1.22	1.03	0.45
MHT-7C	92	2.69	3.31	0.57	2.29	1.70	1.14
MHT-7C	95	1.35	1.13	0.15	1.20	1.26	0.69
MHT-7C	97	5.75	4.68	0.46	0.58	4.00	4.59
MHT-7C	99	2.25	0.62	-0.07	1.19	2.27	0.37
MHT-7C	101	3.65	3.46	0.62	2.11	2.25	1.12
MHT-7C	103	1.86	0.73	-0.24	1.22	1.96	0.44
MHT-7C	108	9.13	2.78	0.07	0.79	8.97	2.19
MHT-7C	115	7.46	4.39	-0.16	0.59	8.08	4.25
MHT-7C	118	1.19	1.14	0.20	1.31	1.09	0.65
MHT-7C	124	0.99	2.19	0.48	2.02	0.65	0.92
MHT-7C	126	-0.58	0.90	0.09	1.08	-0.62	0.59
MHT-7C	128	10.19	2.95	-0.31	1.01	10.69	1.95
MHT-7C	133	9.84	3.82	-0.52	1.11	10.99	2.36
MHT-7C	138	1.47	1.75	0.27	1.85	1.41	0.82
MHT-7C	140	1.53	0.83	0.10	1.10	1.47	0.52

Table 4.5 Summary of Sieve Analysis of MHT Well Cores (continued)

Well	Depth	Mean	Std Dev	Skewness	Kurtosis	Median	Sorting
MHT-7C	144	1.10	1.13	0.16	1.05	1.01	0.75
MHT-7C	149	1.92	2.32	0.18	1.58	1.96	1.25
MHT-7C	152	1.32	2.55	0.36	2.23	1.14	1.03
MHT-7C	154	3.01	0.67	0.01	0.74	3.01	0.54
MHT-7C	157	1.50	1.57	0.31	1.63	1.32	0.75
MHT-7C	159	1.67	1.54	0.24	1.42	1.58	0.86
MHT-7C	161	1.10	1.27	0.11	1.58	1.15	0.69
MHT-7C	163	5.58	4.03	0.47	0.87	4.12	2.90
MHT-7C	165	2.56	2.56	0.41	1.98	2.27	1.11
MHT-9C	71	3.95	2.34	3.58	0.73	0.69	3.37
MHT-9C	74	1.12	0.74	-0.02	1.22	1.15	0.44
MHT-9C	77	1.60	0.85	0.07	1.08	1.57	0.55
MHT-9C	80	1.00	0.93	-0.03	1.03	1.04	0.61
MHT-9C	83	1.18	0.76	-0.02	1.09	1.18	0.49
MHT-9C	86	1.24	0.75	0.17	1.46	1.21	0.40
MHT-9C	89	8.86	10.39	4.11	3.68	-0.46	0.64
MHT-9C	92	3.55	4.93	0.61	2.00	1.26	1.48
MHT-9C	96	1.71	0.96	0.07	1.45	1.62	0.45
MHT-9C	100	10.25	10.31	2.62	1.88	-0.14	0.96
MHT-9C	104	8.08	9.25	4.26	4.44	-0.30	0.53
MHT-9C	108	1.08	2.17	0.38	2.70	0.89	0.78
MHT-9C	111	7.67	9.07	4.36	3.58	-0.38	0.73
MHT-9C	117	1.32	3.21	0.38	2.15	1.01	1.30
MHT-9C	119	1.55	3.51	0.34	1.58	1.15	1.70
MHT-9C	122	0.45	1.07	-0.06	1.25	0.50	0.63

Table 4.5 Summary of Sieve Analysis of MHT Well Cores (continued)

Well	Depth	Mean	Std Dev	Skewness	Kurtosis	Median	Sorting
MHT-9C	126	0.29	0.82	0.14	1.47	0.26	0.45
MHT-9C	130	6.23	3.96	3.84	3.53	0.73	0.65
MHT-9C	135	0.84	1.60	0.03	1.10	0.85	1.03
MHT-9C	140	1.98	1.14	-0.32	1.15	2.22	0.68
MHT-9C	146	1.46	1.14	0.00	1.21	1.51	0.69
MHT-9C	149	1.07	1.31	0.25	1.22	0.92	0.79
MHT-9C	153	2.97	0.67	-0.19	1.21	3.06	0.40
MHT-9C	154	3.13	0.82	-0.29	1.61	3.22	0.39
MHT-9C	157	1.79	1.04	0.13	1.29	1.69	0.58
MHT-9C	159	1.38	1.23	0.24	1.32	1.26	0.68
MHT-9C	162	4.02	3.38	0.38	1.49	3.36	1.60

**Figure 4.1. Potentiometric Map for Aquifer IA;
elevations in feet above msl.**

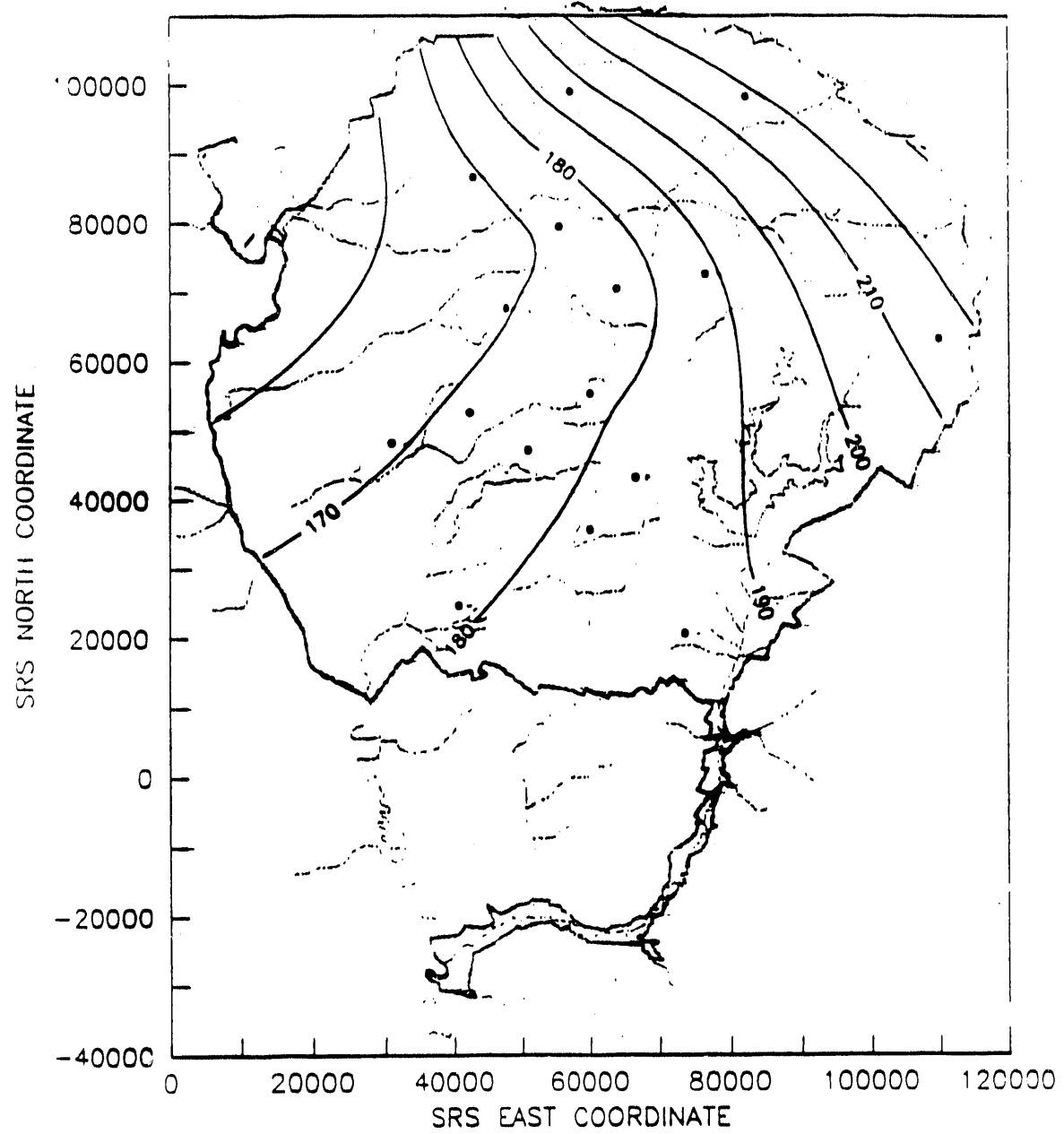


**Figure 4.2. Potentiometric Map for Aquifer IB;
elevations in feet above msl.**

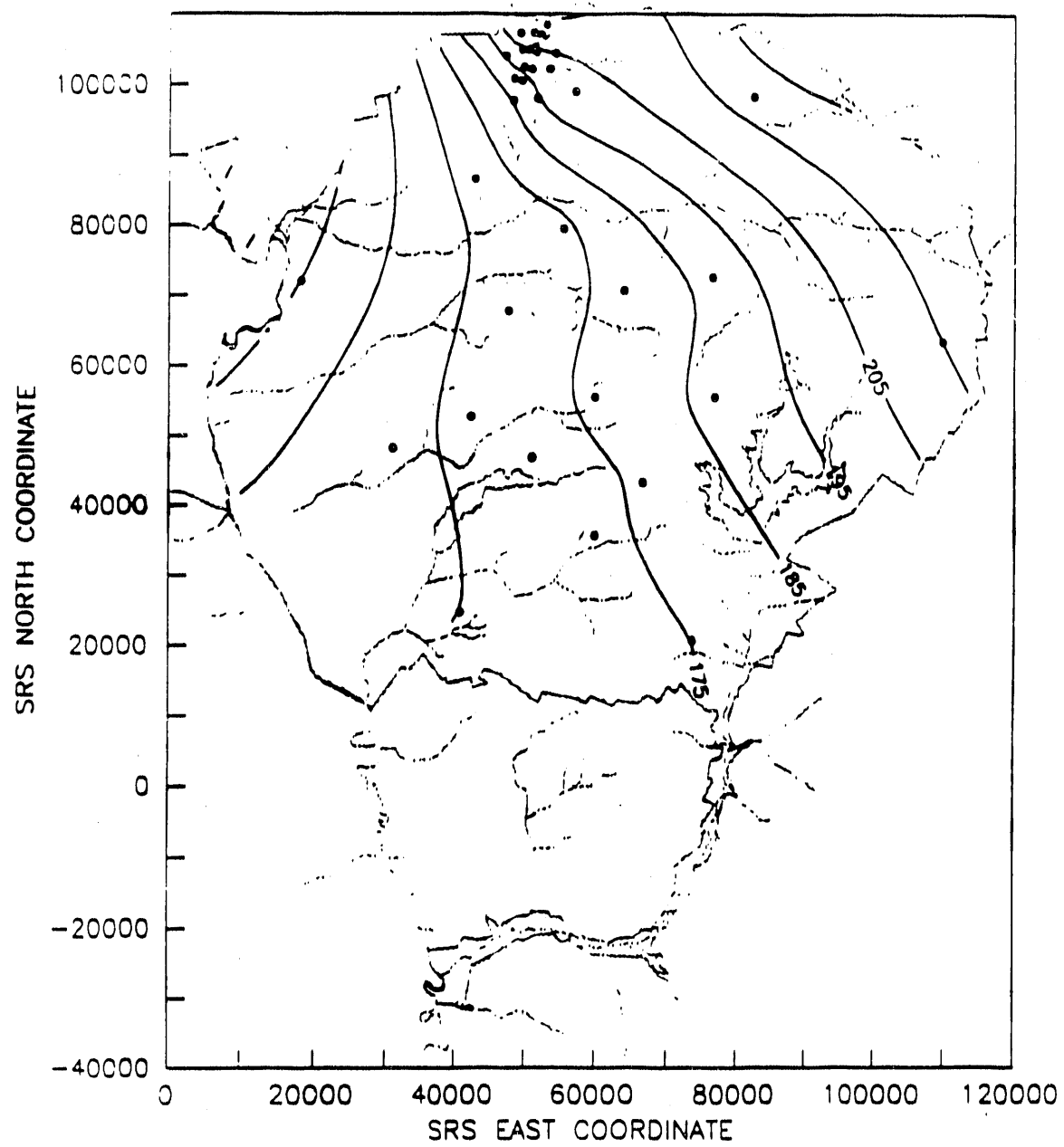


**Figure 4.3. Potentiometric Map for Confined Zones of Aquifer System II;
elevations in feet above msl.**

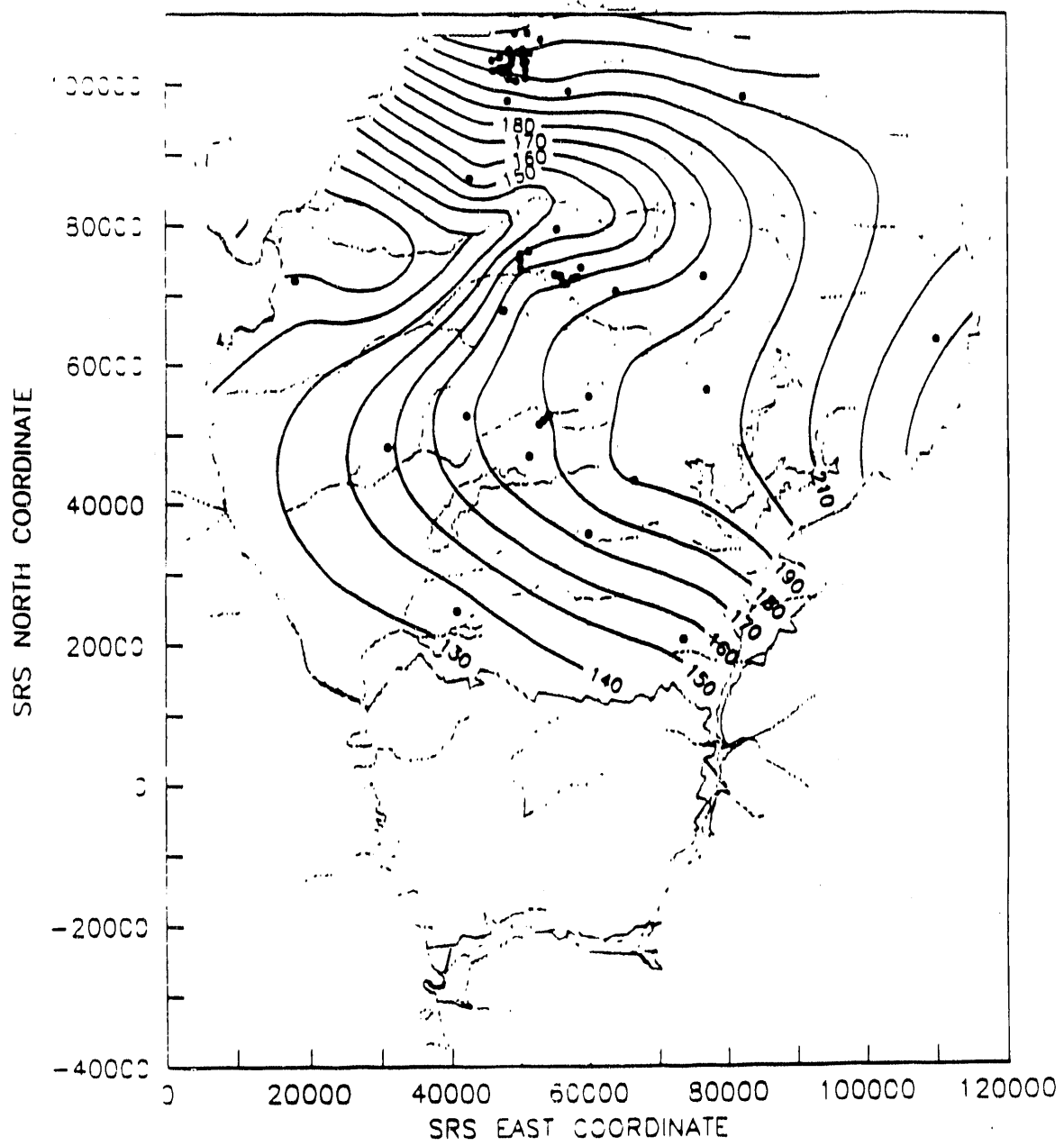


Figure 4.4. Potentiometric Map for the Water Table Zone at the Field Demonstration Site; elevations in feet above msl.

Pretest Potentiometric Surface - Water Table Zone

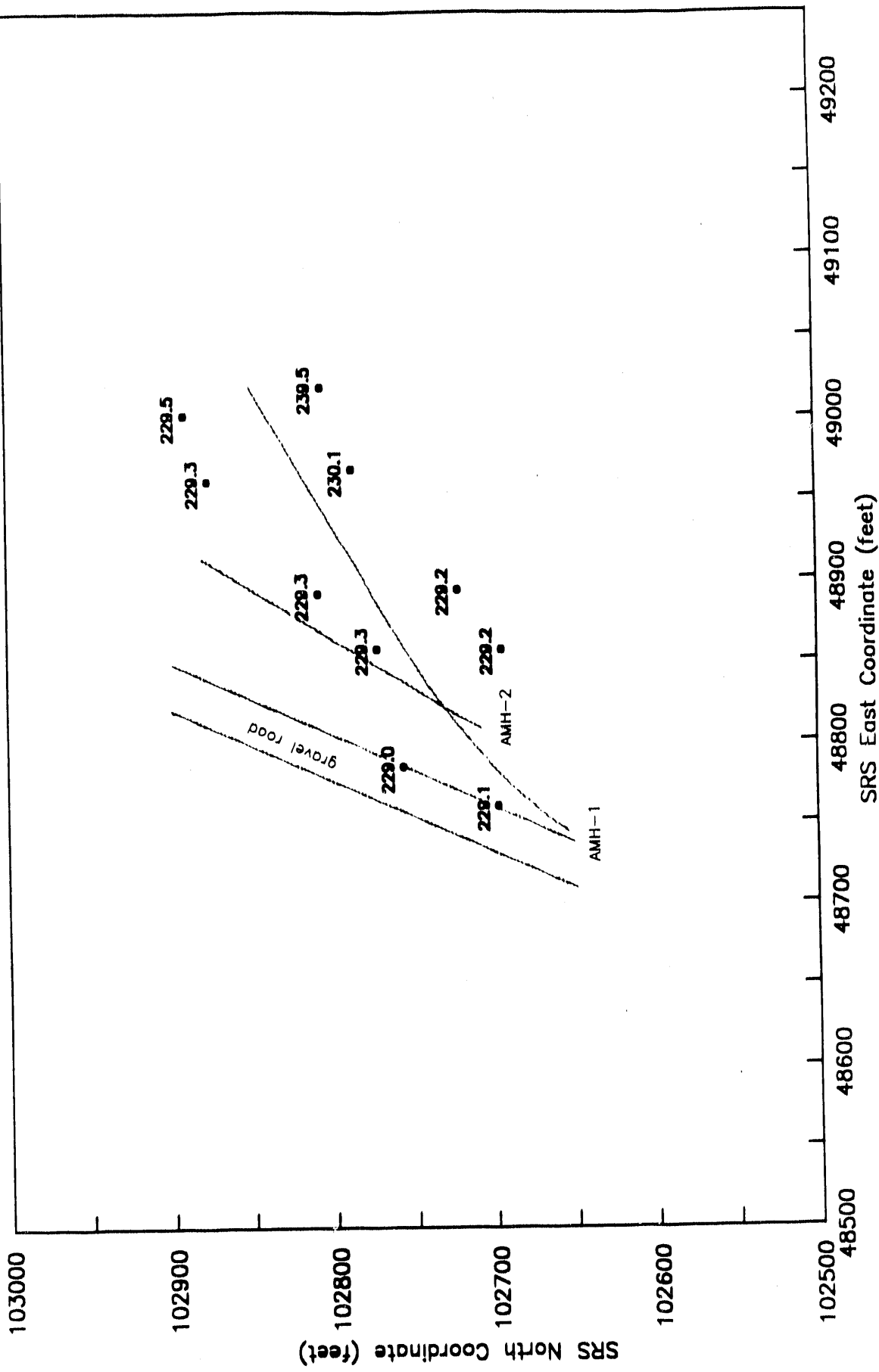


Figure 4.5. Potentiometric Map for the Semiconfined Zone at the Field Demonstration Site; elevations in feet above msl.

Pretest Potentiometric Surface – Semiconfined Zone

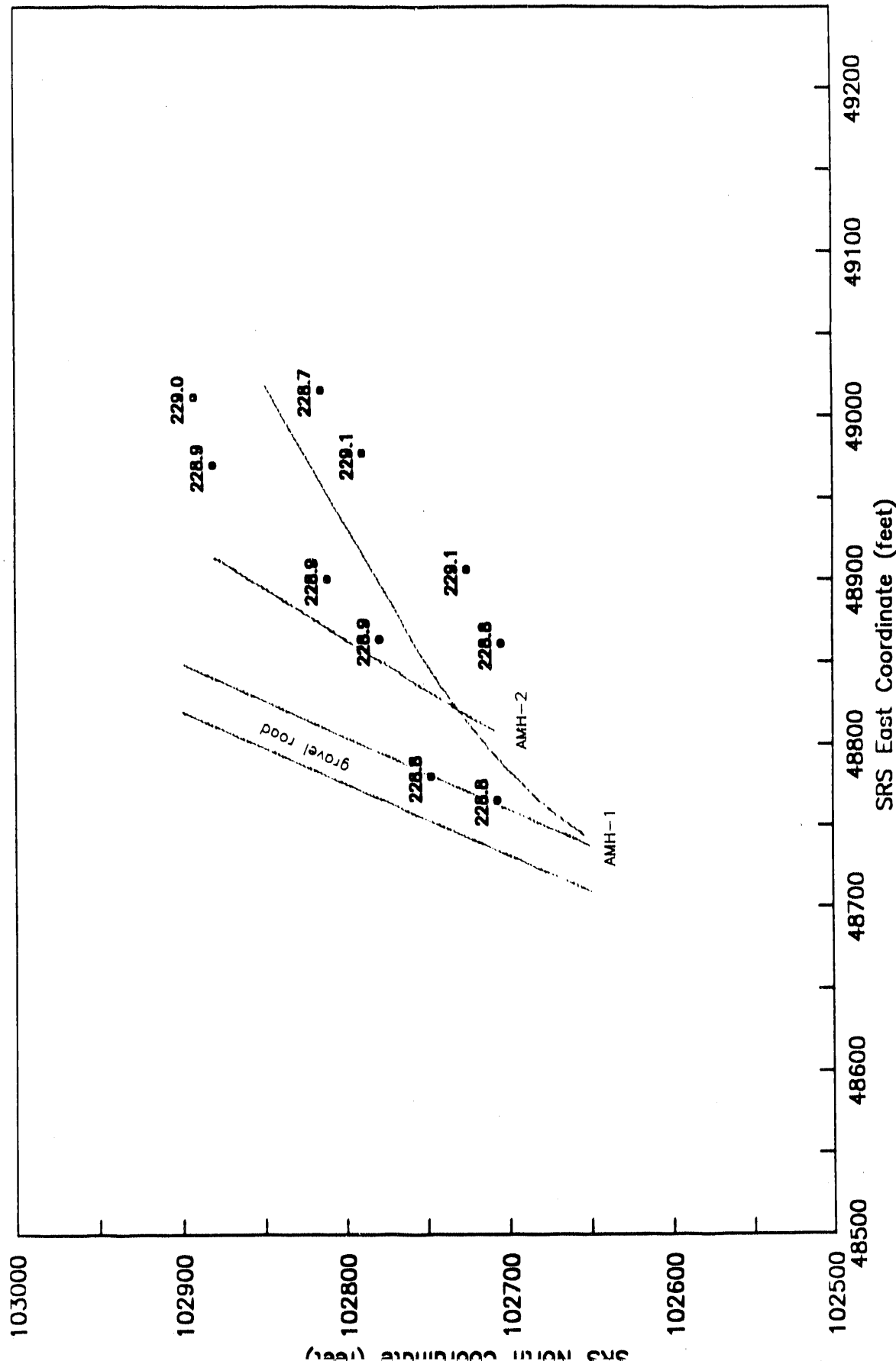
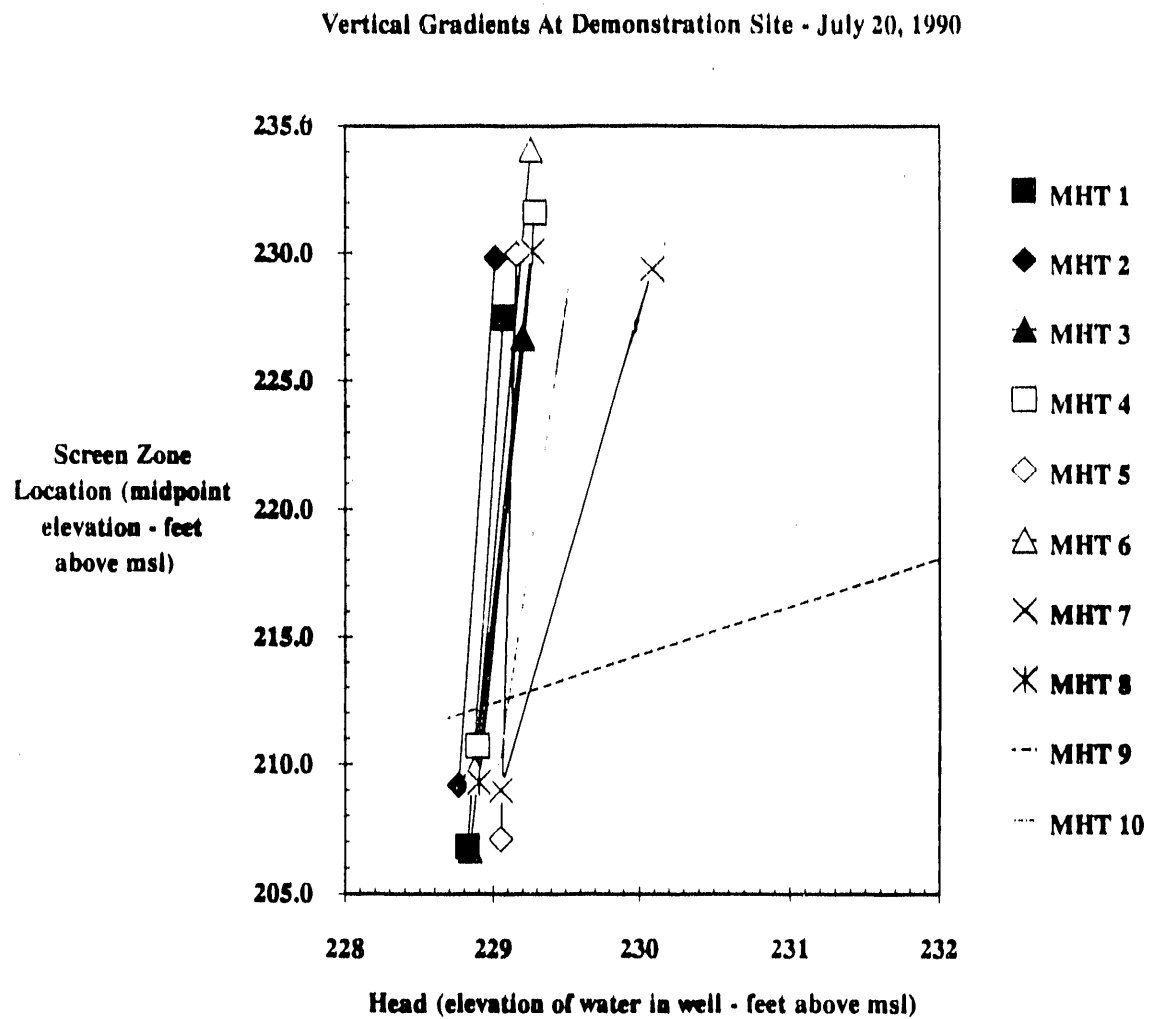


Figure 4.6. Vertical Gradients Measured at Well Clusters at the Field Demonstration Site.



5.0 Sampling

Water Sampling Techniques

Groundwater from Monitoring Wells

Water samples were collected at the beginning of the vapor extraction test. Water samples were collected using dedicated submersible pumps according to documented SRS well sampling protocols (DPSOP 254). Bulk water parameters including temperature, pH, dissolved oxygen (DO), conductivity, and oxidation-reduction potential (ORP) were measured using a Hydrolab. Samples were collected for microbiological studies in a bottle and VOC analysis in a headspace vial.

HydroPunch

The HydroPunch sampler is designed to collect groundwater samples at discrete depths within a single borehole without requiring the installation of a well. This provides information on the vertical distribution of contamination in the groundwater without having to install monitoring wells. This sampling tool can be used in conjunction with a conventional drilling rig with hollow stem augers or mud rotary drilling equipment. The sampler consists of a stainless steel drive point, a perforated section of stainless steel pipe covered by a screen, and a stainless steel and Teflon sample chamber. As the sampler is advanced, the sample intake pipe is shielded by housing. The sampler is attached to a soil sampling rod, advanced through the hollow stem auger or drill pipe, and pushed below the borehole into sediment relatively undisturbed by the drilling process. The sampler is pulled back about a foot in order to expose the perforated zone to the saturated zone and groundwater flows into the sampling chamber. Once the sample chamber is filled, the sampler is pulled toward the surface and the increase in hydrostatic pressure closes two Teflon check valves. The sample is transferred at the surface through a discharge tube into a sample container.

Samples were collected by HydroPunch adjacent to the well clusters at MHT2, MHT3, MHT4, MHT5, MHT7, MHT8, MHT9, and MHT10. Each sample was analyzed for VOC content and for baseline microbial characteristics if sufficient sample was available. The analytical results for these samples have been compared with samples collected at the same depth interval from adjacent wells and sediment cores.

Water samples were not collected at 5 foot intervals below the water table with the HydroPunch due to operational problems with the sampler. Practical problems encountered at the demonstration site in the use of the HydroPunch sampler included: (1) the sampler did not fill due to insufficient head (too close to water table), fine grained sediments or sampler not opening; (2) the sample was contaminated with drilling fluids (due to fluid pressure in the hole affecting the seating of the check valve). This problem was corrected by running a separate air line to the valve to keep it closed during sample retrieval and; (3) damage to the sampler due to the force required to advance it beyond the predrilled hole. In addition, field decontamination and operating procedures are relatively complicated and extensive for this device. Nonetheless, the detailed vertical contaminant information provided by the HydroPunch is an extremely valuable part of the characterization data base.

Sediment Sampling Techniques

For all borings done in the MHT and MHV well series, sediment samples were collected at five foot intervals and, in addition, at all significant lithologic changes in the core. Samples were collected using a modified syringe tube and plunger. This technique results in the collection of a consistent volume of sediment. Immediately after collection, the sediment sample was placed in a headspace vial. Five milliliters of solution, comprised of 10 grams of sodium sulfate and 0.3 milliliters of

phosphoric acid (0.15%) added to 200 milliliters of distilled water, was added to the vial. The vials were sealed with crimped aluminum rings over teflon-lined septa. Samples were placed in a cooler on ice. The samples were collected daily and refrigerated in the lab. Prior to sample analysis, the samples were weighed in order to determine the mass of the sample. Samples were then placed in the sonic dismembrator for fifteen minutes in order to disaggregate the sediment.

Core specimens for microbial analysis were obtained directly from the split spoon or barrel. Cores were sectioned into 3 inch lengths with sterile spatulas and the outermost layer (about 1/4 the diameter of the core) was scraped off using a sterile scoopula. Samples were collected approximately every 10 feet in conjunction with chemical sampling.

6.0 Analytical Techniques

Analysis of VOC in Sediment and Groundwater

VOC analyses were performed on a Hewlett-Packard 5890 Gas Chromatograph with an electron capture detector, an HP 19395A Headspace Sampler, an HP 3392A Networking Integrator, and a 60 m x 0.75 mm ID Supelco VOCOL wide bore capillary column coated with a 1.5 μ m film. The instrument was calibrated using samples spiked with standard solution. Within the headspace sampler, the teflon-lined vials are punctured, and the gases are released into the gas chromatograph. The gases are analyzed in the gas chromatograph, and the analysis is printed out.

Microbiological Analytical Techniques

Several methods were used to define the baseline microbiology of the site including: 1. Direct Counts (microscopy of stained sediments), 2. Plate Counts (enriched and low nutrient media), 3. Community Diversity (cultural identification, cataloging of isolates, nucleic acid analysis), 4. Phospholipid Fatty Acid Analysis (of selected sediment samples for community identification and physiological characterization), and 5. Qualitative and Quantitative Determinations of Functional Groups and Specific Populations (fluorescent antibodies, nucleic acid probes). The specific methods are described below.

Acridine Orange Direct Counts (AODC)

Samples were preserved in phosphate buffered formalin. Samples (1 to 3 grams) were extracted three times with a non-ionic homogenizing detergent to remove bacteria from the sediment particles. Homogenates were cleared by low speed centrifugation and the supernatants were pooled. Ten microliters of supernatant was spotted onto each well of a toxoplasmosis microscope slide, stained with 0.01% acridine orange, then rinsed with distilled water. The number of cells stained with acridine orange were counted by epifluorescence microscopy. The number of cells per sample was normalized by dividing by the dry weight of the sediment. Counts were reported as cells per gram.

Enumeration by Plate Count (Spread Plate)

Samples (1 to 3 grams) were weighed directly into 15 ml conical centrifuge tubes containing 9 ml of pyrophosphate buffer. Subsequent serial dilutions were made in phosphate buffered saline. 0.1 ml of each appropriate dilution was inoculated onto a corresponding plate of appropriate medium. For this study, 1% and full strength formulation of peptone trypticase yeast extract (PTYG) were used. A glass rake and turntable were used to spread the inoculum evenly over the entire surface of the agar. Plates were incubated at room temperature for at least two weeks prior to counting. Bacterial colonies were counted with the aid of low power magnification. Counts were normalized to sediment dry weights and reported as colony forming units (CFU) per gram.

Community Diversity

Every bacterial colony type was noted, counted, and cataloged for calculation of diversity indices (Shannon) and measurement of structural diversity. Representatives of these isolates were grown in pure culture and frozen for future biochemical studies and measurement of functional diversity.

Phospholipid Fatty Acid Analysis

(Note: All data analyses on phospholipid fatty acids were done under contract with Drs. Tom Phelps and David White, University of Tennessee, through Oak Ridge National Laboratory).

Ester-linked phospholipid fatty acids (PLFA) were extracted from sediment samples via inverse serial extraction, fractionated and methylated by microtechnique. Identifications were made by comparison of retention times to standards after extracting specific ions from a total ion chromatogram obtained with electron impact GC/MS. These techniques minimized the input of contaminants while maximizing sample input.

Fluorescent Antibody Analysis

Samples were prepared as for AODC described above. Samples fixed on slides were stained by incubation with fluorescien isothiocyanate labeled antibodies (specific for a TCE-degrading bacteria isolated from M area sediment) for 1 hour and then excess stain was washed away with buffer. The stained slides were then examined with a fluorescent microscope and the number of yellow/green fluorescing cells enumerated as with AODC. Fluorescent antibodies for several nitrogen transforming organisms are also being tested.

Nucleic Acid Analysis

(Note: All of the following nucleic acid analysis was done through a contract with Drs. Luis Jimenez and Gary Saylor, University of Tennessee, through Oak Ridge National Laboratory).

Total DNA was extracted from sediment samples by placing the sample into a solution of 2.5% Sodium Dodecyl Sulfate (SDS) in (0.1 M) sodium phosphate buffer, pH 8.0 for 1 hour to lyse the cells. After a 1 hour incubation at 70°C proteins and cells debris were separated from the DNA by the addition of 0.5 volume of sodium acetate or ammonium acetate. The sample was incubated then for 30 minutes at -20 °C. After incubation the mixture was centrifuged at 12,000 x g for 15 minutes. The supernatants were pooled and transferred to another container and 2 volumes of 95% ethanol were added, then DNA was precipitated overnight at room temperature. Samples were centrifuged at 12,000 x g for 30 minutes to recover the DNA. Buoyant density centrifugation in Cesium Chloride-Ethidium Bromide Gradients was performed as described elsewhere (Maniatis et al., 1987). DNA was extracted and purified from the gradients as described by Maniatis et al. (1987). Concentration of DNA and purity was determined by absorbance at 260 nm and 280 nm. If the ratio of 260/280 was lower than 1.8 the solution was purified by a cesium chloride-ethidium bromide gradient. DNA concentration per gram sediment was then calculated from the initial dry weight used.

Slot blots were used to further purify genomic fragments before hybridization with a TCE-degrading type I methanotroph (68-1) probe. The probe is DNA fragment that encodes a putative gamma subunit of methane monooxygenase. DNA hybridizations were carried out under stringent conditions. Similar probes, e. g., TOI-1 etc. are also being tested.

Total DNA is also being subjected to thermal melting point determinations via a melting point spectrophotometer and subsequent calculation of mol% G+C for diversity estimates.

7.0 Results

Groundwater

Groundwater from Wells

Analytical results for bulk parameters are given in Table 7.1. Measured pH values in several of the wells are high indicating contamination of the screen zone by grout. Many of the measured conductivity values are also high and may reflect the presence of relatively conductive contaminant phases from the drilling mud or the process sewer line in some of the wells.

Well water samples were analyzed for PCE and TCE at the beginning of the demonstration. The results are summarized in Table 7.2. Maps of TCE and PCE contamination in the water table and semi-confined aquifer are shown in Figures 7.1 through 7.4. In the MHT-C wells, initial concentrations ranged from a high of 1807 ppm TCE and 184 ppm PCE in MHT6C to a low of 108 ppm PCE and 20 ppm PCE in MHT9C. In the three water table wells that could be sampled, initial concentrations ranged from 1776 ppm TCE and 193 ppm PCE in MHT9D to 500 ppm TCE and 51 ppm PCE in MHT2D.

HydroPunch

Approximately 40 samples of water were collected using the HydroPunch sampler. Average analytical results from duplicate samples are tabulated in Table 7.3.

Sediments

Over 1000 sediment samples from the MHT and MHV cores were analyzed for TCE and PCE. Concentrations of PCE and TCE are plotted against depth for each of the MHT wells in Figures 7.5 through 7.24. Maximum values from each well are tabulated in Table 7.4. The highest value for TCE was measured in MHT6C at 103 feet and for PCE in MHV4 at 43 feet. Generally, the highest levels of contamination were found slightly above and within the clay rich zones. In general, the most contaminated zone in most of the borings was found slightly above, at, or less than 15 feet below the top of tan clay zone (elevation 270 feet). Analytical results for the MHT and MHV sediments are reported in Appendix II.

3D Modeling

The results from chemical analysis of the MHV and MHT cores were entered into a database and several 3-dimensional representations of the data were prepared using a Silicon Graphics Workstation with Dynamic Graphics Software. Several approaches were used in modeling the data to produce the optimal representation of the site.

Six models of the TCE data from the MHV and MHT wells were prepared for this report. All models were gridded with a 25 by 2.5 by 40 grid resulting in a 17 ft by 13 ft by 5 ft spacing between the 25,000 grid nodes. The top of the grid was bounded by the topographic land surface, and the bottom of the grid was bounded by the top of the "green clay". The edges of the model were clipped by a polygonal boundary file that extends approximately ten feet beyond the exterior data points in order to reduce excess extrapolation of the data. Measured values in the data set ranged from 0 to 16 ppm. In order to best represent the range of contamination, concentrations were contoured with the following modified log scale: 0.0025, 0.005, 0.01, 0.025, 0.05, 0.1, 0.25, 0.5, 1, 2.5, 5, 10, and 25 ppm.

Three models were prepared in linear space each with different Z factors (Figures 7.25, 7.26, 7.27). The Dynamic Graphics software allows the user to choose a Z-influence factor prior to gridding. The Z-influence factor controls the vertical influence versus the horizontal during gridding. A factor of one uses the normal 3-D minimum tension gridding method, i.e., data in the Z-direction influence grid node calculations as much as data in the X and Y direction. A value of zero gives a 2-D minimum tension gridding on each X/Y plane, i.e. data in the Z-direction has almost no influence over data in each X/Y plane. This is important as the density of environmental data is much greater in the vertical direction than in the horizontal direction. Models were prepared with a Z factor of 1, 0.1, and .001 (Figures 7.25-7.27). As the Z value decreases, the lamination or lateral continuity of the layers of the model increases.

Additionally, several models were prepared using the log values of the contaminant data (Figures 7.28-7.30). After the three dimensional grid was prepared, the antilog is then taken of the grid nodes. Only the grid values are transformed, i.e., the location of the isoconcentration surfaces does not change. The advantage of this technique is that isoconcentration levels are calculated over an order of magnitude rather over several orders of magnitudes. This method produces more finely layered isoconcentration surfaces.

The results are presented in Figures 7.25 to 7.30. Each figure is a representation of the pretest core data with some of the lower isoconcentration shells removed. Figures 7.25 to 7.29 show the distribution of TCE greater than 2.5 ppm. The distribution of TCE is clearly heterogeneous and concentrated below 300 feet elevation. Figures 7.25 and 7.27 have the same orientation and the differences between the models result from changes in the Z factor. The individual zones of contamination are increasingly laterally continuous with decreasing Z factor and the models with low Z factors seem more geologically reasonable. The observed layering of the contamination is clearly confined to zones that correlate with the location of the clay zones identified during drilling. Contamination is present in a layer at 325' elevation, a layer at 300' elevation, and a thick zone above, at, and below 300 foot elevation. The model produced using a Z-factor of essentially zero (0.001) is preferred over models produced with higher Z-factor as the stratified nature of the contamination is more clearly presented.

Figures 7.28 and 7.29 show the results of gridding the log of the contaminant values and taking the antilog of the grid nodes. Only the grid values are transformed, i.e., the location of the isoconcentration surfaces does not change. This technique result in an increase in the lateral continuity of the isoconcentration surfaces. Figures 7.28 and 7.29 show the effects of a decrease in Z-value from 0.1 to 0.001 on the transformed grids.

For this site, the most appropriate model is shown in Figure 7.29 and 7.30. The distribution of contaminants at the Integrated Demonstration Site is controlled by the stratification of the clay layers in the Coastal Plain sediments. These figures clearly show that the 325 foot clay and the 300 foot clay control the distribution of contamination along the western side of the site and that the 'tan clay' zone (below 300 feet elevation) concentrates most of the contamination in the deeper part of the site.

Comparison of Water and Sediment Data

The detailed depth sampling of sediment core and vertical profiles of water concentrations provided by the HydroPunch sampler provide unique data. Comparison of HydroPunch to bulk sediment samples and HydroPunch data to wells provides data on the heterogeneity of the site and will assist in interpretation of the site characterization, in situ air stripping demonstration monitoring, and other related studies.

Figure 7.31 is a plot of HydroPunch TCE concentration vs. bulk sediment TCE concentration. As expected, as the total TCE concentration increases (as determined by the sediment plug sample), the

TCE concentration in the interstitial water (as measured by the HydroPunch) increases. Note that the samples from sediments with less than 30% clay are skewed slightly toward the HydroPunch axis on the graph relative to samples from sediments that are more clay rich; this skew suggests that VOC loss during sediment sampling may be more significant for the sandier samples.

These data can also be used to calculate distribution coefficients (K_d values) for the sample pairs (assuming a bulk density of approximately 1.6 g/cm^3 and a porosity of approximately 0.3). The resulting data are shown on Figure 7.32. A K_d of zero implies that all of the contaminant is in the water (i.e., that there is no affinity to the solid). A K_d greater than 0 indicates that some fraction of the contaminant is associated with the solid. Finally, a field measured K_d less than 0 indicates that VOC has been lost from the bulk sediment analysis (because the amount of contaminant measured in the interstitial water is greater than the sum of the water plus sediment from the plug sampling). It is clear from Figure 7.32 that significant quantities of VOC are lost from the bulk sediment samples; several of the field estimated K_d values are below zero. Negative K_d values are observed for both lithology classes. Similar to Figure 7.31, however, Figure 7.32 suggests that the loss mechanisms are more acute for the sandier sediments than for the clayier sediments. Approximately 70% of the sandy samples have a field estimated K_d below zero while approximately 50% of the clayey samples have a field estimated K_d below zero.

Sims et al. (1991) demonstrate that the sampling method employed for the bulk sediment analysis (plug sampling of the core within a few seconds of collection followed by sealing in the headspace vial) is superior to typical methods of sample collection/analysis. In this study, the headspace method was compared to standard methods carefully performed by an independent laboratory. Most of the volatile contaminants were lost from the samples that were collected and analyzed using the "standard" methods while the headspace method provided representative analyses on all but the highest samples (since the samples are sealed in final form in the field, they can not be diluted). The headspace sampling methods employed during the pretest characterization of the field demonstration site eliminate most of the potential for loss of constituent from the core once it is brought to the surface and sampled. This suggests that the loss of VOC may be occurring in the hole (by drainage during retrieval or by invasion of uncontaminated drilling fluid). Both of these mechanisms would result in relatively higher losses from more permeable sand zones. Fluorescent dye studies at the study site indicated some penetration of the core by drilling fluid. Note that the loss mechanisms listed above are common to site characterizations across the country; the data suggest that inventories estimated based only on core samples from saturated sediments may be too low. If the true K_d value for all samples was 0.1, the average loss of VOC from the samples at the field demonstration site would have been approximately 50%. Less robust sampling and analysis techniques that are typically used would cause even higher losses.

Figure 7.33 is an example plot showing the depth discrete HydroPunch VOC concentrations compared with the well screened at approximately the same location. The data for this well, MHT 4, is typical of all of the wells at the field demonstration site. The HydroPunch data indicate significant vertical heterogeneity in the VOC concentration with the highest concentrations at the water table and below the green clay. The HydroPunch data from the elevations where the nearby well was screened are almost identical to the composite sample that is produced by the 5 foot well screen. The contamination below the green clay has a different ratio of TCE to PCE (approximately 100% TCE) suggesting that it may be flowing beneath the demonstration site from a site that is upgradient (in the confined aquifer). The data indicate that the HydroPunch sampler (as modified to work with mud rotary drilling) is collecting good quality water samples that provide a valuable information about the site.

Microbiology

Bacterial counts were determined on 117 vadose zone samples (10 wells); 36 saturated sediments (8 wells); 30 HydroPunch samples (6 wells). In addition 12 samples of drilling muds were analyzed to assess potential for contamination of saturated zone samples.

Tables 7.5 through 7.14 show results of both the direct and plate counts (number of bacteria or colony forming units per gram of dry soil, respectively) from wells MHT 1C through 10C. In general, direct counts were higher in the near-surface depths and the capillary fringe. Fluctuations in the vadose zone count appeared to be attributable to changes in lithology or degree of sediment saturation; i.e., changes in the clay and sand content, or in water content of the sediment. (As an example, see Table 7.7, MHT 3C, where at a depth of 47 feet, there is an approximate doubling of the count relative to the surrounding depths.) Otherwise, direct counts remained relatively constant throughout the vadose zone. This is depicted graphically in Figure 7.34. Direct counts were 4 to 6 orders of magnitude higher than plate counts. This is typical of low nutrient environment when the microflora is under stress and thus injured so that they are surviving but do not go readily on nutrient media.

Overall, plate counts were relatively low, especially in the vadose zone. In general, plate counts were higher in near-surface depths and in the saturated zone. Fluctuations in the vadose zone counts appeared to be attributable to changes in lithology or degree of saturation, i.e. higher counts are associated with sandy or moist sediments, while clayey or dry sediments have low densities of bacteria. This type of change can be seen in Table 7.5, MHT 1C, where increases are seen at 25 to 37 feet and 83 and 95 feet (1% PTYG). No apparent correlation was seen among plate counts with either TCE or PCE concentrations. The results for MHT 2C and 8C are portrayed graphically in Figures 7.35 and 7.36, respectively. For MHT 2C, changes can be seen at 25 and 75 feet. The increased counts at near surface depths and in the saturated zone are obvious. The increased count at 105 feet may also be the result of increased saturation. Similar changes were apparent in MHT 8C (Figure 7.36). Figure 7.37 is a composite graph depicting the average plate counts for all wells (1% PTYG). Unlike the direct counts, which remained relatively high and constant throughout the vadose zone, plate counts showed order-of-magnitude fluctuations and relatively low counts in the vadose zone. One possible explanation is that heterogeneity of nutrient availability in the vadose zone caused heterogeneity in microbial community stress as suggested by the difference in ability to grow.

Extremely high counts were observed in the drilling fluids (see Tables 7.6, 7.8, 7.12, and 7.14). These counts were orders of magnitude higher than anything seen in the sediments. Figure 7.38 graphically illustrates differences seen between plate counts of sediments and drilling fluids collected at similar depths.

The ratio of plate counts to direct counts can give a measure of the viability of the organisms for a particular sample. A high ratio is proportional to high organism viability. Data tabulated in this form are shown in Tables 7.15 through 7.19 for wells MHT 2C, 3C, 5C, 7C, and 9C. Viability as measured by the ratio of plate to direct count was quite low in the vadose zone. Viability was much higher in the near-surface depths and the saturated zone. A comparison of the direct and plate counts is shown in Figure 7.39. Another way of looking at these data is shown in Figure 7.40. This figure shows the ratio of direct to plate counts. (Data are plotted as the log of the ratio of the AODC to CFU.) This is a measure of the sensitivity of AODC versus culturing. The data show orders-of-magnitude higher sensitivity of direct counting when compared to culturing for this system. This is most pronounced in the vadose zone, less so in the near-surface depths and the water table.

All bacterial colonies present on both media formulations were described and cataloged for diversity studies. These descriptions will be coded and analyzed statistically to determine if diversity differences exist between depths within a well, at the same depths between wells, and at differing concentrations of TCE and PCE. Over 500 isolates from both media formulations were preserved. These isolates can be retrieved at a later date and tested for novel or potentially useful metabolic capabilities.

Figures 7.41 and 7.42 illustrate the number of different colony types cultured from 1% and full-strength PTYG, respectively, in MHT 3C. Generally, the number of different colony types isolated in near-surface depths and in the saturated zone was higher than the number of colony types isolated from the vadose zone. Regardless of depth, higher numbers of colony types were isolated from the low nutrient formulation than from the high nutrient formulation (see Figure 7.43). In fact, at some depths, only 1% PTYG was capable of enumerating the bacterial community. This observation further suggests that the ambient microbial community is adapted to low nutrient stress and have been adapted to low nutrient conditions for so long that high nutrient conditions have become toxic.

Figures 7.44 and 7.45 illustrate the diversity of the subsurface microbial community of MHT 3C (1% and full-strength PTYG respectively). Each bar represents one "species" (colony type); its height represents its relative contribution to the community for that depth. Communities which show domination by one or two species are considered low diversity systems. Low diversity systems are typical of highly stressed or limited environments. High diversity communities are characterized by many rare species (species that comprise a small percentage of the total number of individuals), and a few common species (species that comprise a large percentage of the total number of individuals). The communities of the near-surface, capillary fringe, and water table-zones appeared to be high diversity communities (compared to the low diversity communities of the vadose zone).

The direct phospholipid fatty acid (PLFA) analysis verified that biomass in the sediment was usually quite low - usually < 1.0 picamole/gdw, except at the 5 ft zone in MHT-4C and MHT-7C (Tables 7.20 to 7.22). PLFA concentrations of 1.0 pmole/gdw are equivalent to 3.5×10^5 cells/gdw, this is remarkably similar to the direct count estimates (AODC) from the same samples. These biomass values are typical of vadose zones. The surface soils have 10 Me 16:0 and 10 Me 18:0 which are biomarkers for actinomycetes (10 Me 18:0 is tuberculostearic acid). Where microbes were detected in the subsurface there are high proportions of cyclopropane fatty acids (these accumulate when bacteria are in stationary growth phase) and cis/trans monoenoic which correlates with ultramicrocell formation and starvation if it is > 0.10. The trans/cis ratios increase when organisms are starved or subjected to some form of environmental stress as seen in Tables 7.20 to 7.22.

Of the nucleic acid samples done to date 7 of 20 samples were positive for the MMO1 probe (Table 7.23). This was further verified by cultural enrichment for methanotrophs for positive probe analyses. Plasmid frequency seemed to increase slightly with depth. Total DNA concentration ranged from 0.05 to 3.73 μg DNA/gdw. The total DNA mol% G+C analysis for diversity is not complete.

Fluorescent antibody analysis has so far indicated that TCE-degraders are present in most of the sites. Nitrogen transforming bacteria are also present in most of the sites examined so far. This analysis is incomplete at this time.

Table 7.1 Bulk Parameters of Groundwater

	Date	Temperature	pH	DO	Conductivity	ORP
		degrees C		mg/l	μmhos/cm	volts
MHT-1C	8/5/90	18.60	5.28	6.15	38	0.570
MHT-2C	8/5/90	18.71	5.23	7.67	38	0.576
MHT-2D	8/5/90	20.83	5.68	6.43	50	0.546
MHT-3C	8/22/90	20.41	6.46	4.06	192	0.424
MHT-4C	8/22/90	20.41	6.23	5.47	155	0.424
MHT-5C	8/6/90	19.06	5.57	6.63	43	0.526
MHT-5D	8/22/90	20.00	6.65	2.68	230	0.446
MHT-6C	8/6/90	20.14	7.65	5.72	86	0.353
MHT-7C	8/22/90	19.70	9.26	5.40	211	0.252
MHT-8C	8/22/90	19.90	6.47	2.70	134	0.389
MHT-9C	8/22/90	20.54	5.80	4.08	93	0.427
MHT-9D	8/6/90	24.17	6.34	6.98	20	0.505
MHT-10C	8/22/90	20.96	6.53	2.93	104	0.382

Table 7.2 TCE and PCE Results for Groundwater in the MHT Wells

Well I.D.	TCE	PCE
MHT-1C	543	128
MHT-2C	858	84.5
MHT-2D	499.5	51
MHT-3C	482.5	73
MHT-4C	1576	75.5
MHT-5C	787	125
MHT-5D	768.5	63.5
MHT-6C	1807	184
MHT-7C	114	65
MHT-8C	395	37.5
MHT-9C	108	19.5
MHT-9D	1776	193
MHT-10C	427	49.5

Table 7.3 Average of Duplicate Analysis of TCE and PCE Results from HydroPunch Samples

Borehole	Depth (feet)	TCE (ug/L)	PCE (ug/L)	Elevation (feet)
MHP2B	143	473	35	221
MHP2B	160	1055	144	204
MHP2B	188	13080	<1	176
MHP2B	197	1492	<1	167
MHP 3	147	2829	26	215
MHP 3	151	862	22	211
MHP 3	156	484	68	206
MHP 3	167	589	87	195
MHP 3	170	219	37	192
MHP 3	185	13050	2	177
MHP3B	193	10150	<1	169
MHP 4	145	7899	204	222
MHP 4	154	4810	159	214
MHP 4	159	450	53	208
MHP 4	163	1033	174	204
MHP 4	169	438	55	198
MHP 4	172	150	83	195
MHP 4	176	1931	27	191
MHP 5	144	666	159	220
MHP 5	148	544	89	216
MHP 5	161	1660	201	203
MHP 7	142	64	5	226
MHP 7	150	3950	194	218
MHP 7	156	100	127	212
MHP 7	162	168	239	206
MHP 7	172	134	55	196
MHP 7	179	3130	282	189
MHP 7	195	7685	2	173
MHP 8	155	584	96	214
MHP 8	159	564	8	210
MHP 8	171	628	40	198
MHP 9	143	173	22	225
MHP 9	148	622	118	219
MHP 9	150	350	50	217
MHP 9	154	547	124	214
MHP 9 B	145	52	11	222
MHP 9 B	152	60	103	215
MHP 9 B	188	5925	1	179
MHP 9 B	190	5035	1	177
MHP 10	148	481	102	220
MHP 10	173	46	2	195

Table 7.4 Maximum Values of TCE and PCE Measured in MHT and MHV Sediment Samples

WELL I.D.	TCE ($\mu\text{G/G}$)	PCE ($\mu\text{G/G}$)
MHT1C	11.46	3.46
MHT2C	11.22	7.03
MHT3C	8.02	0.66
MHT4C	11.96	4.30
MHT5C	11.65	0.99
MHT6C	16.32	2.97
MHT7C	1.26	0.17
MHT8C	3.02	0.11
MHT9C	1.53	0.093
MHT10C	2.77	0.034
MHV1	14.46	4.93
MHV2	9.98	2.20
MHV3	1.28	0.64
MHV4	14.21	8.75
MHV5	14.34	0.73

Table 7.5 Density of Bacteria in Sediment from MHT-1C

WELL #	DEPTH (ft)	PTYG ¹	1% PTYG ²	AODC ³	TCE ⁴	PCE ⁴
MHT-1C	10	3.77	2.25	6.38	<0.002	0.004
MHT-1C	17	3.39	<1.5	7.06	0.023	0.058
MHT-1C	25	1.87	2.47	ND ⁵	0.312	0.565
MHT-1C	35	2.52	3.07	ND	1.082	1.434
MHT-1C	37	2.79	2.97	ND	1.496	3.461
MHT-1C	43	<1.5	<1.5	ND	0.139	0.375
MHT-1C	52	<1.5	<1.5	ND	1.033	0.819
MHT-1C	62	<1.5	<1.5	ND	<0.002	0.008
MHT-1C	73	<1.5	<1.5	6.98	0.109	0.216
MHT-1C	83	1.83	2.07	6.94	<0.002	0.159
MHT-1C	95	<1.5	2.25	5.95	0.557	0.197
MHT-1C	105	<1.5	<1.5	6.18	<0.002	<0.002

¹ Log₁₀ colony forming units on peptone trypticase yeast glucose per gram dry soil.

² Log₁₀ colony forming units on 1% peptone trypticase yeast glucose per gram dry soil.

³ Acridine Orange Direct Count (log₁₀ cells per gram dry soil).

⁴ Trichloroethylene and tetrachloroethylene concentrations in µg/g soil.

⁵ Not Determined.

Table 7.6 Density of Bacteria in Sediment from MHT-2C

WELL #	DEPTH (ft)	PTYG ¹	1% PTYG ²	AODC ³	TCE ⁴	PCE ⁴
MHT-2C	5	4.41	4.52	7.17	<0.002	0.010
MHT-2C	15	<1.5	<1.5	7.50	0.122	0.432
MHT-2C	25	2.09	2.63	7.23	0.050	0.076
MHT-2C	35	<1.5	<1.5	7.47	4.948	7.028
MHT-2C	45	<1.5	<1.5	6.73	0.186	0.376
MHT-2C	55	<1.5	<1.5	6.68	1.838	2.340
MHT-2C	75	<1.5	2.03	6.60	0.008	0.005
MHT-2C	85	<1.5	<1.5	6.58	0.014	0.022
MHT-2C	95	<1.5	<1.5	7.01	5.718	0.819
MHT-2C	105	<1.5	2.12	6.62	0.229	<0.002
MHT-2C	115	<1.5	<1.5	6.82	0.014	0.003
MHT-2C	125	2.05	2.34	7.32	0.063	0.011
MHT-2C	135	3.07	2.91	7.06	0.493	0.177
MHT-2C	145	4.49	4.42	7.03	0.282	0.065
MHT-2C	158 (ML) ⁶	5.81	6.17	ND ⁵	0.016	<0.002
MHT-2C	168 (ML)	4.34	4.52	ND	0.057	0.011
MHT-2C	178 (ML)	5.46	6.2	ND	0.024	<0.002
MHT-2C	187 (ML)	3.82	4.01	ND	7.473	<0.002
MHT-2C	146 (DF) ⁷	7.18	7.77	ND	ND	ND
MHT-2C	191 (DF)	6.67	7.08	ND	ND	ND

¹ Log₁₀ colony forming units on peptone trypticase yeast glucose per gram dry soil.

² Log₁₀ colony forming units on 1% peptone trypticase yeast glucose per gram dry soil.

³ Acridine Orange Direct Count (log₁₀ cells per gram dry soil).

⁴ Trichloroethylene and tetrachloroethylene concentrations in $\mu\text{g/g}$ soil.

⁵ Not Determined.

⁶ Collected by mud rotoring, with lexan core liner.

⁷ Drilling Fluids.

Table 7.7 Density of Bacteria in Sediment from MHT-3C

WELL #	DEPTH (ft)	PTYG ¹	1% PTYG ²	AODC ³	TCE ⁴	PCE ⁴
MHT-3C	3	5.27	5.8	7.74	<0.002	<0.002
MHT-3C	7	3.98	3.59	7.26	<0.002	<0.002
MHT-3C	15	1.82	<1.5	7.20	0.007	0.014
MHT-3C	25	1.85	<1.5	6.74	0.027	0.068
MHT-3C	35	<1.5	<1.5	6.97	0.013	0.044
MHT-3C	47	<1.5	2.38	6.32	<0.002	0.002
MHT-3C	57	2.48	<1.5	6.06	0.085	0.097
MHT-3C	65	2.69	1.95	6.07	0.217	0.347
MHT-3C	73	2.28	2.86	6.44	<0.002	<0.002
MHT-3C	85	3.31	3.52	6.45	0.019	0.027
MHT-3C	105	<1.5	2.07	7.55	8.021	0.656
MHT-3C	115	3.54	3.58	7.18	0.793	0.075

¹ Log₁₀ colony forming units on peptone trypticase yeast glucose per gram dry soil.

² Log₁₀ colony forming units on 1% peptone trypticase yeast glucose per gram dry soil.

³ Acridine Orange Direct Count (log₁₀ cells per gram dry soil).

⁴ Trichloroethylene and tetrachloroethylene concentrations in $\mu\text{g/g}$ soil.

Table 7.8 Density of Bacteria in Sediment from MHT-4C

WELL #	DEPTH (ft)	PTYG ¹	1% PTYG ²	AODC ³	TCE ⁴	PCE ⁴
MHT-4C	5	5.09	5.14	ND ⁵	<0.002	<0.002
MHT-4C	15	<1.5	<1.5	ND	<0.002	<0.002
MHT-4C	25	1.88	<1.5	ND	<0.002	0.005
MHT-4C	35	<1.5	<1.5	ND	0.004	0.010
MHT-4C	55	<1.5	<1.5	ND	0.083	0.083
MHT-4C	65	1.87	2.86	ND	0.730	0.622
MHT-4C	75	<1.5	2.02	ND	<0.002	<0.002
MHT-4C	87	1.92	<1.5	ND	<0.002	<0.002
MHT-4C	95	<1.5	<1.5	ND	11.964	4.303
MHT-4C	105	<1.5	<1.5	ND	8.202	1.295
MHT-4C	115	2.28	2.37	ND	3.048	0.911
MHT-4C	125	2.3	2.38	ND	0.911	0.094
MHT-4C	138	2.61	<1.5	ND	0.402	0.027
MHT-4C	145	<1.5	<1.5	ND	0.971	0.027
MHT-4C	152 (ML) ⁶	3.25	3.51	ND	1.288	0.037
MHT-4C	162 (ML)	5.34	5.83	ND	0.013	0.003
MHT-4C	171 (ML)	3.27	3.37	ND	0.029	0.025
MHT-4C	181 (ML)	5.86	6.15	ND	0.143	0.002
MHT-4C	190 (ML)	4.19	4.47	ND	7.812	<0.002
MHT-4C	148 (DF) ⁷	7.12	7.28	ND	ND	ND
MHT-4C	191 (DF)	6.98	7.44	ND	ND	ND

¹ Log₁₀ colony forming units on peptone trypticase yeast glucose per gram dry soil.

² Log₁₀ colony forming units on 1% peptone trypticase yeast glucose per gram dry soil.

³ Acridine Orange Direct Count (log₁₀ cells per gram dry soil).

⁴ Trichloroethylene and tetrachloroethylene concentrations in $\mu\text{g/g}$ soil.

⁵ Not Determined.

⁶ Collected by mud rotoring, with lexan core liner.

⁷ Drilling Fluids.

Table 7.9 Density of Bacteria in Sediment from MHT-5C

WELL #	DEPTH (ft)	PTYG ¹	1% PTYG ²	AODC ³	TCE ⁴	PCE ⁴
MHT-5C	5	5.26	5.62	8.05	<0.002	<0.002
MHT-5C	15	3.23	3.51	7.38	<0.002	<0.002
MHT-5C	25	<1.5	<1.5	6.95	<0.002	<0.002
MHT-5C	45	1.93	<1.5	7.30	0.022	0.038
MHT-5C	55	2.03	<1.5	6.93	<0.086	0.091
MHT-5C	65	2.29	<1.5	7.10	0.194	0.324
MHT-5C	75	1.86	2.46	7.53	<0.002	<0.002
MHT-5C	85	2.53	<1.5	7.78	0.028	0.020
MHT-5C	93	3.01	2.41	7.72	1.081	0.521
MHT-5C	101	<1.5	<1.5	6.40	0.140	0.133
MHT-5C	117	2.62	2.96	8.02	5.775	0.985
MHT-5C	126 (MS) ⁵	5.3	5.22	7.09	1.002	0.063
MHT-5C	138 (MS)	5.16	5.33	6.77	0.025	0.002
MHT-5C	162 (MS)	4.13	4.35	7.79	0.058	0.007
MHT-5C	187 (MS)	5.55	5.74	8.06	3.634	<0.002

¹ Log₁₀ colony forming units on peptone trypticase yeast glucose per gram dry soil.

² Log₁₀ colony forming units on 1% peptone trypticase yeast glucose per gram dry soil.

³ Acridine Orange Direct Count (log₁₀ cells per gram dry soil).

⁴ Trichloroethylene and tetrachloroethylene concentrations in $\mu\text{g/g}$ soil.

⁵ Collected by mud rotoring, with 2 inch split spoon.

Table 7.10 Density of Bacteria in Sediment from MHT-6C

WELL #	DEPTH (ft)	PTYG ¹	1% PTYG ²	AODC ³	TCE ⁴	PCE ⁴
MHT-6C	5	4.17	4.53	ND ⁵	<0.002	<0.002
MHT-6C	15	4.05	4.39	ND	<0.002	<0.002
MHT-6C	25	<1.5	<1.5	ND	<0.002	<0.002
MHT-6C	36	2.59	<1.5	ND	<0.002	<0.002
MHT-6C	45	<1.5	<1.5	ND	0.006	0.018
MHT-6C	55	<1.5	<1.5	ND	0.010	0.015
MHT-6C	65	2.04	<1.5	7.20	0.028	0.025
MHT-6C	75	<1.5	<1.5	ND	0.038	0.009
MHT-6C	85	1.80	<1.5	7.08	0.010	<0.002
MHT-6C	95	2.67	<1.5	6.82	<0.002	<0.002
MHT-6C	115	2.12	<1.5	7.03	5.121	0.155
MHT-6C	125	3.71	3.21	ND	0.215	0.005
MHT-6C	137	2.18	1.88	6.86	0.610	0.009
MHT-6C	141	3.11	3.04	ND	0.156	0.007
MHT-6C	145	3.97	4.24	ND	0.386	0.004
MHT-6C	158 (ML) ⁶	5.99	6.08	ND	0.170	0.007
MHT-6C	165 (ML)	6.11	6.39	ND	<0.002	<0.002
MHT-6C	175 (ML)	4.05	4.23	6.88	0.027	0.010
MHT-6C	185 (ML)	6.06	6.22	ND	<0.002	<0.002
MHT-6C	190 (ML)	6.03	6.26	ND	ND	ND

¹ Log₁₀ colony forming units on peptone trypticase yeast glucose per gram dry soil.

² Log₁₀ colony forming units on 1% peptone trypticase yeast glucose per gram dry soil.

³ Acridine Orange Direct Count (log₁₀ cells per gram dry soil).

⁴ Trichloroethylene and tetrachloroethylene concentrations in $\mu\text{g/g}$ soil.

⁵ Not Determined.

⁶ Collected by mud rotoring, with lexan core liner.

Table 7.11 Density of Bacteria in Sediment from MHT-7C

WELL #	DEPTH (ft)	PTYG ¹	1% PTYG ²	AODC ³	TCE ⁴	PCE ⁴
MHT-7C	5	5.21	5.84	8.78	<0.002	<0.002
MHT-7C	15	3.68	4.29	8.36	<0.002	<0.002
MHT-7C	25	2.24	<1.5	8.17	<0.002	<0.002
MHT-7C	35	2.82	2.78	7.85	<0.002	<0.002
MHT-7C	45	3.48	3.91	7.94	<0.002	<0.002
MHT-7C	71	<1.5	<1.5	6.76	0.017	0.011
MHT-7C	85	3.25	3.20	7.13	<0.002	<0.002
MHT-7C	95	<1.5	<1.5	7.90	0.992	0.172
MHT-7C	105	<1.5	<1.5	8.04	0.204	<0.002
MHT-7C	115	2.63	3.39	8.29	0.208	0.012
MHT-7C	143 (MS) ⁵	>6.5	5.68	7.71	0.004	<0.002
MHT-7C	155 (MS)	5.45	5.94	7.76	0.006	<0.002
MHT-7C	179 (MS)	4.56	5.28	7.42	1.260	<0.002
MHT-7C	191 (MS)	5.58	6.14	9.09	0.004	<0.002

¹ Log₁₀ colony forming units on peptone trypticase yeast glucose per gram dry soil.

² Log₁₀ colony forming units on 1% peptone trypticase yeast glucose per gram dry soil.

³ Acridine Orange Direct Count (log₁₀ cells per gram dry soil).

⁴ Trichloroethylene and tetrachloroethylene concentrations in $\mu\text{g/g}$ soil.

⁵ Collected by mud rotoring, with lexan core liner.

Table 7.12 Density of Bacteria in Sediment from MHT-8C

WELL #	DEPTH (ft)	PTYG ¹	1% PTYG ²	AODC ³	TCE ⁴	PCE ⁴
MHT-8C	5	4.76	4.99	7.80	<0.002	<0.002
MHT-8C	15	2.62	3.35	6.54	<0.002	<0.002
MHT-8C	25	2.16	<1.5	7.29	<0.002	<0.002
MHT-8C	35	2.69	3.17	7.60	<0.002	<0.002
MHT-8C	65	2.09	<1.5	7.23	0.010	<0.002
MHT-8C	75	<1.5	<1.5	7.08	0.633	0.064
MHT-8C	85	<1.5	<1.5	7.18	0.271	0.022
MHT-8C	95	1.98	1.98	6.72	0.101	0.006
MHT-8C	105	<1.5	2.13	7.54	<0.002	<0.002
MHT-8C	113	2.36	1.97	7.93	1.250	0.004
MHT-8C	125 (ML) ⁶	4.62	4.75	ND ⁵	3.017	0.109
MHT-8C	134 (ML)	5.64	6.00	ND	0.154	0.003
MHT-8C	144 (ML)	3.51	3.95	ND	0.023	0.010
MHT-8C	154 (ML)	5.53	5.80	ND	0.052	<0.002
MHT-8C	164 (ML)	4.24	4.36	ND	<0.015	0.004
MHT-8C	174 (ML)	5.42	5.72	ND	0.233	<0.002
MHT-8C	184 (ML)	5.51	5.76	ND	0.267	<0.002
MHT-8C	120 (DF) ⁷	>6.5	7.39	ND	ND	ND
MHT-8C	190 (DF)	>6.5	>6.5	ND	ND	ND

¹ Log₁₀ colony forming units on peptone trypticase yeast glucose per gram dry soil.

² Log₁₀ colony forming units on 1% peptone trypticase yeast glucose per gram dry soil.

³ Acridine Orange Direct Count (log₁₀ cells per gram dry soil).

⁴ Trichloroethylene and tetrachloroethylene concentrations in $\mu\text{g/g}$ soil.

⁵ Not Determined.

⁶ Collected by mud rotoring, with lexan core liner.

⁷ Drilling Fluids.

Table 7.13 Density of Bacteria in Sediment from MHT-9C

WELL #	DEPTH (ft)	PTYG ¹	1% PTYG ²	AODC ³	TCE ⁴	PCE ⁴
MHT-9C	5	4.49	5.12	7.36	<0.002	<0.002
MHT-9C	15	3.66	3.98	7.34	<0.002	<0.002
MHT-9C	25	1.85	2.60	6.73	<0.002	<0.002
MHT-9C	37	<1.5	3.64	6.76	<0.002	<0.002
MHT-9C	45	<1.5	1.81	6.94	0.003	<0.002
MHT-9C	65	<1.5	2.45	6.88	0.005	<0.002
MHT-9C	75	<1.5	2.21	6.82	0.005	<0.002
MHT-9C	85	2.43	2.26	6.85	<0.002	<0.002
MHT-9C	95	2.74	2.86	7.28	<0.002	<0.002
MHT-9C	105	<1.5	<1.5	8.02	0.126	<0.002
MHT-9C	115	2.02	1.79	7.54	0.006	<0.002
MHT-9C	143 (MB) ⁶	<1.5	<1.5	ND ⁵	0.012	0.006
MHT-9C	155 (MB)	2.20	2.31	8.25	<0.002	<0.002
MHT-9C	167 (MS) ⁷	4.24	4.29	8.18	0.176	0.005

¹ Log₁₀ colony forming units on peptone trypticase yeast glucose per gram dry soil.

² Log₁₀ colony forming units on 1% peptone trypticase yeast glucose per gram dry soil.

³ Acridine Orange Direct Count (log₁₀ cells per gram dry soil).

⁴ Trichloroethylene and tetrachloroethylene concentrations in µg/g soil.

⁵ Not Determined.

⁶ Collected by mud rotoring, with brass core liner in a 2 inch split spoon.

⁷ Collected by mud rotoring, with a 2 inch split spoon.

Table 7.14 Density of Bacteria in Sediment from MHT-10C

WELL #	DEPTH (ft)	PTYG ¹	1% PTYG ²	AODC ³	TCE ⁴	PCE ⁴
MHT-10C	7	3.73	4.17	ND ⁵	<0.002	<0.002
MHT-10C	15	1.95	3.80	ND	<0.002	<0.002
MHT-10C	25	1.67	2.35	ND	<0.002	<0.002
MHT-10C	35	2.75	2.72	ND	<0.002	<0.002
MHT-10C	45	1.83	2.13	ND	0.012	<0.002
MHT-10C	55	3.70	4.03	ND	0.042	0.005
MHT-10C	65	<1.5	<1.5	ND	0.049	<0.002
MHT-10C	75	<1.5	<1.5	ND	0.037	<0.002
MHT-10C	87	<1.5	<1.5	ND	<0.002	<0.002
MHT-10C	95	<1.5	<1.5	ND	0.390	0.026
MHT-10C	105	1.86	2.18	ND	0.037	<0.002
MHT-10C	148 (ML) ⁶	3.35	3.49	ND	0.016	0.012
MHT-10C	167 (ML)	3.11	3.43	ND	0.025	0.011
MHT-10C	175 (ML)	5.70	6.26	ND	<0.002	<0.002
MHT-10C	185 (ML)	>6.5	6.23	ND	0.304	<0.002
MHT-10C	142 (DF) ⁷	>6.5	7.41	ND	ND	ND
MHT-10C	148 (DF)	>6.5	7.29	ND	ND	ND
MHT-10C	163 (DF)	>6.5	7.18	ND	ND	ND
MHT-10C	176 (DF)	>6.5	7.45	ND	ND	ND
MHT-10C	181 (DF)	>6.5	7.27	ND	ND	ND
MHT-10C	190 (DF)	>6.5	7.53	ND	ND	ND

¹ Log₁₀ colony forming units on peptone trypticase yeast glucose per gram dry soil.

² Log₁₀ colony forming units on 1% peptone trypticase yeast glucose per gram dry soil.

³ Acridine Orange Direct Count (log₁₀ cells per gram dry soil).

⁴ Trichloroethylene and tetrachloroethylene concentrations in $\mu\text{g/g}$ soil.

⁵ Not Determined.

⁶ Collected by mud rotoring, with lexan core liner.

⁷ Drilling Fluids.

Table 7.15 Viable vs. Direct Counts of Bacteria in MHT-2C Sediment

WELL	DEPTH	% CFU/AODC ¹	RATIO AODC/CFU ²
MHT-2C	5	0.22007	4.54E+02
MHT-2C	15	0.00010	1.00E+06
MHT-2C	25	0.00250	4.01E+04
MHT-2C	35	0.00011	9.27E+05
MHT-2C	45	0.00059	1.69E+05
MHT-2C	55	0.00066	1.52E+05
MHT-2C	75	0.00267	3.74E+04
MHT-2C	85	0.00083	1.21E+05
MHT-2C	95	0.00031	3.22E+05
MHT-2C	105	0.00320	3.13E+04
MHT-2C	115	0.00048	2.09E+05
MHT-2C	125	0.00106	9.47E+04
MHT-2C	135	0.00707	1.41E+04
MHT-2C	145	0.24555	4.07E+02
MHT-2C	158	ND ³	ND
MHT-2C	168	ND	ND
MHT-2C	178	ND	ND
MHT-2C	187	ND	ND

¹ (Colony Forming Units/Acridine Orange Direct Count) X 100%

² Acridine Orange Direct Count/Colony Forming Units

³ Not Determined

Table 7.16 Viable vs. Direct Counts of Bacteria in MHT-3C Sediment

WELL	DEPTH	% CFU/AODC ¹	RATIO AODC/CFU ²
MHT-3C	3	1.15767	8.64E+01
MHT-3C	7	0.02110	4.74E+03
MHT-3C	15	0.00020	5.00E+05
MHT-3C	25	0.00057	1.75E+05
MHT-3C	35	0.00034	2.95E+05
MHT-3C	47	0.01142	8.75E+03
MHT-3C	57	0.00278	3.59E+04
MHT-3C	65	0.00759	1.32E+04
MHT-3C	73	0.02595	3.85E+03
MHT-3C	85	0.11974	8.35E+02
MHT-3C	105	0.00034	2.97E+05
MHT-3C	115	0.02529	3.95E+03

¹ (Colony Forming Units/Acidine Orange Direct Count) X 100%

² Acidine Orange Direct Count/Colony Forming Units

Table 7.17 Viable vs. Direct Counts of Bacteria in MHT-5C Sediment

WELL	DEPTH	% CFU/AODC ¹	RATIO AODC/CFU ²
MHT-5C	5	0.37360	2.68E+02
MHT-5C	15	0.01367	7.32E+03
MHT-5C	25	0.00035	2.85E+05
MHT-5C	45	0.00016	6.33E+05
MHT-5C	55	0.00037	2.69E+05
MHT-5C	65	0.00025	4.03E+05
MHT-5C	75	0.00084	1.19E+05
MHT-5C	85	0.00005	1.91E+06
MHT-5C	93	0.00049	2.06E+05
MHT-5C	101	0.00125	7.99E+04
MHT-5C	117	0.00087	1.15E+05
MHT-5C	126	1.35143	7.40E+01
MHT-5C	138	3.64265	2.75E+01
MHT-5C	162	0.03609	2.77E+03
MHT-5C	187	0.48135	2.08E+02

¹ (Colony Forming Units/Acidine Orange Direct Count) X 100%

² Acidine Orange Direct Count/Colony Forming Units

Table 7.18 Viable vs. Direct Counts of Bacteria in MHT-7C Sediment

WELL	DEPTH	% CFU/AODC ¹	RATIO AODC/CFU ²
MHT-7C	5	0.11678	8.56E+02
MHT-7C	15	0.00839	1.19E+04
MHT-7C	25	0.00002	4.71E+06
MHT-7C	35	0.00086	1.17E+05
MHT-7C	45	0.00919	1.09E+04
MHT-7C	71	0.00056	1.80E+05
MHT-7C	85	0.01188	8.42E+03
MHT-7C	95	0.00004	2.49E+06
MHT-7C	105	0.00003	3.49E+06
MHT-7C	115	0.00127	7.89E+04
MHT-7C	143	0.94036	1.06E+02
MHT-7C	155	1.50266	6.65E+01
MHT-7C	179	0.72446	1.38E+02
MHT-7C	191	0.11197	8.93E+02

¹ (Colony Forming Units/Acridine Orange Direct Count) X 100%

² Acridine Orange Direct Count/Colony Forming Units

Table 7.19 Viable vs. Direct Counts of Bacteria in MHT-9C Sediment

WELL	DEPTH	% CFU/AODC ¹	RATIO AODC/CFU ²
MHT-9C	5	0.57375	1.74E+02
MHT-9C	15	0.04379	2.28E+03
MHT-9C	25	0.00746	1.34E+04
MHT-9C	37	0.07551	1.32E+03
MHT-9C	45	0.00075	1.34E+05
MHT-9C	65	0.00376	2.66E+04
MHT-9C	75	0.00241	4.15E+04
MHT-9C	85	0.00254	3.93E+04
MHT-9C	95	0.00384	2.61E+04
MHT-9C	105	0.00003	3.33E+06
MHT-9C	115	0.00018	5.60E+05
MHT-9C	143	ND ³	ND
MHT-9C	155	0.00011	8.71E+05
MHT-9C	167	0.01302	7.68E+03

¹ (Colony Forming Units/Acridine Orange Direct Count) X 100%

² Acridine Orange Direct Count/Colony Forming Units

³ Not Determined

Table 7.20 Phospholipid Fatty Acid Analysis of Sediments from MHT-2C by Depth (all data in Mol %)

Table 721: Proximate and Fatty Acid Analysis of Sediment from MHT 4C by Depth (all data is Mean \pm S)

Table 7.22. Phospholipid Fatty Acid Analysis of Sediment from MHT-7C by Depth (all data in Mole %)

Sample	Depth	5'	15'	25'	35'	45'	55'	71'	85'	95'	105'	115'	143'	155'	175'	191'	253'	258'
PLFA	#156	0.00	0.00	0.00	0.00	0.00	0.00	0.00	0.00	0.00	0.00	0.00	0.25	0.00	0.00	0.38		
	114-0	0.00	0.00	0.00	0.00	0.00	0.00	0.00	0.00	0.00	0.00	0.00	1.59	0.00	1.86			
	14-0	0.11	0.00	0.00	0.00	0.00	0.00	0.00	0.00	0.00	0.00	0.00	0.00	0.00	0.00	0.00	0.00	
	br15-1	0.08	0.00	0.00	0.00	0.00	0.00	0.00	0.00	0.00	0.00	0.00	0.00	0.00	0.00	0.00	0.00	0.00
	115-0	6.48	0.00	0.00	0.00	0.00	0.00	0.00	0.00	0.00	0.00	0.00	4.30	0.00	3.75			
	115-0	1.20	0.00	0.00	0.00	0.00	0.00	0.00	0.00	0.00	0.00	0.00	4.84	2.45	0.00	2.34		
	115-0	0.26	0.00	0.00	0.00	0.00	0.00	0.00	0.00	0.00	0.00	0.00	0.00	1.20	0.00	0.01		
	115-0	1.04	0.00	0.00	0.00	0.00	0.00	0.00	0.00	0.00	0.00	0.00	0.00	0.00	0.00	0.00	0.00	
poly16:6	116-0	5.00	0.00	0.00	0.00	0.00	0.00	0.00	0.00	0.00	0.00	0.00	2.88	1.67	0.00	1.99		
	116-0	0.59	0.00	0.00	0.00	0.00	0.00	0.00	0.00	0.00	0.00	0.00	0.00	0.00	0.00	0.00	0.00	
	116-0	2.32	3.76	0.00	0.00	1.50	0.00	0.00	0.00	0.00	0.00	0.00	3.81	5.25	0.00	7.69		
	116-0	0.00	0.00	0.00	0.00	0.00	0.00	0.00	0.00	0.00	0.00	0.00	0.00	0.16	0.00	0.28		
	116-0	0.60	0.00	0.00	0.00	0.00	0.00	0.00	0.00	0.00	0.00	0.00	0.00	0.96	0.00	0.31		
	116-0	14.17	72.18	70.91	0.00	65.24	0.00	29.32	0.00	68.09	46.15	0.00	34.77	62.05	36.78			
poly16:1a	117-0	1.78	0.00	0.00	0.00	0.00	0.00	0.00	0.00	0.00	0.00	0.00	0.00	0.00	0.00	0.00	0.00	
poly16:1b	117-0	0.38	0.00	0.00	0.00	0.00	0.00	0.00	0.00	0.00	0.00	0.00	0.00	0.00	0.00	0.00	0.00	
	117-1	1.55	0.00	0.00	0.00	0.00	0.00	0.00	0.00	0.00	0.00	0.00	0.00	0.00	0.00	0.00	0.00	
	100m 16:0	6.65	0.00	0.00	0.00	0.00	0.00	0.00	0.00	0.00	0.00	0.00	0.00	0.00	3.32	0.00	1.39	
	110m 16:0	1.28	0.00	0.00	0.00	0.00	0.00	0.00	0.00	0.00	0.00	0.00	0.00	0.00	0.00	0.00	0.00	
	120m 16:0	2.50	0.00	0.00	0.00	0.00	0.00	0.00	0.00	0.00	0.00	0.00	0.00	0.00	0.00	0.00	0.00	
	br16:1	0.54	0.00	0.00	0.00	0.00	0.00	0.00	0.00	0.00	0.00	0.00	0.00	0.00	0.46	0.00	0.00	
	117-0	4.97	0.00	0.00	0.00	0.00	0.00	0.00	0.00	0.00	0.00	0.00	0.00	0.00	0.00	0.00	0.00	
	117-0	1.97	3.76	0.00	0.00	0.00	0.00	0.00	0.00	0.00	0.00	0.00	0.00	0.00	0.00	0.00	0.00	
	171-8c	0.11	0.00	0.00	0.00	0.00	0.00	0.00	0.00	0.00	0.00	0.00	0.00	0.00	0.00	0.00	0.00	
	c17:3	1.19	0.00	0.00	0.00	0.00	0.00	0.00	0.00	0.00	0.00	0.00	0.00	0.00	0.00	0.00	0.00	
	17-0	0.24	0.00	0.00	0.00	0.00	0.00	0.00	0.00	0.00	0.00	0.00	0.00	0.00	0.00	0.00	0.00	
poly16:1a	14-3	0.00	0.00	0.00	0.00	0.00	0.00	0.00	0.00	0.00	0.00	0.00	0.00	0.00	0.00	0.00	0.00	
poly16:1b	0.33	0.00	0.00	0.00	0.00	0.00	0.00	0.00	0.00	0.00	0.00	0.00	0.00	0.00	0.00	0.00	0.00	
	100m 17:0	1.18	0.00	0.00	0.00	0.00	0.00	0.00	0.00	0.00	0.00	0.00	0.00	0.00	0.00	0.00	0.00	
	br17:1	0.36	0.00	0.00	0.00	0.00	0.00	0.00	0.00	0.00	0.00	0.00	0.00	0.00	0.00	0.00	0.00	
	18-2m6	7.93	0.00	0.00	0.00	0.00	0.00	0.00	0.00	0.00	0.00	0.00	0.00	0.00	3.76	0.00	2.25	
	18-1m9c	4.15	0.00	0.00	0.00	0.00	0.00	0.00	0.00	0.00	0.00	0.00	31.58	11.66	0.00	10.66		
	18-1m7c	1.60	5.64	0.00	0.00	1.50	0.00	0.00	0.00	0.00	0.00	0.00	9.00	12.04	8.26	0.00	5.88	
	18-1m7c	0.52	0.00	0.00	0.00	0.00	0.00	0.00	0.00	0.00	0.00	0.00	0.00	0.00	0.18	0.00	0.10	
	18-1m5c	0.13	0.00	0.00	0.00	0.00	0.00	0.00	0.00	0.00	0.00	0.00	0.00	0.00	0.18	0.00	0.00	
	18-0	2.67	14.66	29.09	0.00	21.43	0.00	56.33	0.00	28.75	44.85	0.00	31.19	37.95	7.55			
	br19-1	0.19	0.00	0.00	0.00	0.00	0.00	0.00	0.00	0.00	0.00	0.00	0.00	0.00	0.00	0.00	0.00	
	100m 18:0	2.04	0.00	0.00	0.00	0.00	0.00	0.00	0.00	0.00	0.00	0.00	0.00	0.00	0.00	0.00	0.00	
	120m 18:0	1.69	0.00	0.00	0.00	0.00	0.00	0.00	0.00	0.00	0.00	0.00	0.00	0.00	0.00	0.00	0.00	
	18-1	0.27	0.00	0.00	0.00	0.00	0.00	0.00	0.00	0.00	0.00	0.00	0.00	0.00	0.00	0.00	0.00	
	c19-0	7.35	0.00	0.00	0.00	0.00	0.00	0.00	0.00	0.00	0.00	0.00	0.00	0.00	2.84	0.00	2.35	
	20-0	0.13	0.00	0.00	0.00	0.00	0.00	0.00	0.00	0.00	0.00	0.00	0.00	0.00	0.00	0.00	0.00	
	20-1m9c	0.00	0.00	0.00	0.00	0.00	0.00	0.00	0.00	0.00	0.00	0.00	0.00	0.00	0.00	0.00	0.00	
	21-0	0.13	0.00	0.00	0.00	0.00	0.00	0.00	0.00	0.00	0.00	0.00	0.00	0.00	0.00	0.00	0.00	
	22-0	0.07	0.00	0.00	0.00	0.00	0.00	0.00	0.00	0.00	0.00	0.00	0.00	0.00	0.00	0.00	0.00	
	24-0	0.13	0.00	0.00	0.00	0.00	0.00	0.00	0.00	0.00	0.00	0.00	0.00	0.00	0.00	0.00	0.00	
Total		100	100	100	100	0	0	100	0	100	100	0	100	100	100	100	100	
pmol/gdw		30.00	0.06	0.03	0.00	0.19	0.00	0.04	0.00	0.12	0.20	0.00	0.21	0.21	0.22	0.22	0.22	

Table 7.23 DNA Analysis of Sediment Samples by Depth

Borehole	DEPTH (ft)	DNA (μ g/gdw)	MMO*	PLASMID FREQUENCY(%)	Methanotrophs (CFU/gdw)
MHT-6C	5	0.19		70	
MHT-6C	15	0.21		25	
MHT-6C	25	0.69		33.3	
MHT-6C	55	2.19	+	66.7	NG
MHT-6C	75	2.7	+	0	3.90×10^5
MHT-6C	95	0.77		46.2	
MHT-6C	115	0.14	+	12.5	5.00×10^6
MHT-6C	141	0.05		71.4	
MHT-6C	145	0.16		71.4	
MHT-6C	165(ML)	3.73	+	41.7	4.60×10^6
MHT-6C	185(ML)	0.68	+	100	1.47×10^7
MHT-6C	190(ML)	2.31	+	58.3	3.20×10^7
<hr/>					
MHT-9C	5	0.28		11.1	
MHT-9C	25	0.6		33.3	
MHT-9C	45	0.61		33.3	
MHT-9C	65	1.15	+	20	5.50×10^4
MHT-9C	85	1.99		ND	
MHT-9C	95	0.14		37.5	
MHT-9C	105	0.13		33.3	
MHT-9C	167(MS)7	0.13		75	

*methane monooxygenase type I (presence/absence), NG = no growth

Figure 7.1 Map of Pretest TCE Contamination in the MHT C Wells

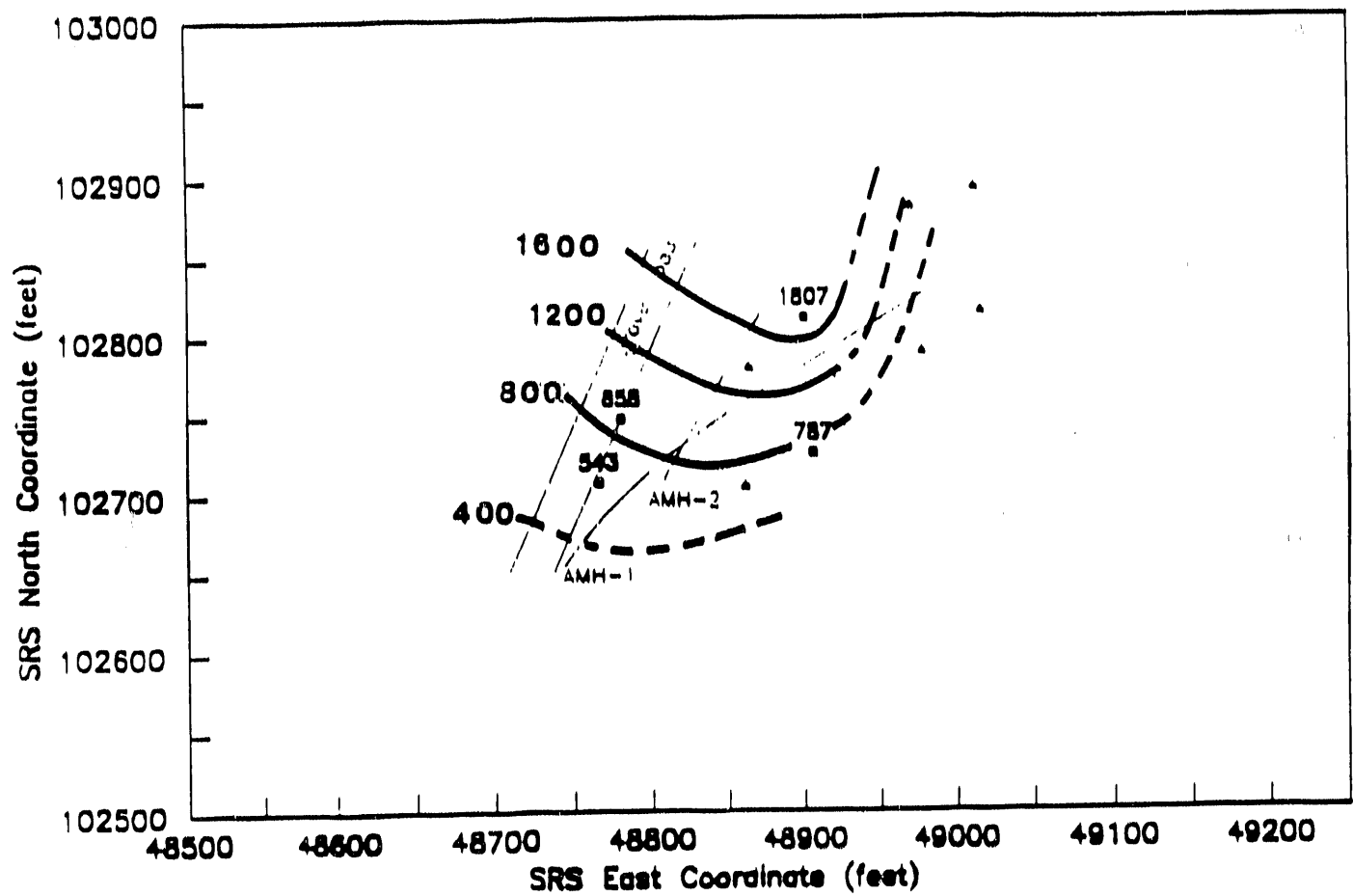


Figure 7.2 Map of Pretest PCE Contamination in the MHT C Wells

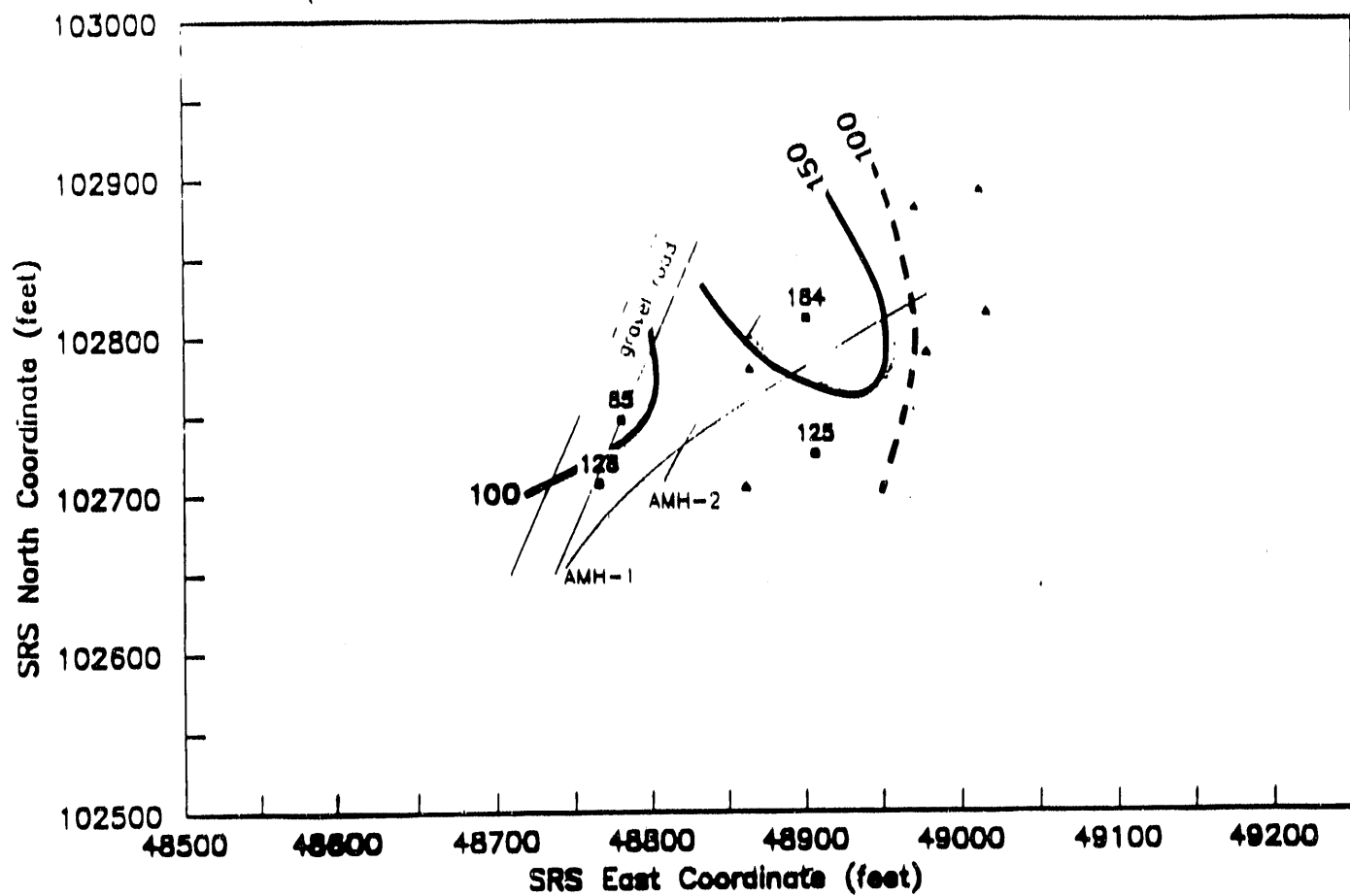


Figure 7.3 Map of Pretest TCE Contamination in the MHT D Wells

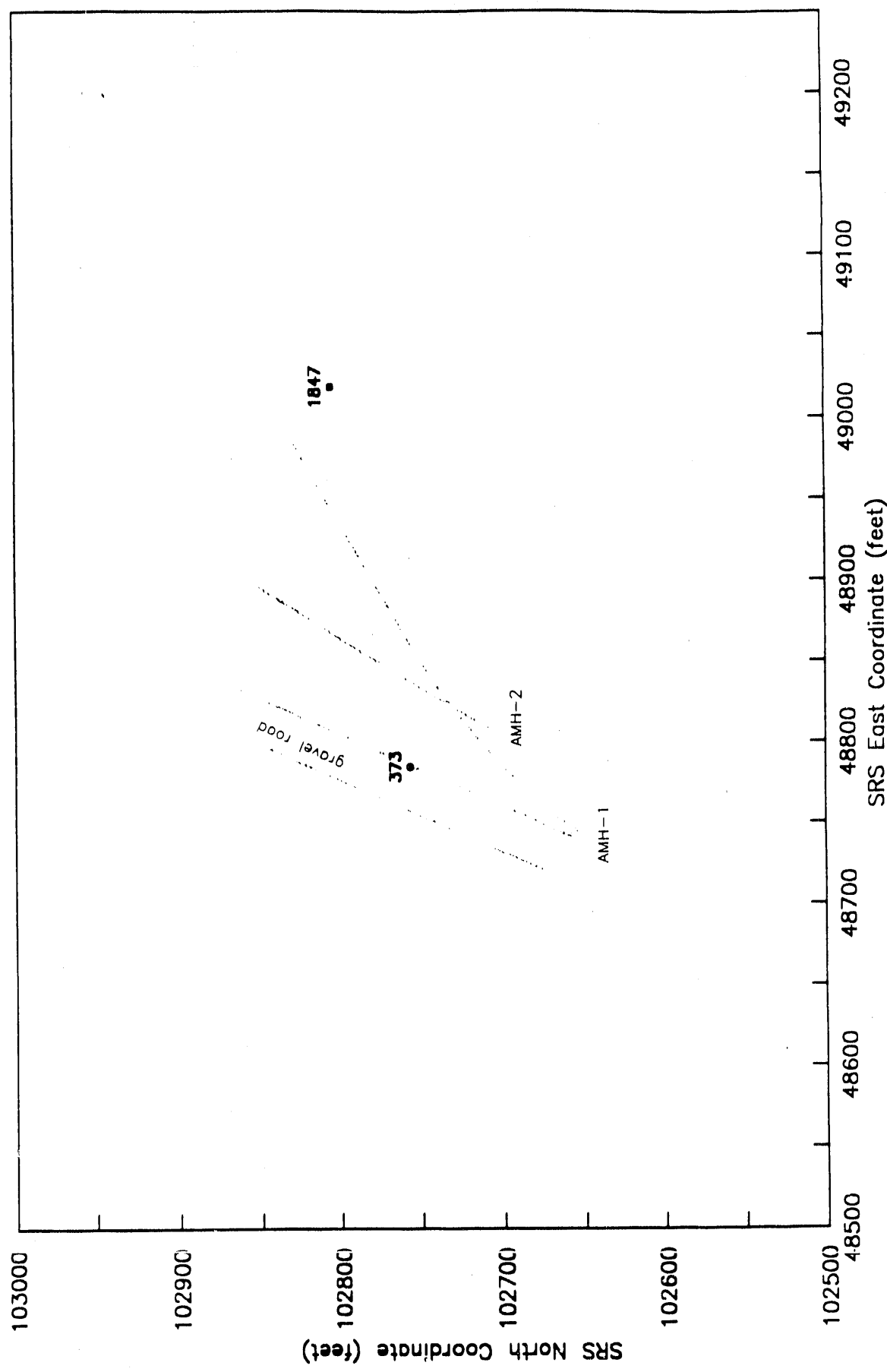


Figure 7.4 Map of Pretest PCE Contamination in the MHT D Wells

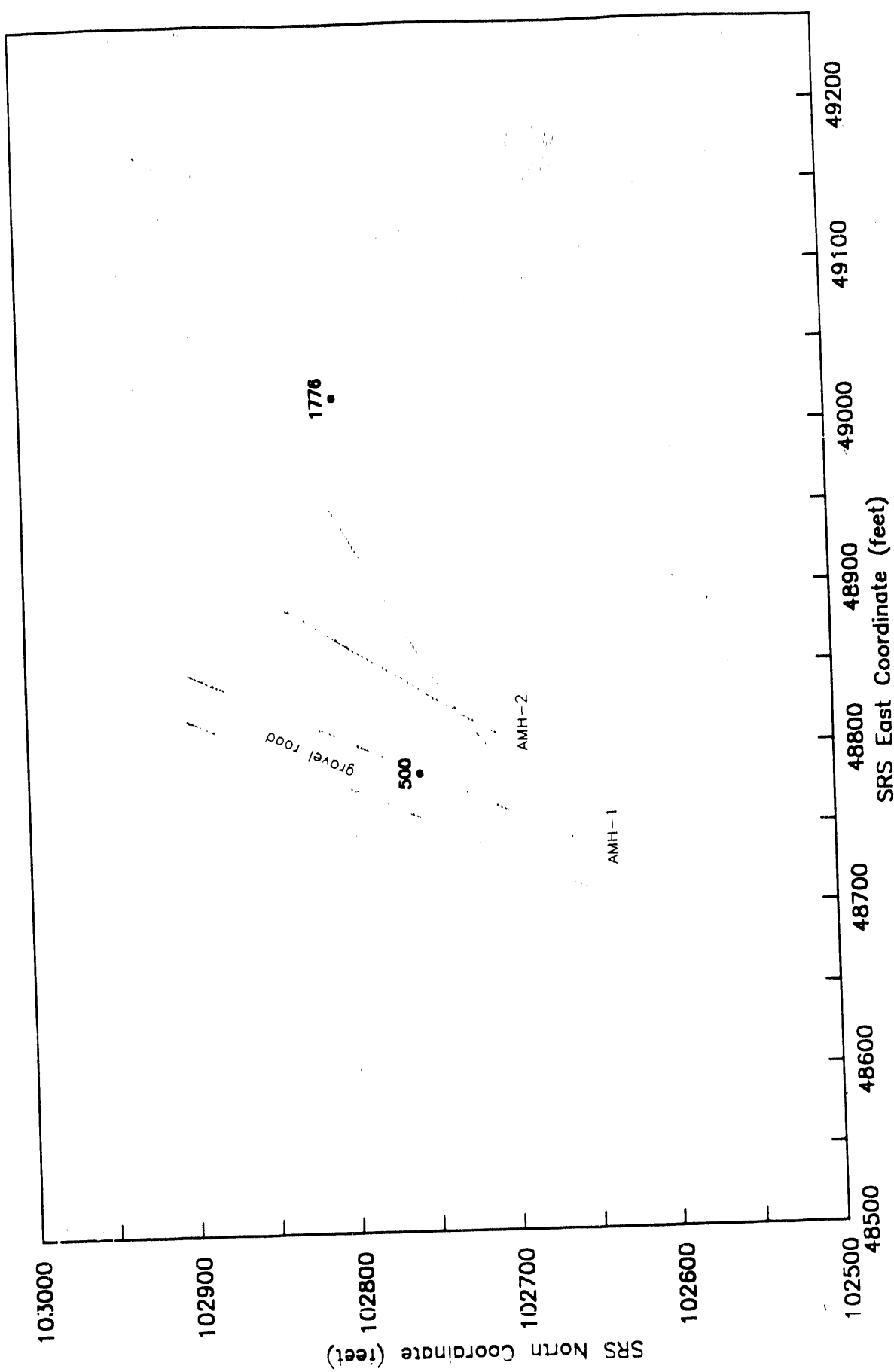


Figure 7.5 Plot of TCE Concentration vs. Depth in Sediment for MHT1C

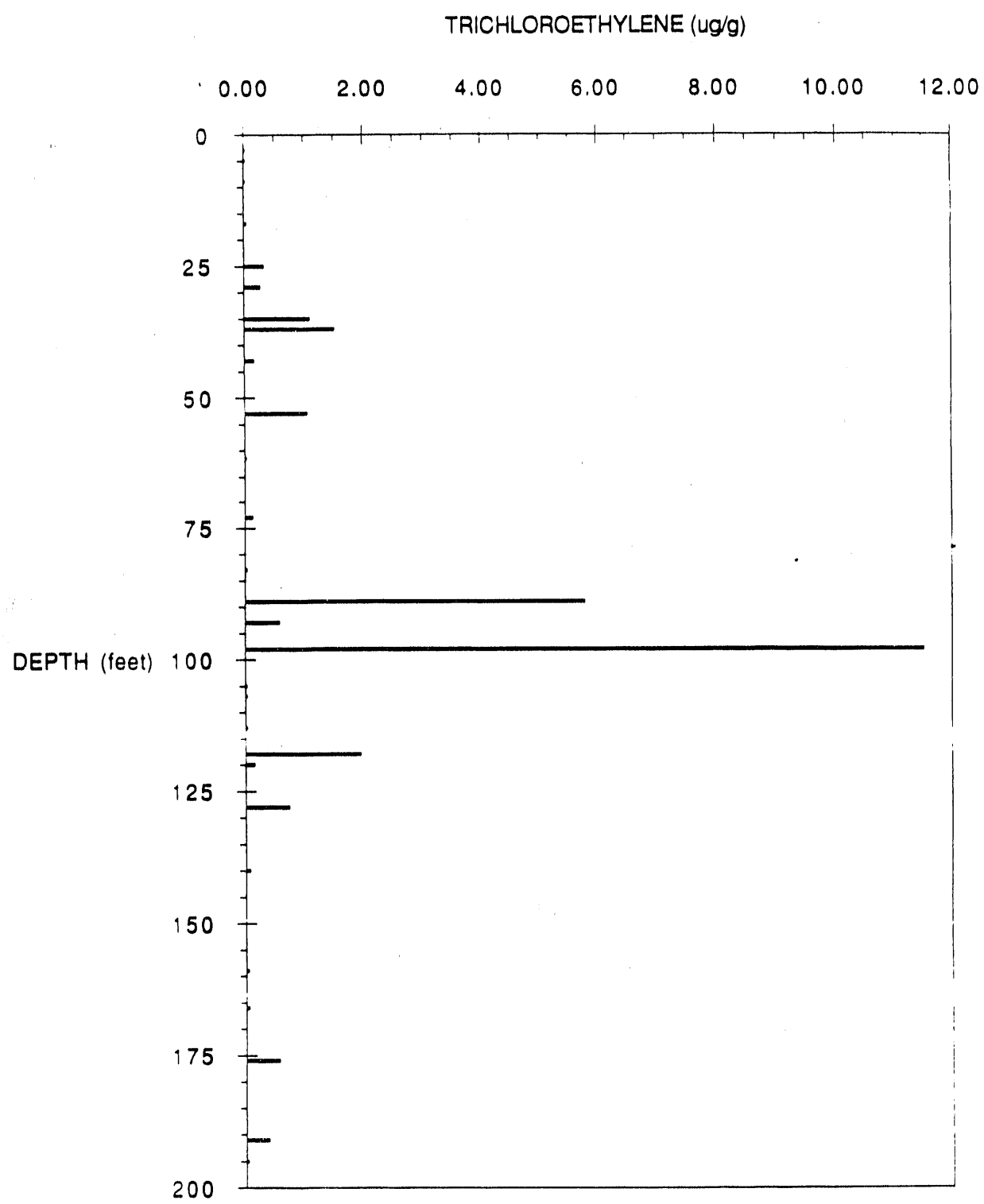


Figure 7.6 Plot of TCE Concentration vs. Depth in Sediment for MHT2C

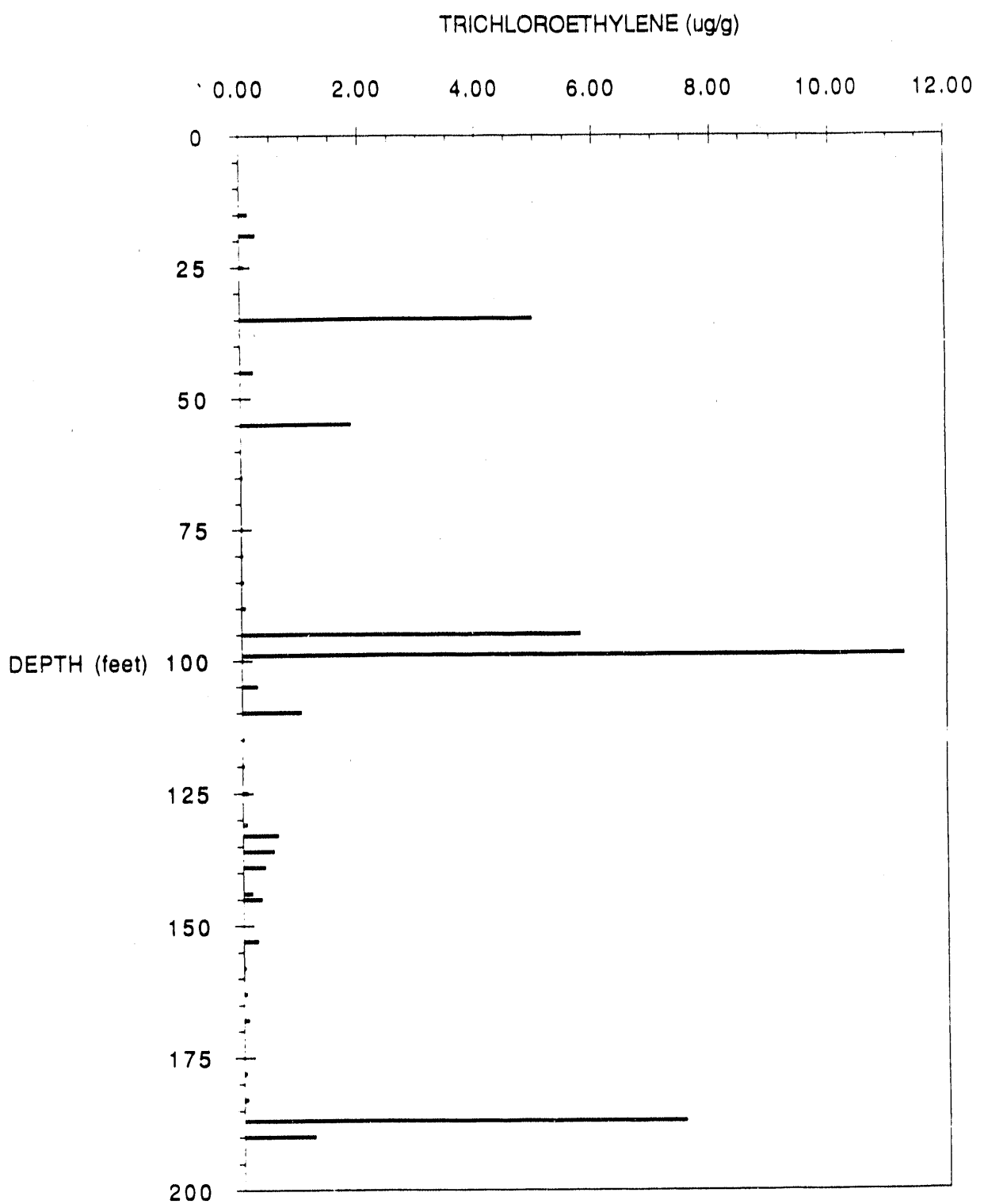


Figure 7.7 Plot of TCE Concentration vs. Depth in Sediment for MHT3C

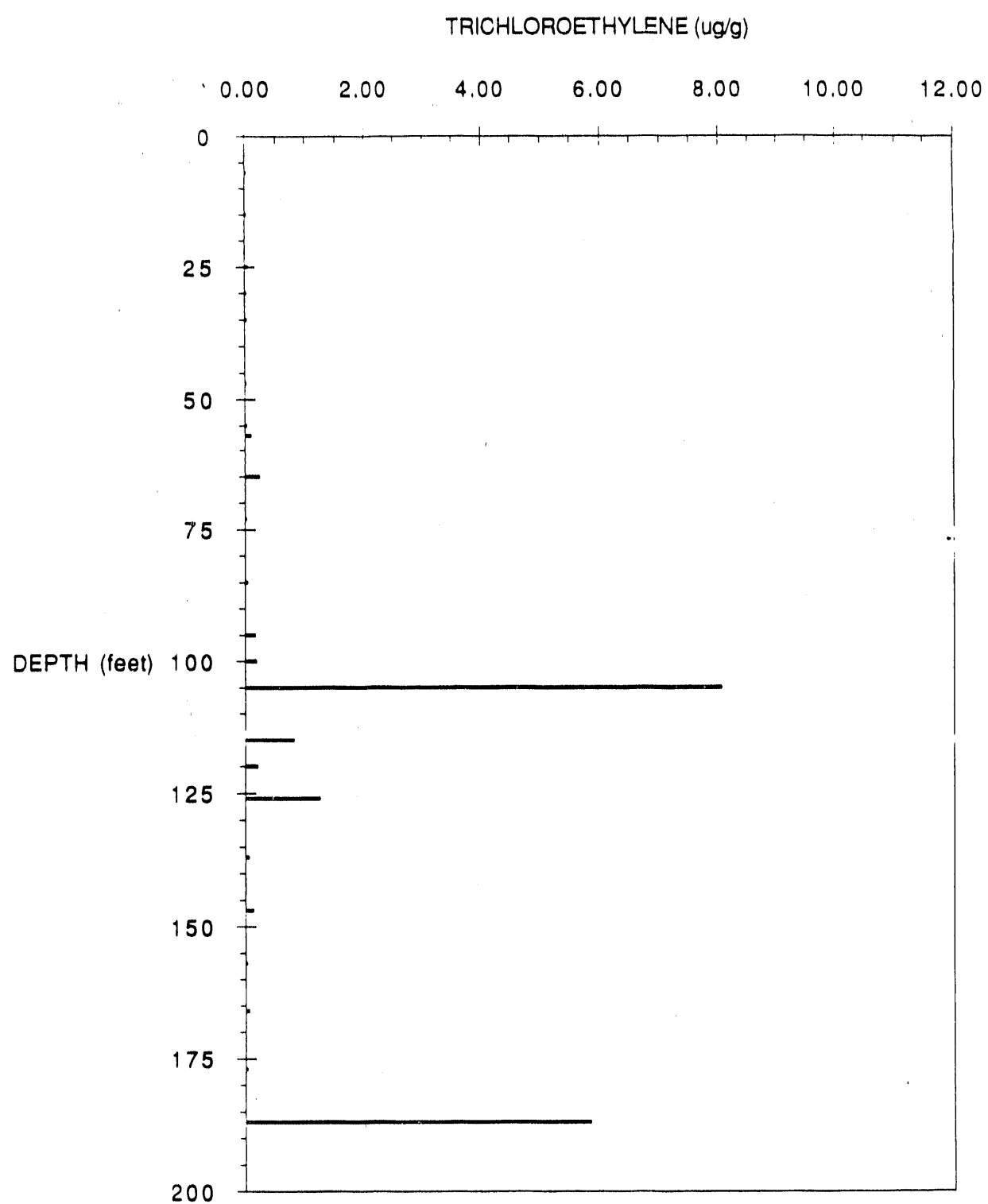


Figure 7.8 Plot of TCE Concentration vs. Depth in Sediment for MHT4C

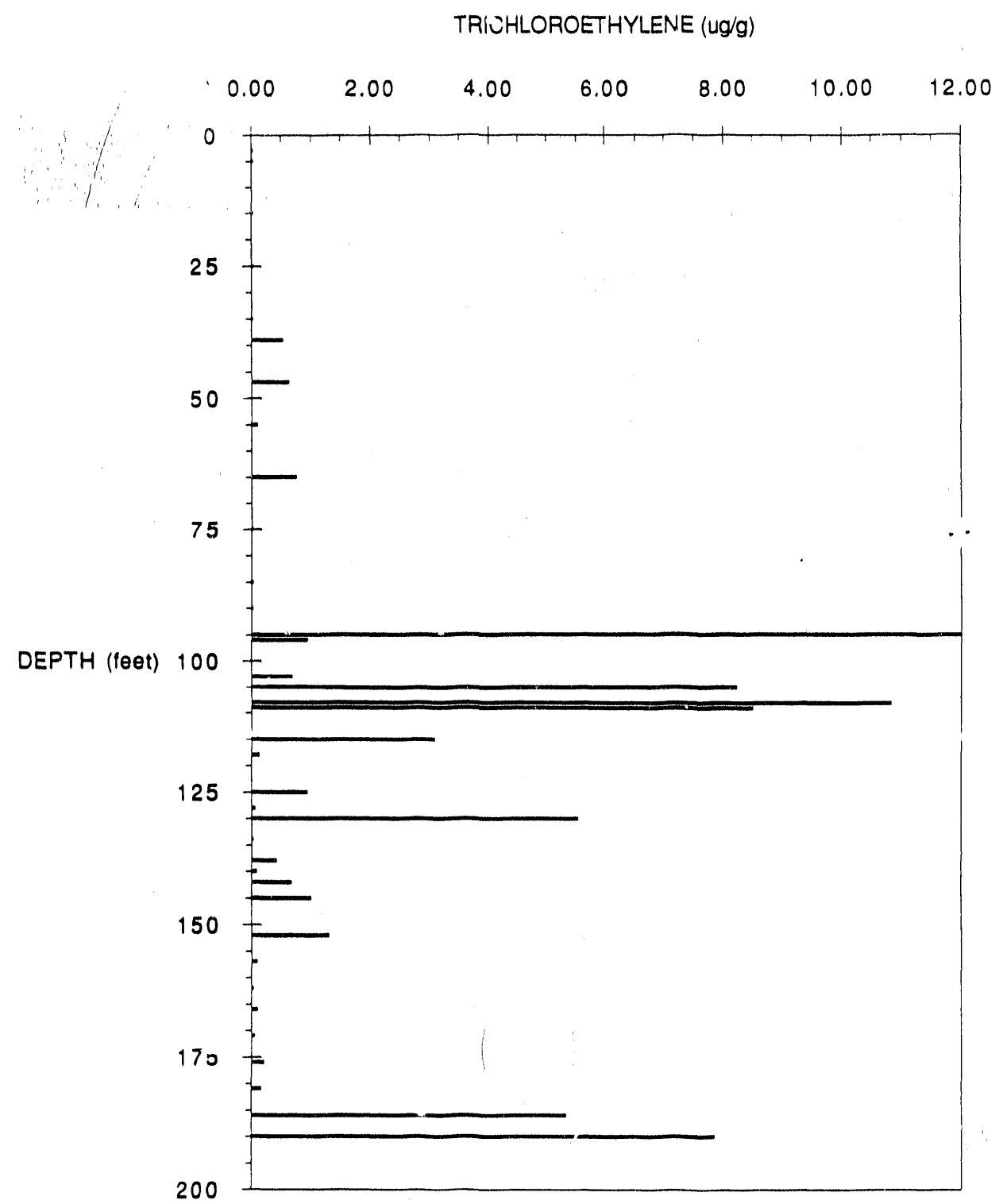


Figure 7.9 Plot of TCE Concentration vs. Depth in Sediment for MHT5C

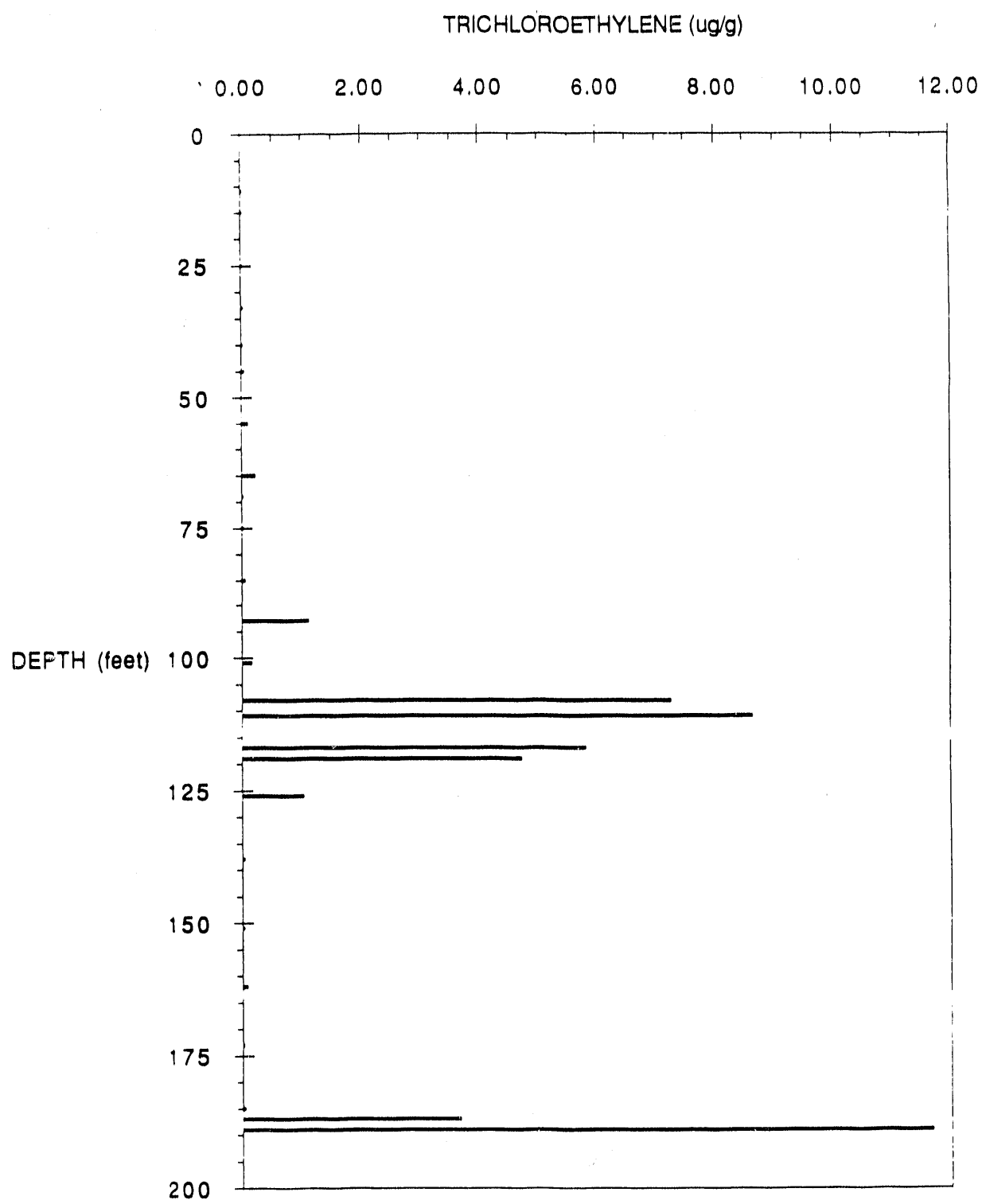


Figure 7.10 Plot of TCE Concentration vs. Depth in Sediment for MHT6C

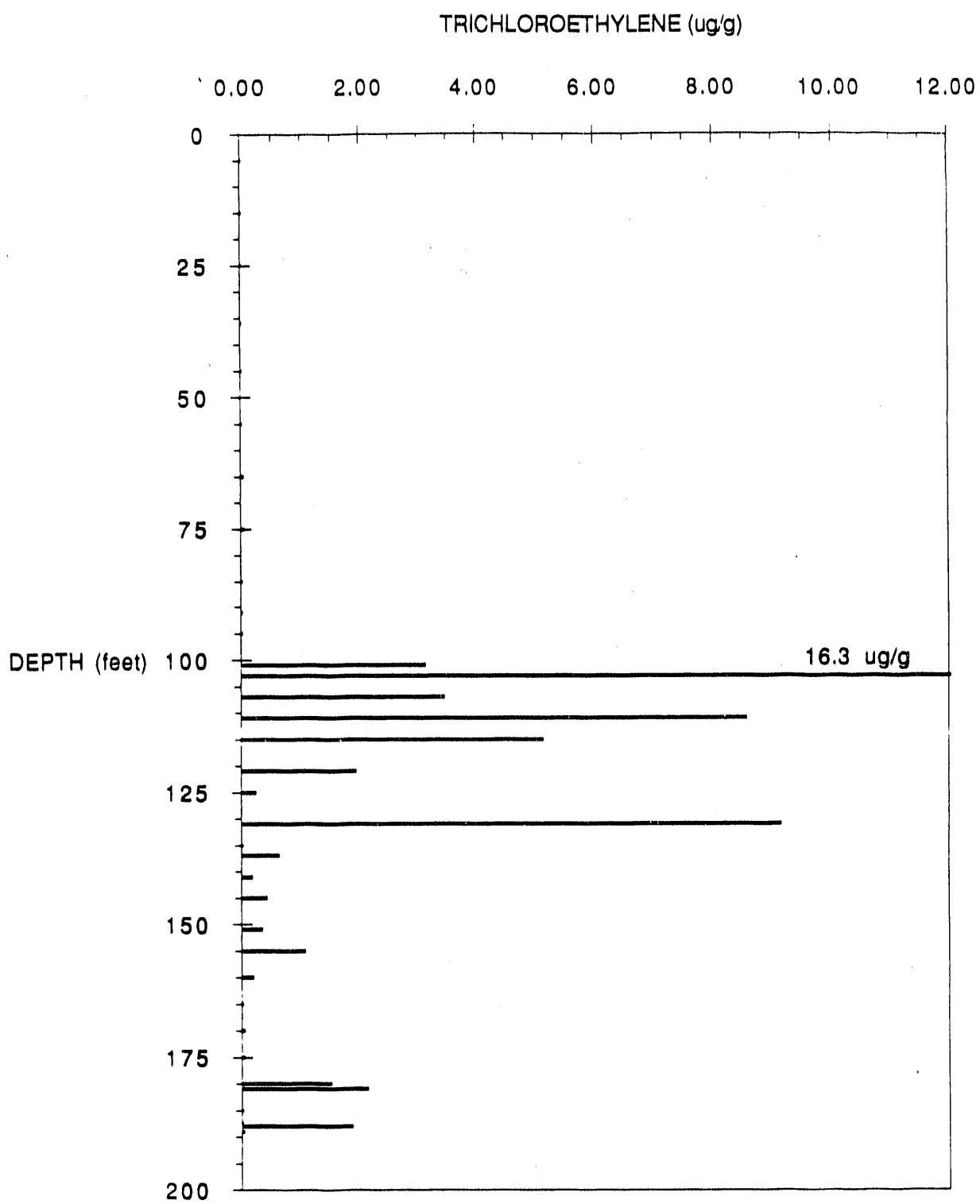


Figure 7.11 Plot of TCE Concentration vs. Depth in Sediment for MHT7C

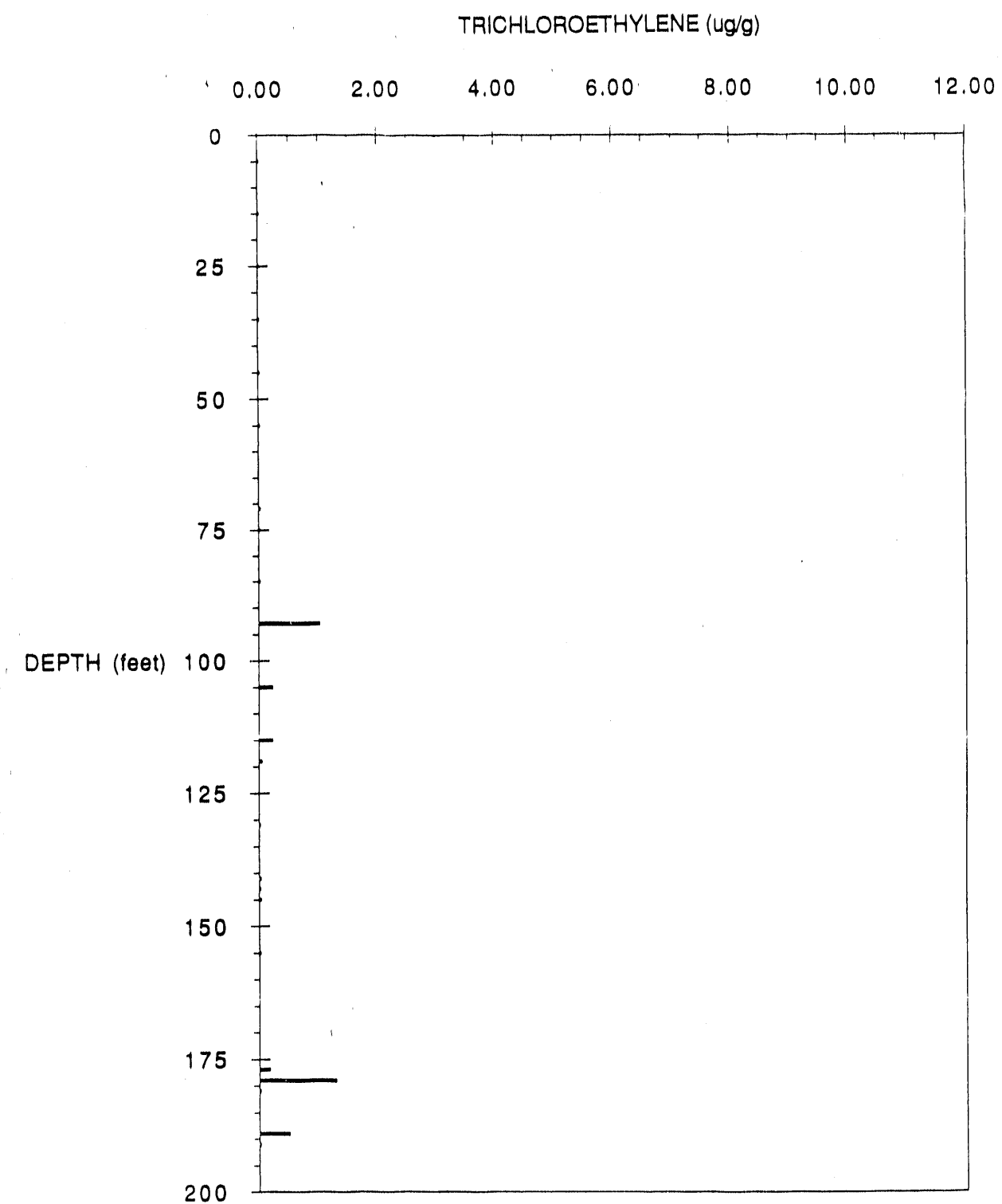


Figure 7.12 Plot of TCE Concentration vs. Depth in Sediment for MHT8C

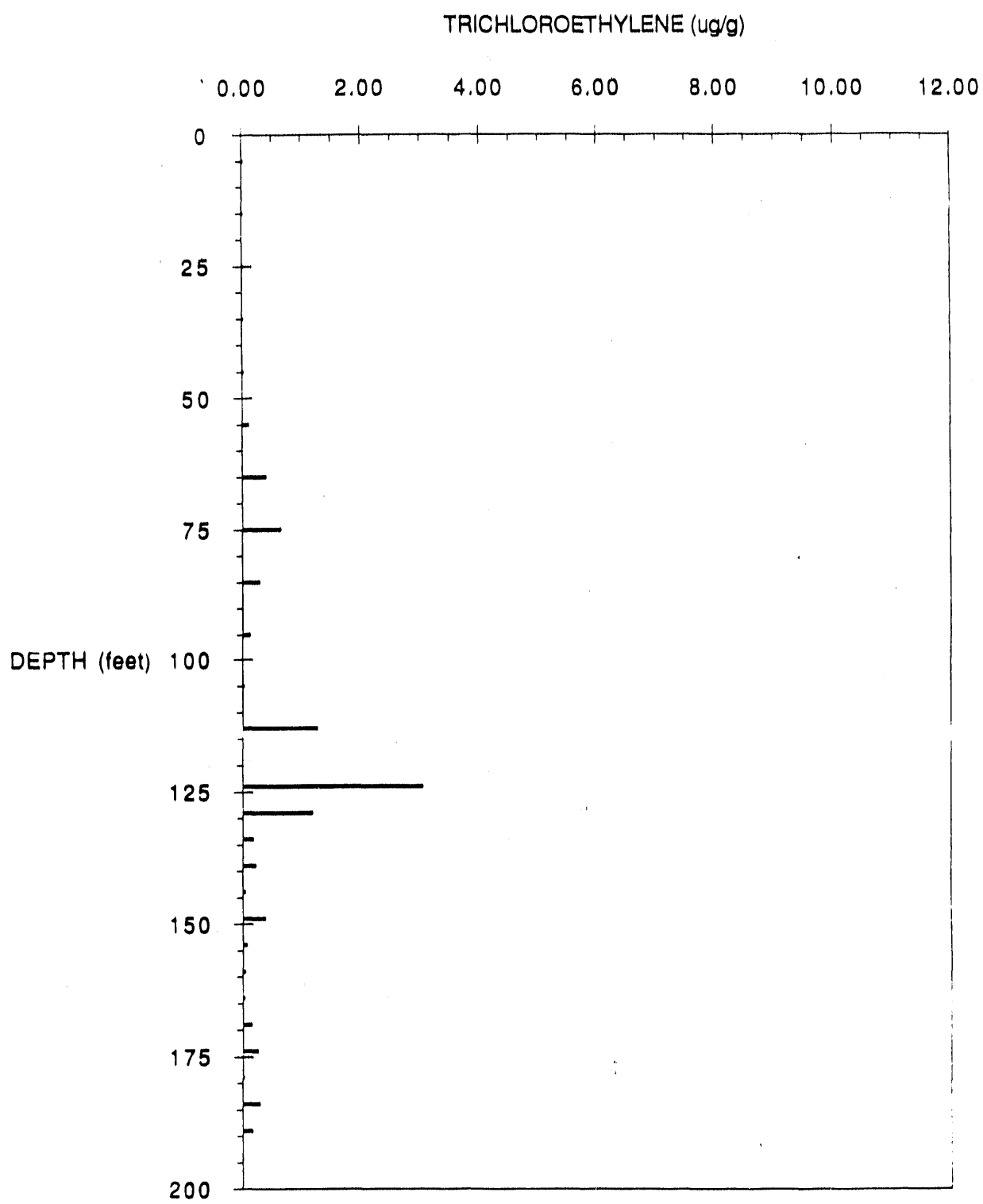


Figure 7.13 Plot of TCE Concentration vs. Depth in Sediment for MHT9C

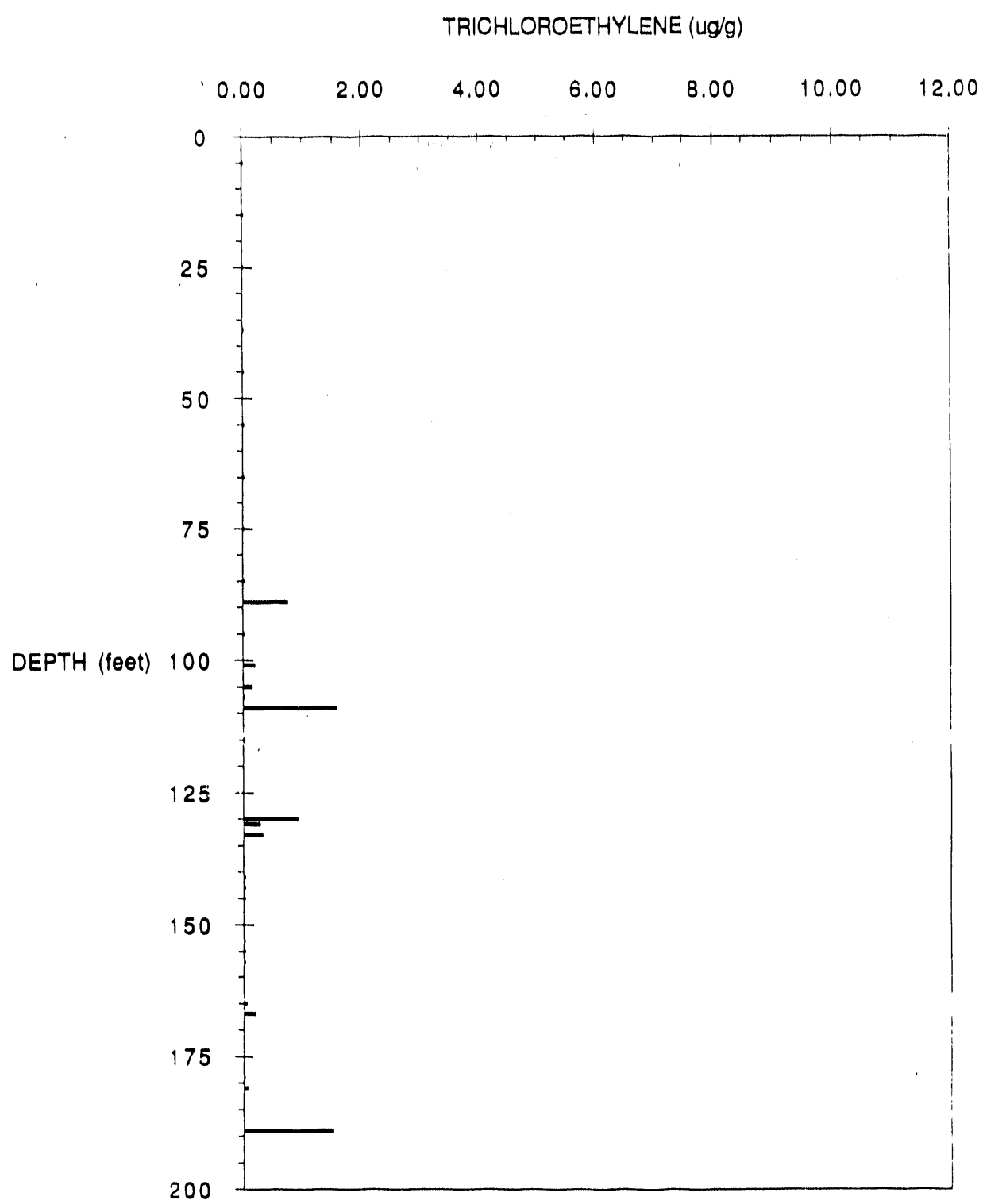


Figure 7.14 Plot of TCE Concentration vs. Depth in Sediment for MHT10C

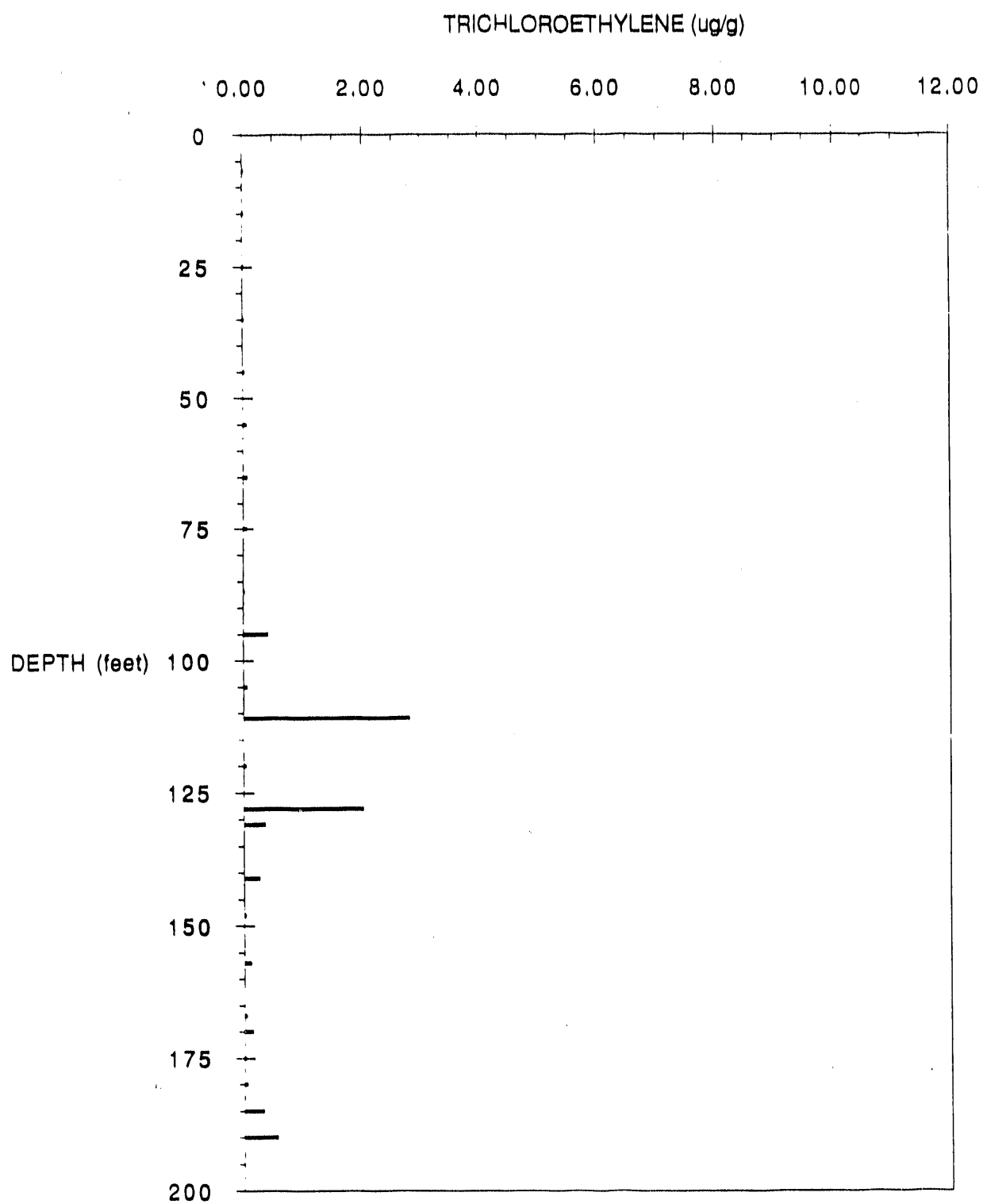


Figure 7.15 Plot of PCE Concentration vs. Depth in Sediment for MHT1C

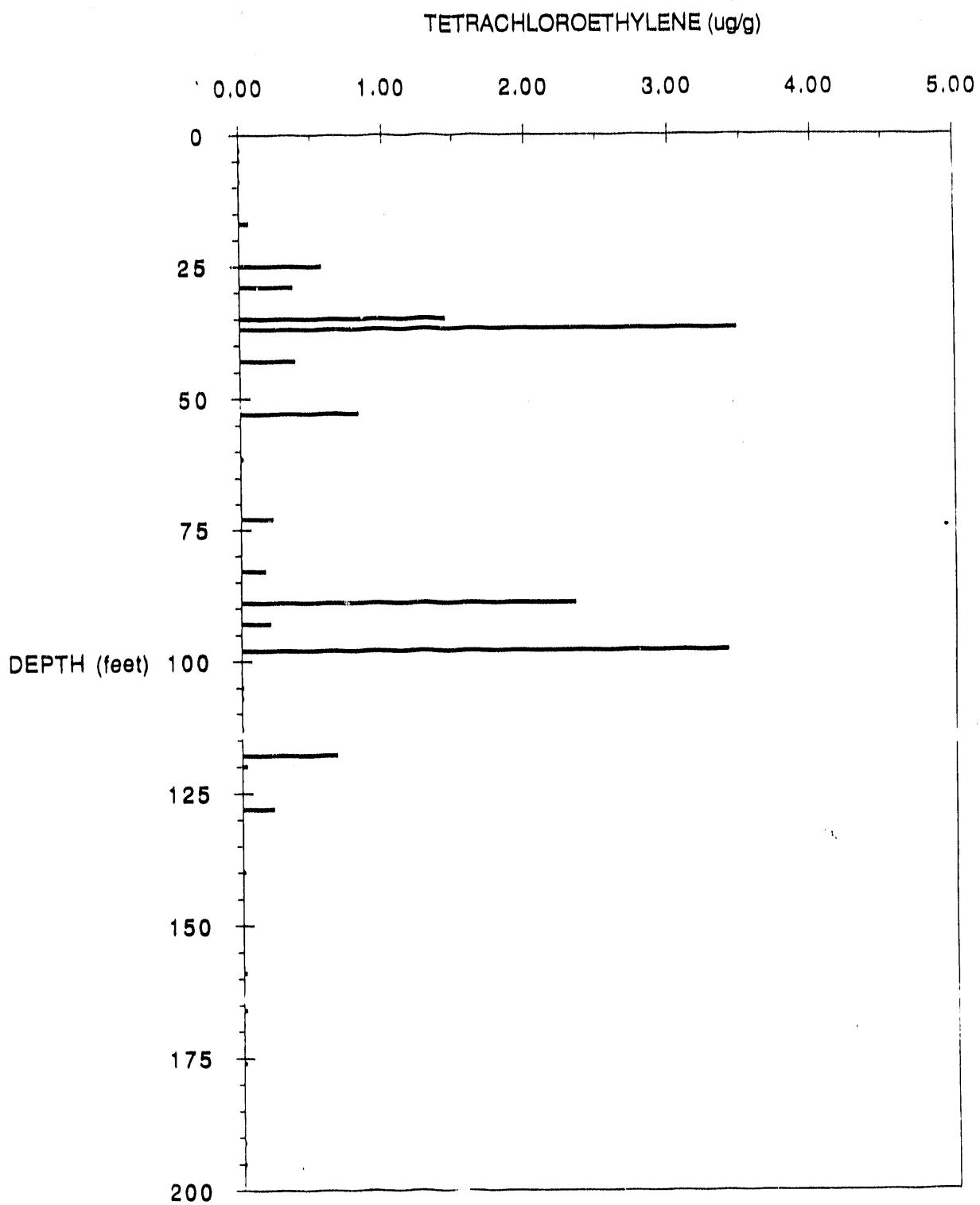


Figure 7.16 Plot of PCE Concentration vs. Depth in Sediment for MHT2C

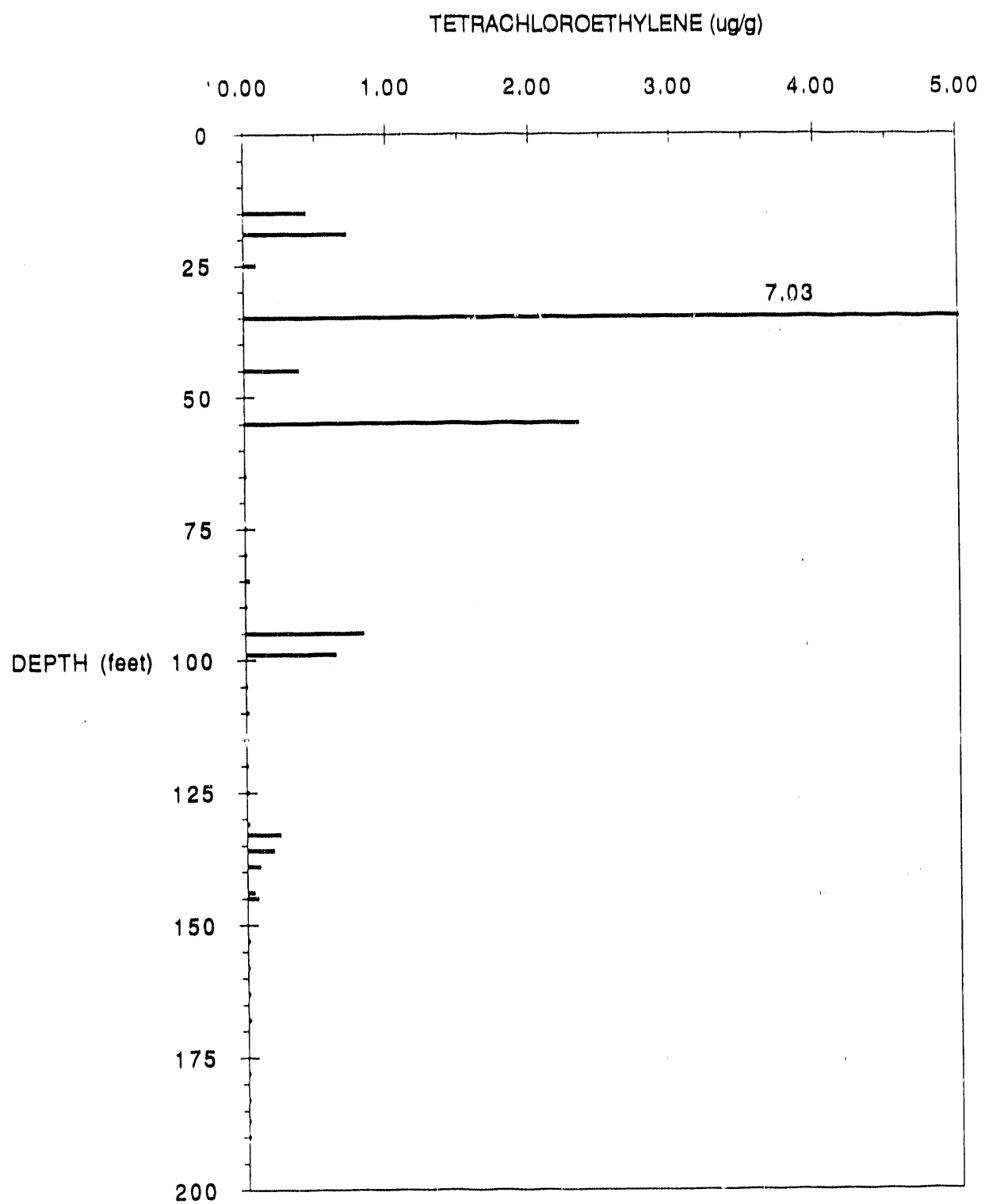


Figure 7.17 Plot of PCE Concentration vs. Depth in Sediment for MHT3C

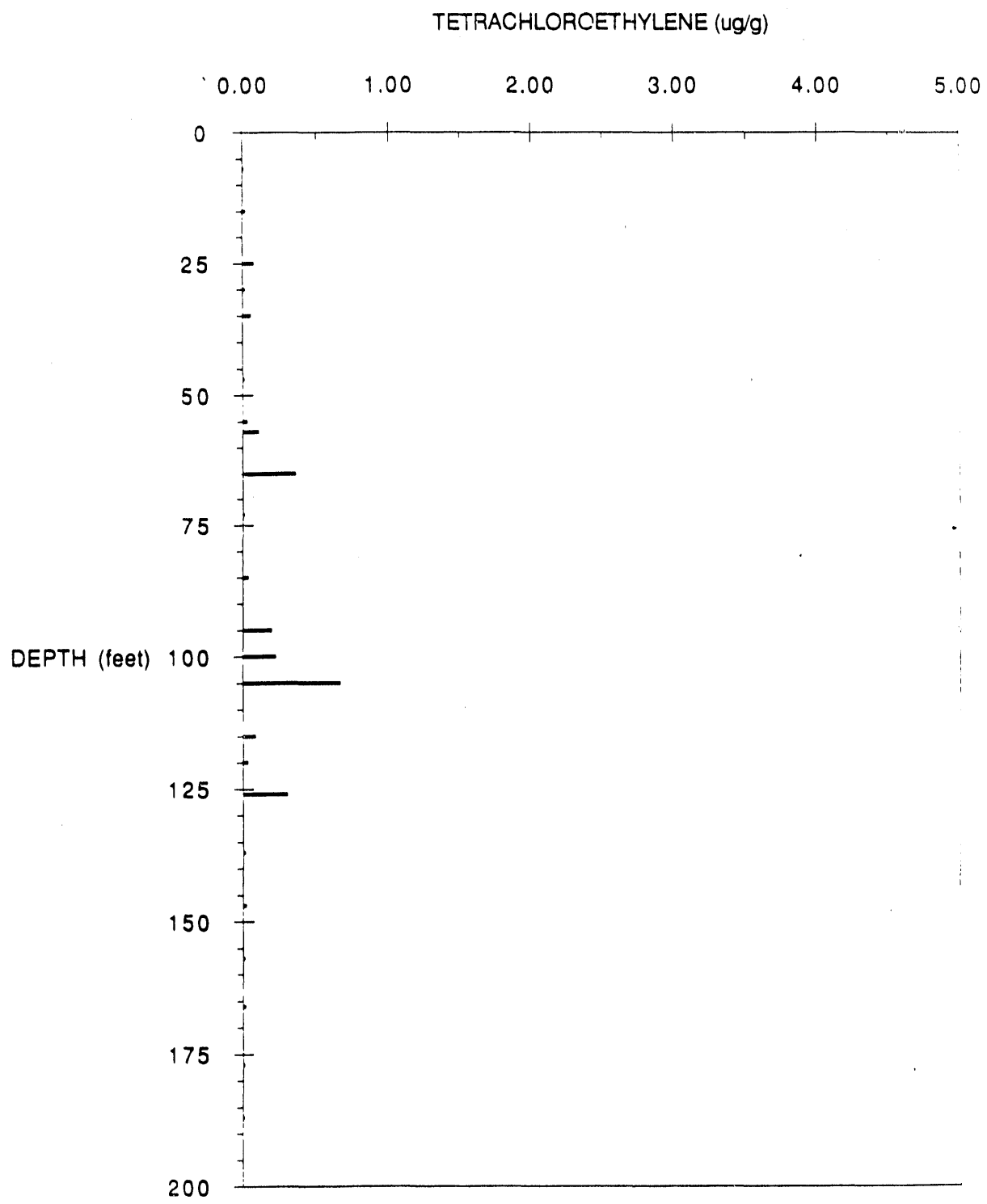


Figure 7.18 Plot of PCE Concentration vs. Depth in Sediment for MHT4C

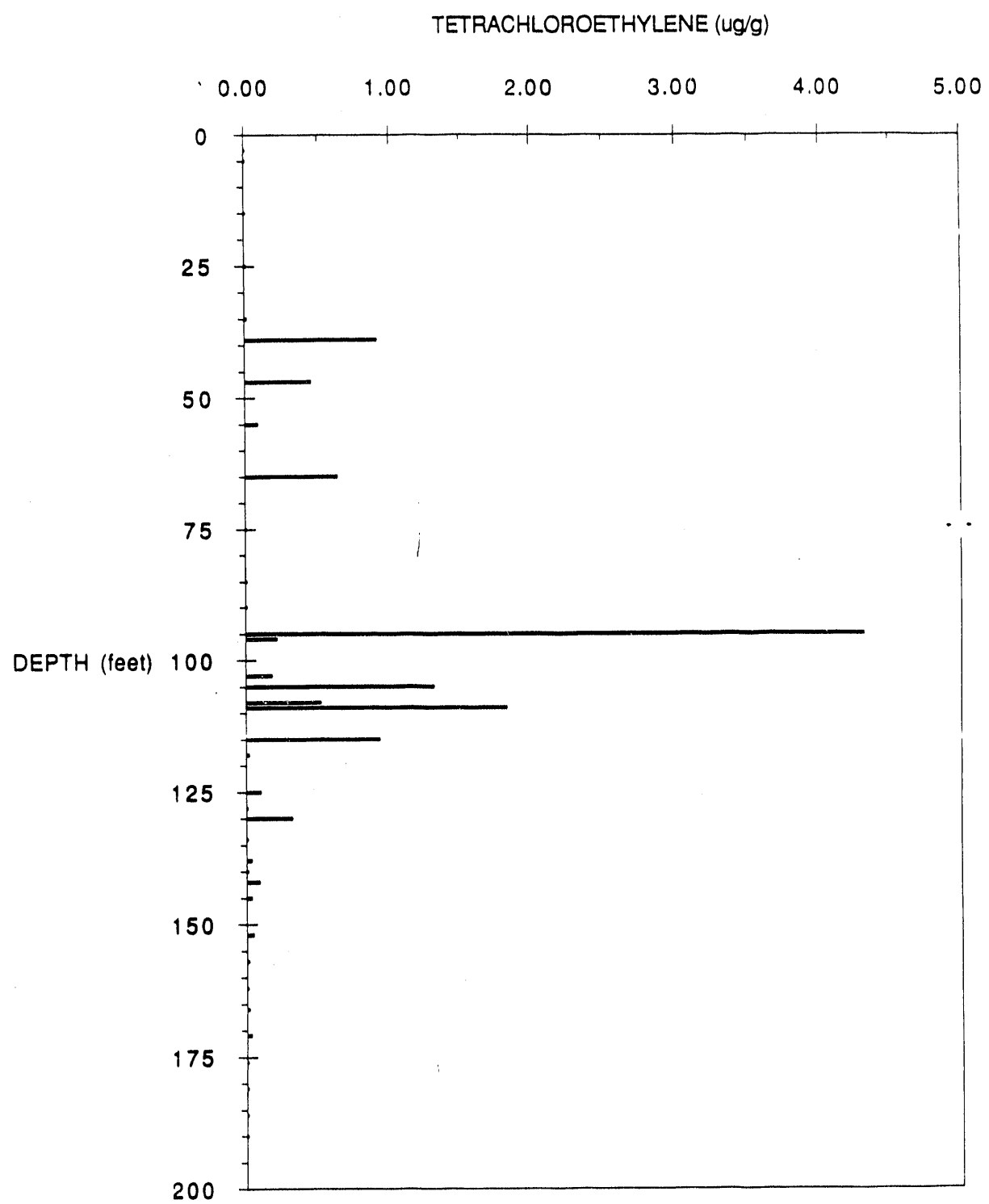


Figure 7.19 Plot of PCE Concentration vs. Depth in Sediment for MHT5C

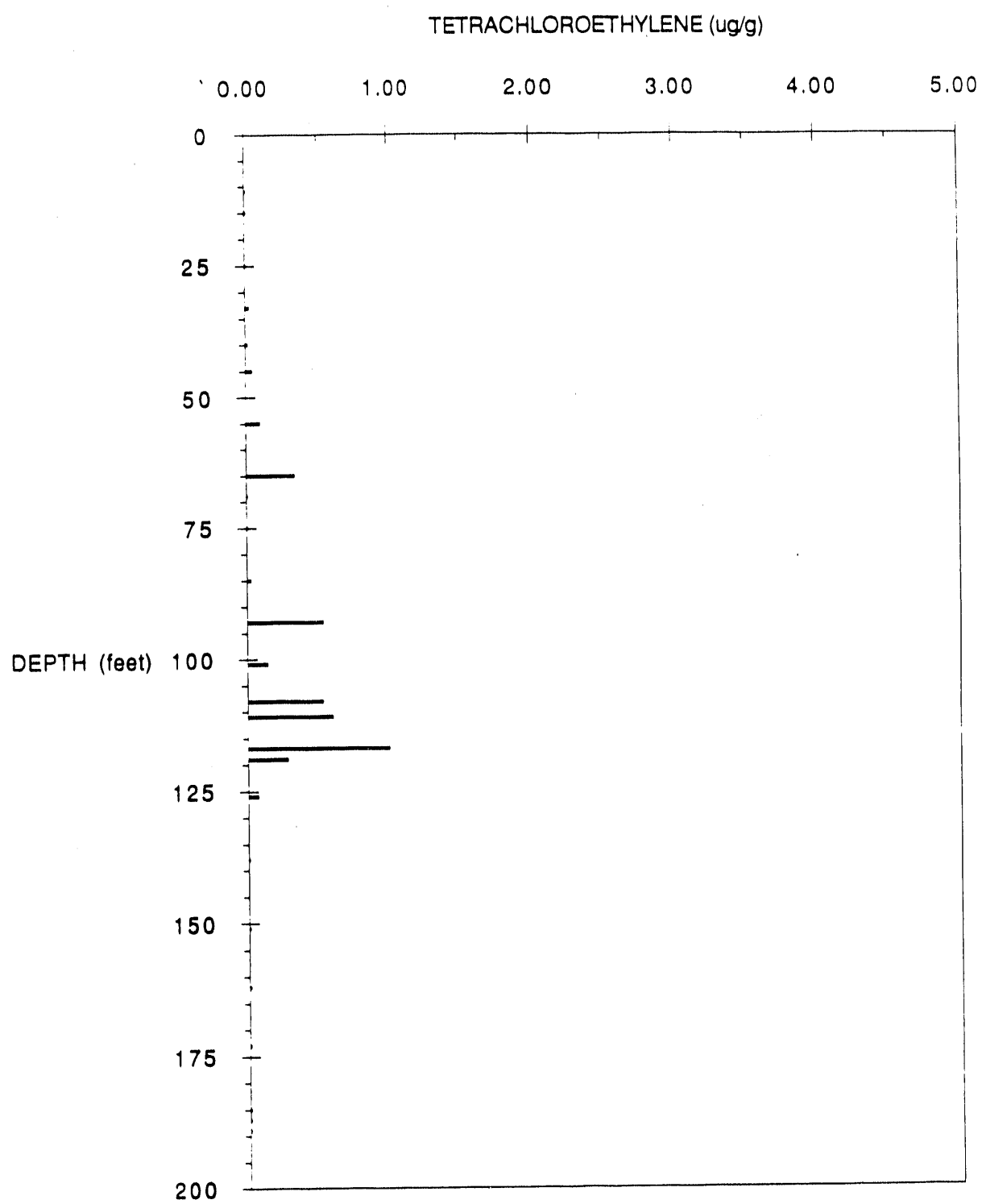


Figure 7.20 Plot of PCE Concentration vs. Depth in Sediment for MHT6C

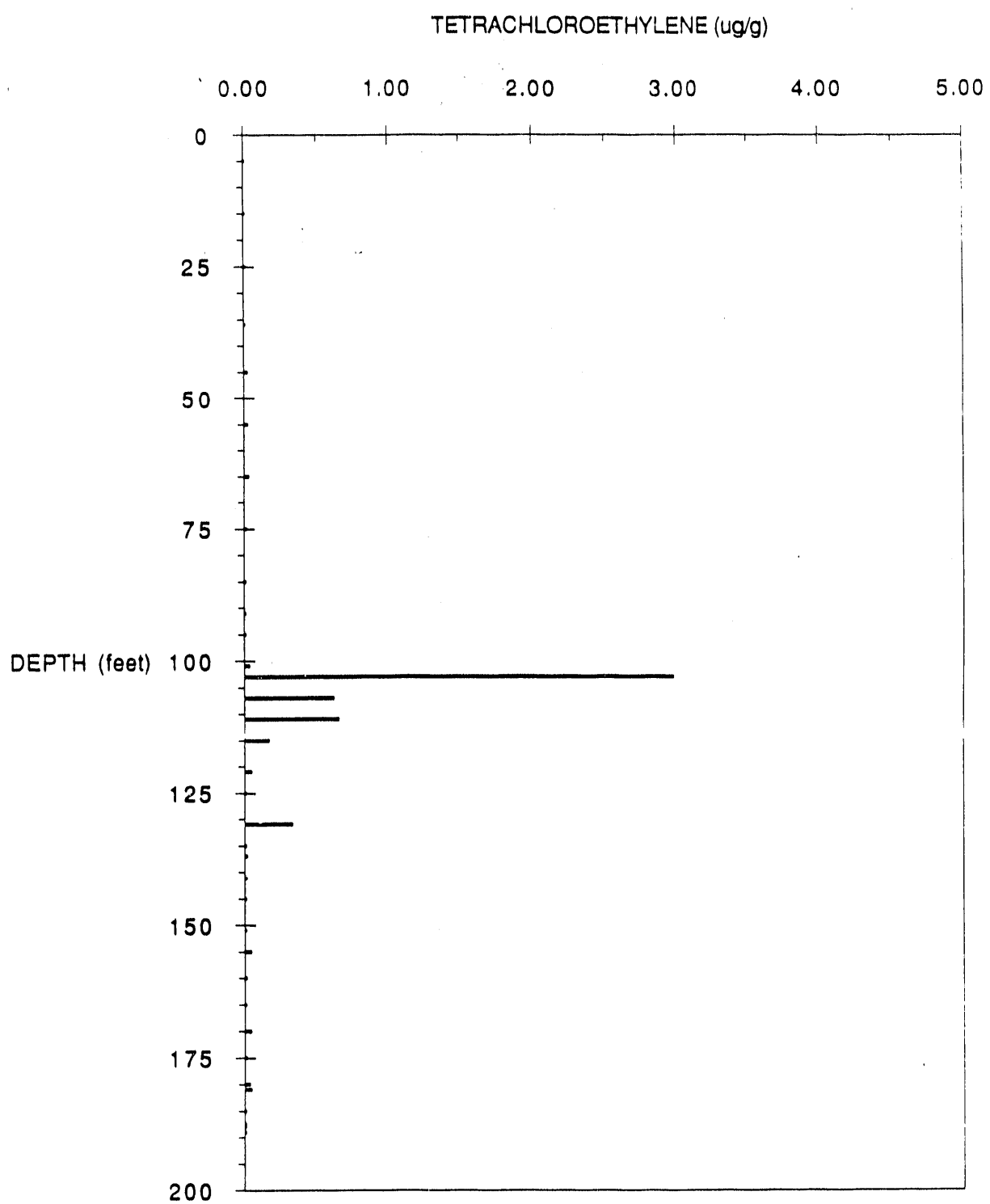


Figure 7.21 Plot of PCE Concentration vs. Depth in Sediment for MHT7C

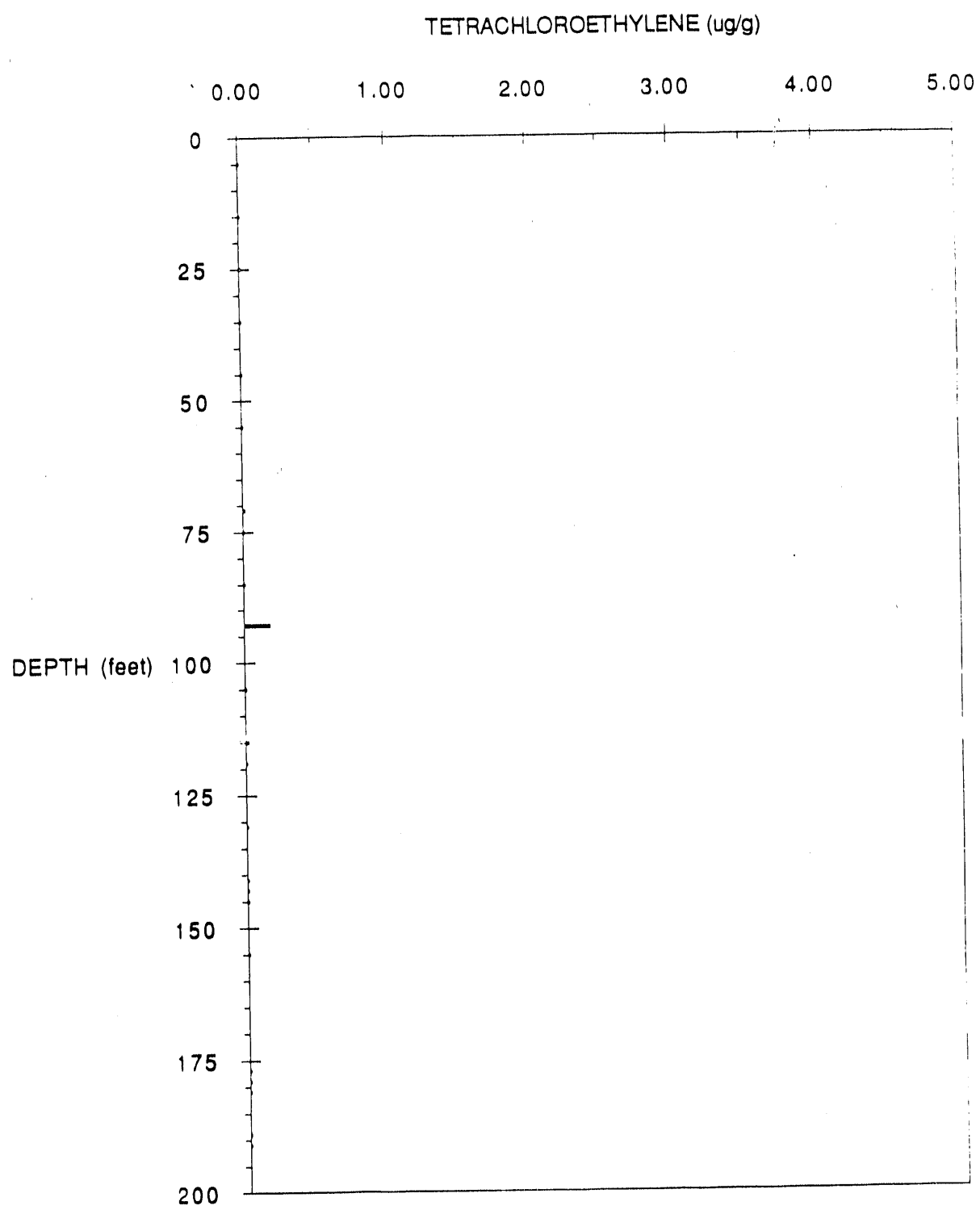


Figure 7.22 Plot of PCE Concentration vs. Depth in Sediment for MHT8C

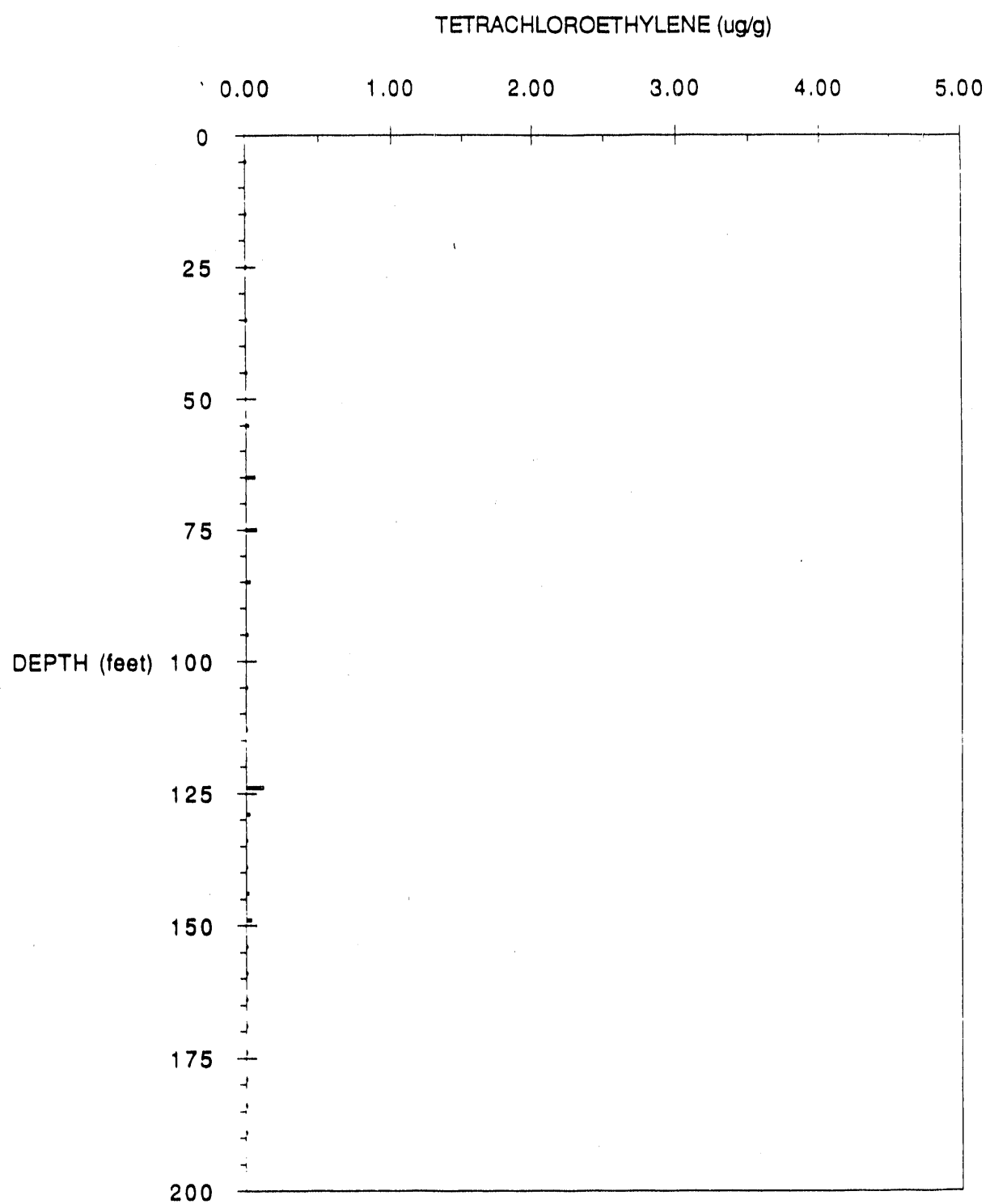


Figure 7.23 Plot of PCE Concentration vs. Depth in Sediment for MHT9C

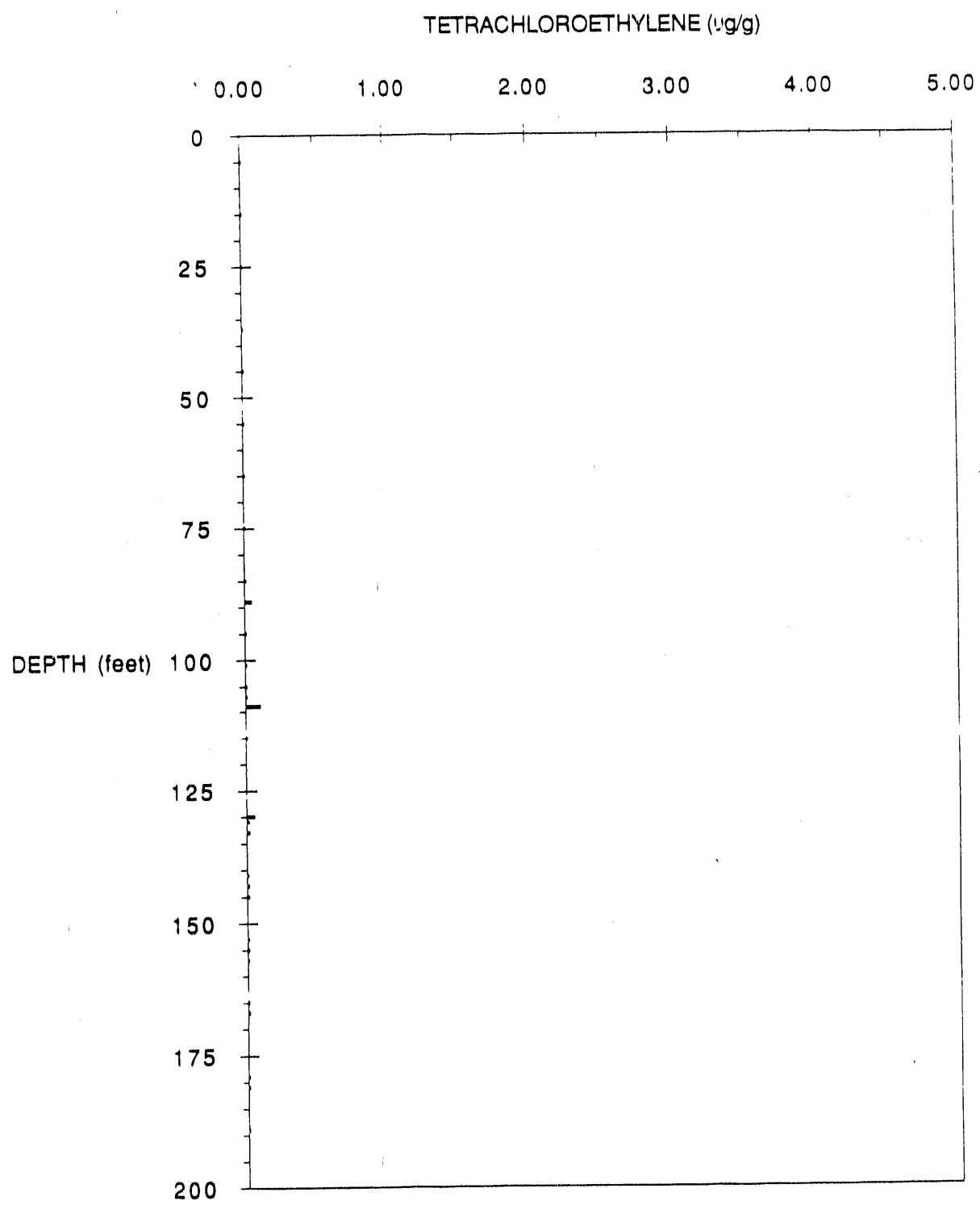


Figure 7.24 Plot of PCE Concentration vs. Depth in Sediment for MHT10C

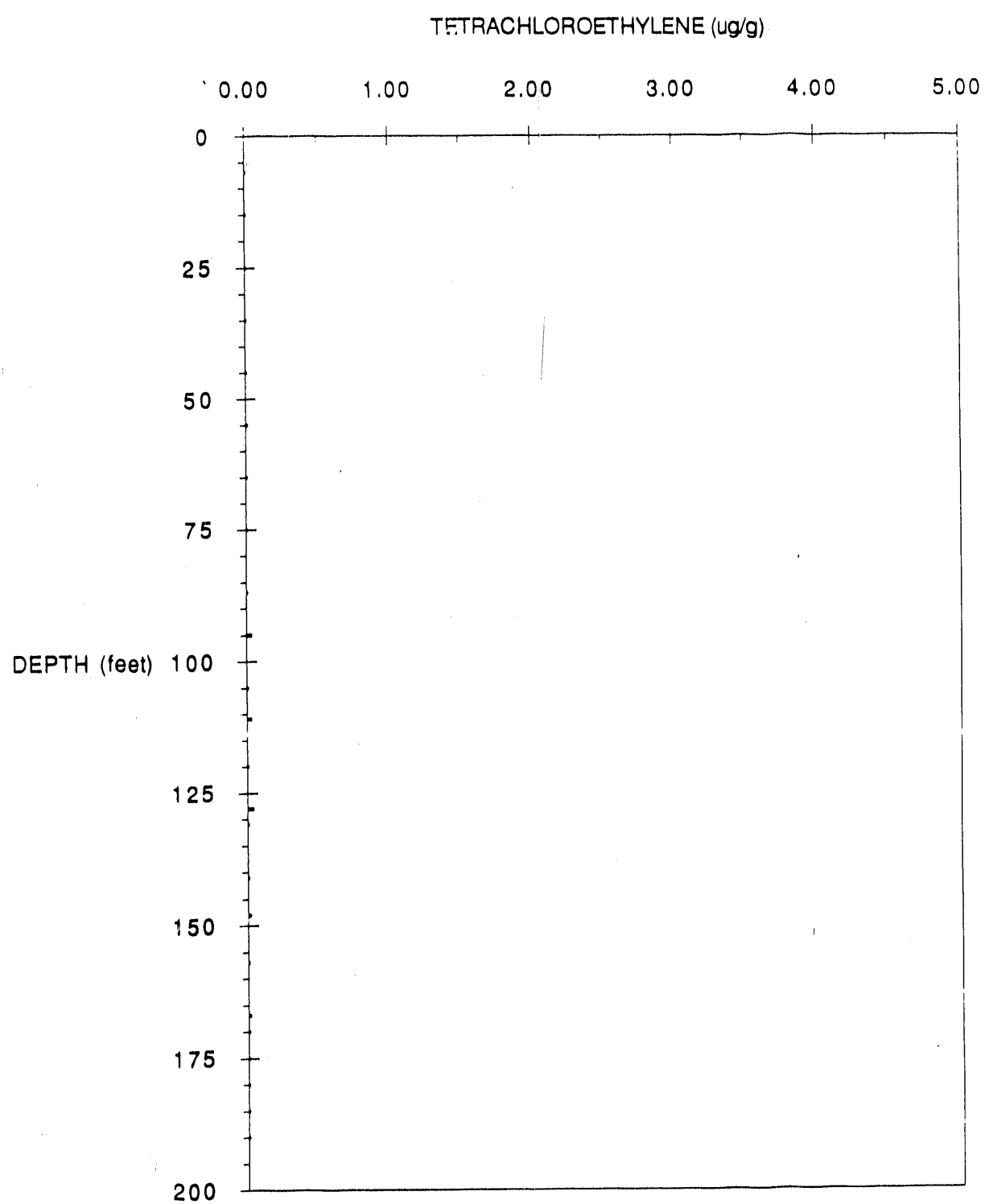


Figure 7.25 Three Dimensional Model of Pretest TCE (Z=1)

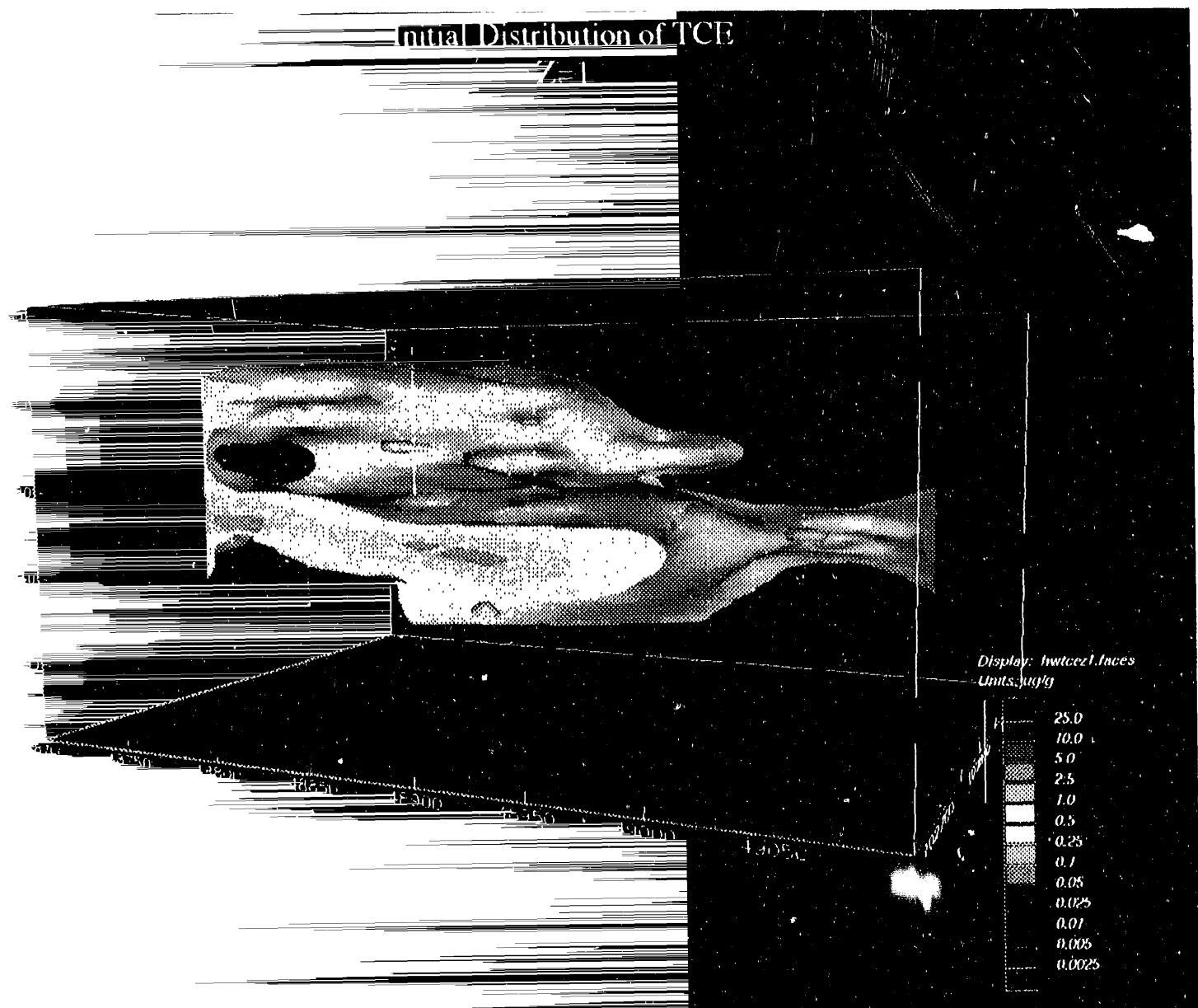


Figure 7.26 Three Dimensional Model of Pretest TCE (Z=0.1)

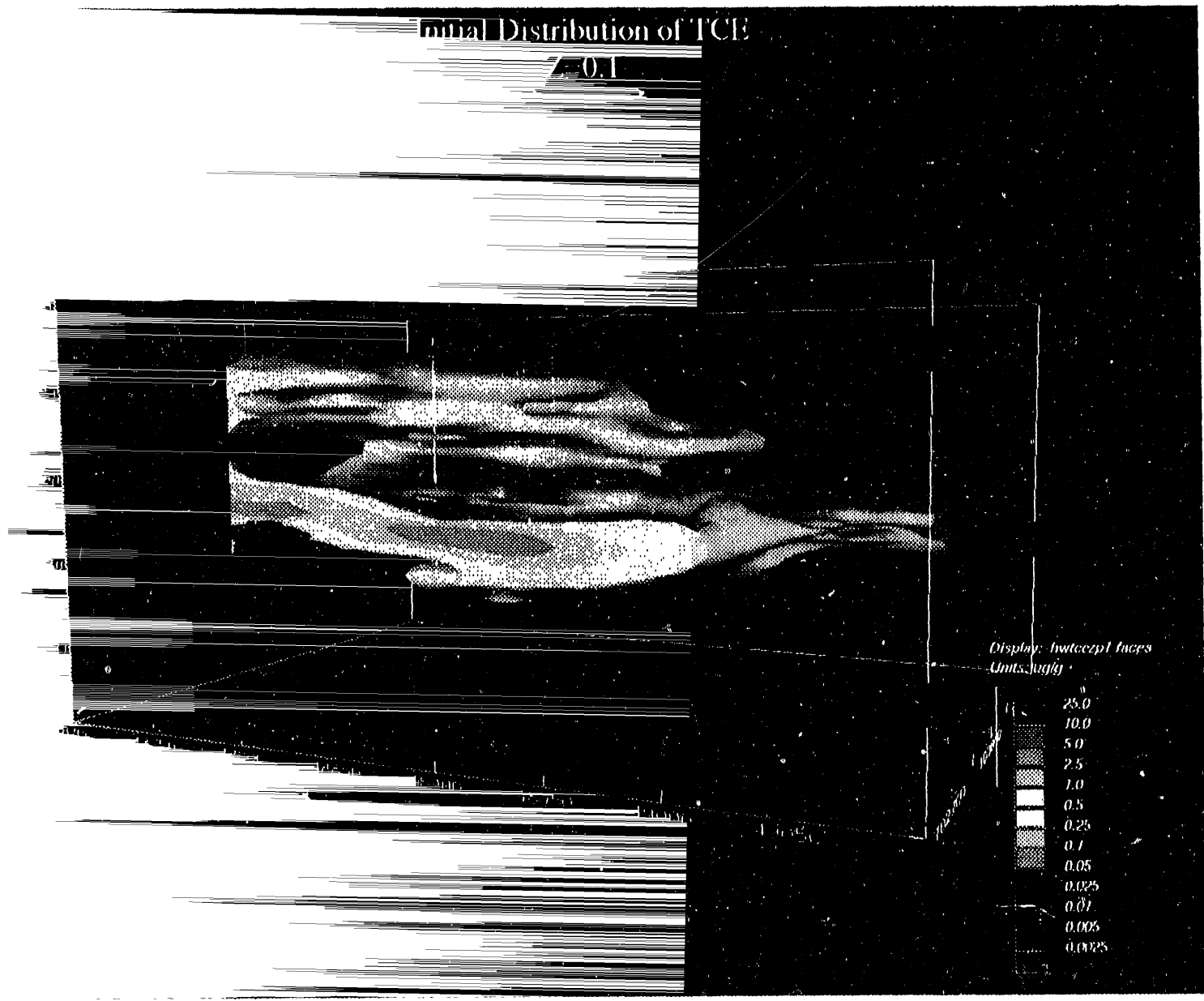


Figure 7.27 Three Dimensional Model of Pretest TCE (Z=0.001)

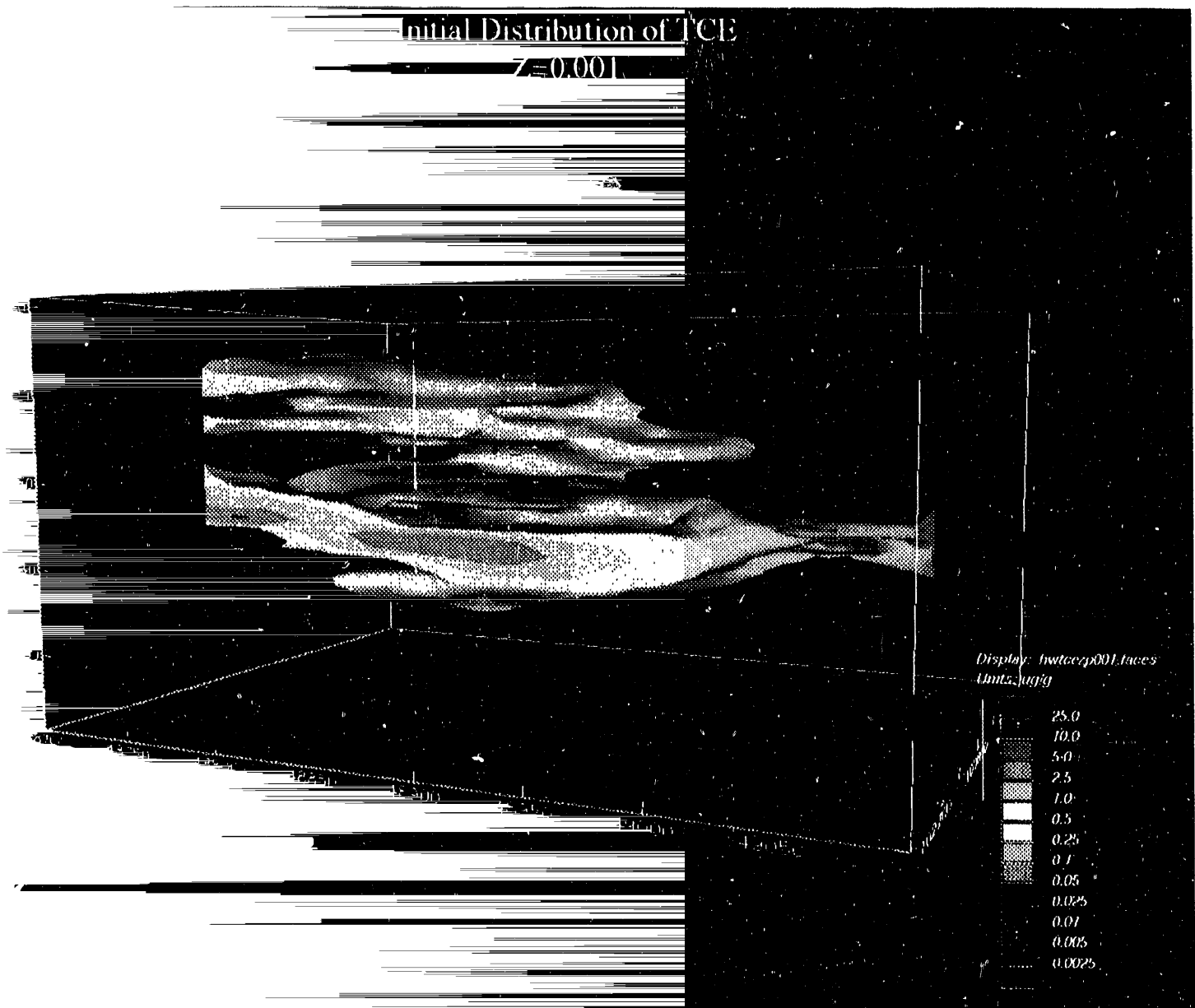


Figure 7.28 Three Dimensional Model of Pretest TCE (Z=0.1, Antilog)

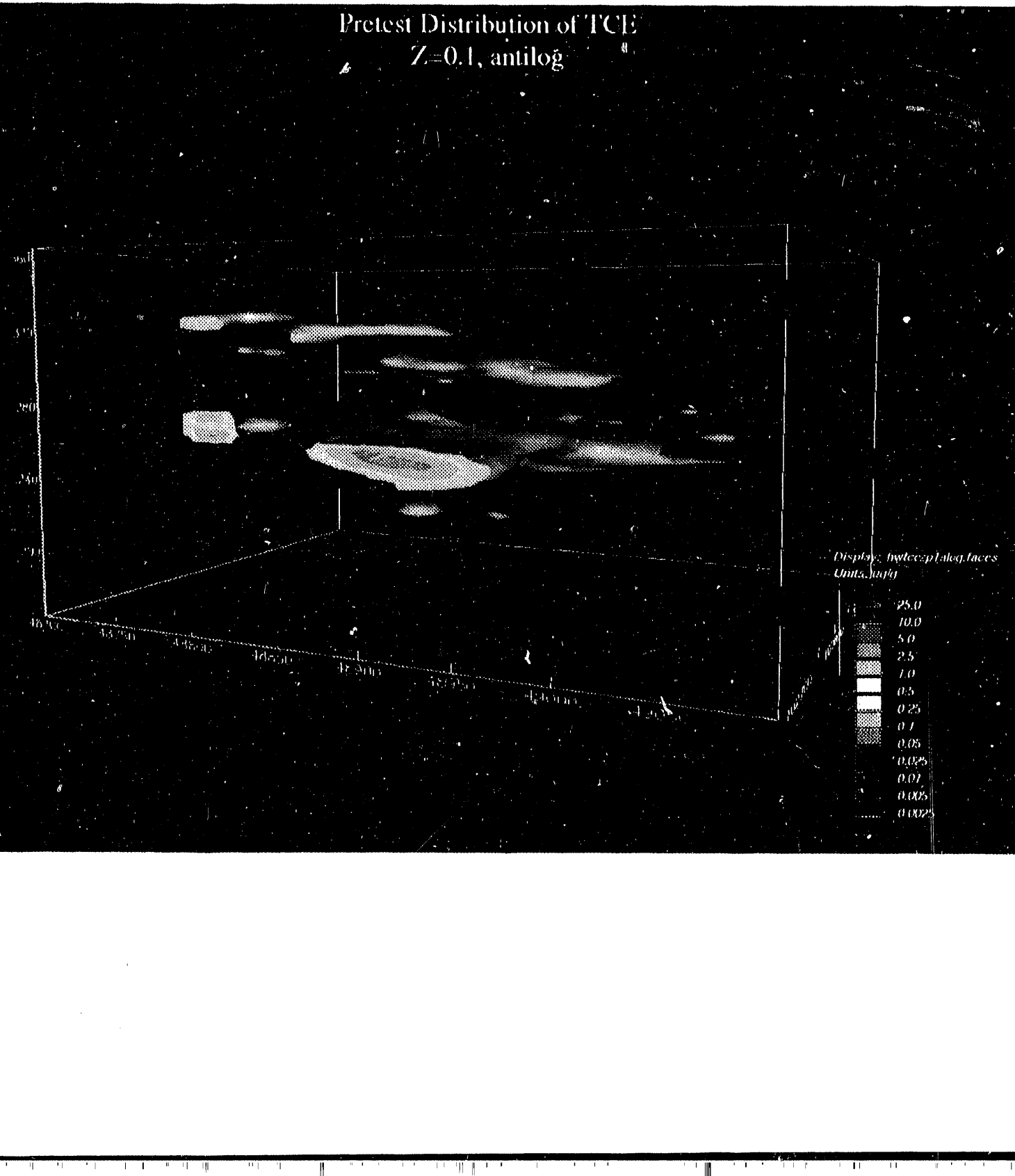
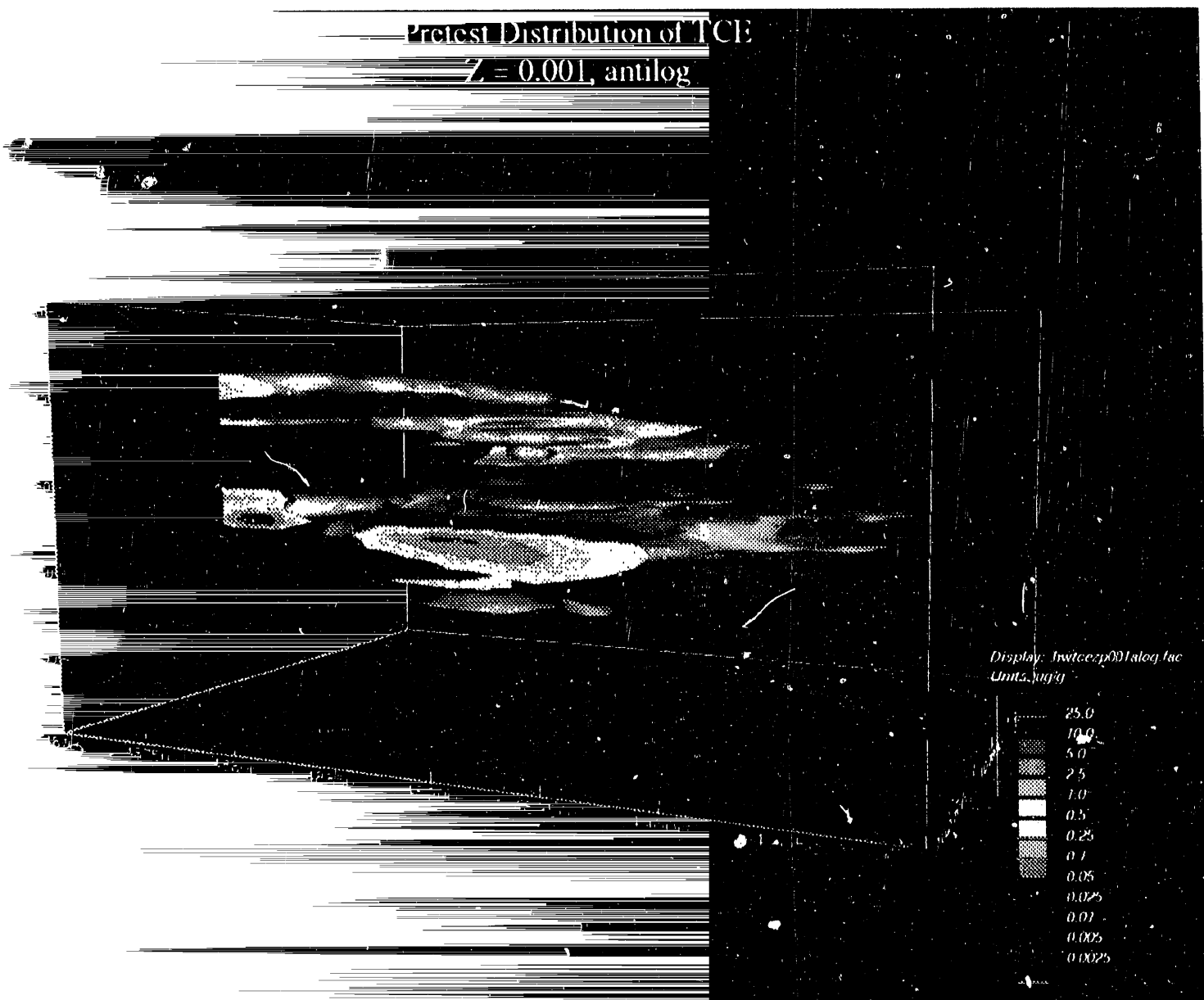


Figure 7.29 Three Dimensional Model of Pretest TCE (Z=0.001, Antilog)



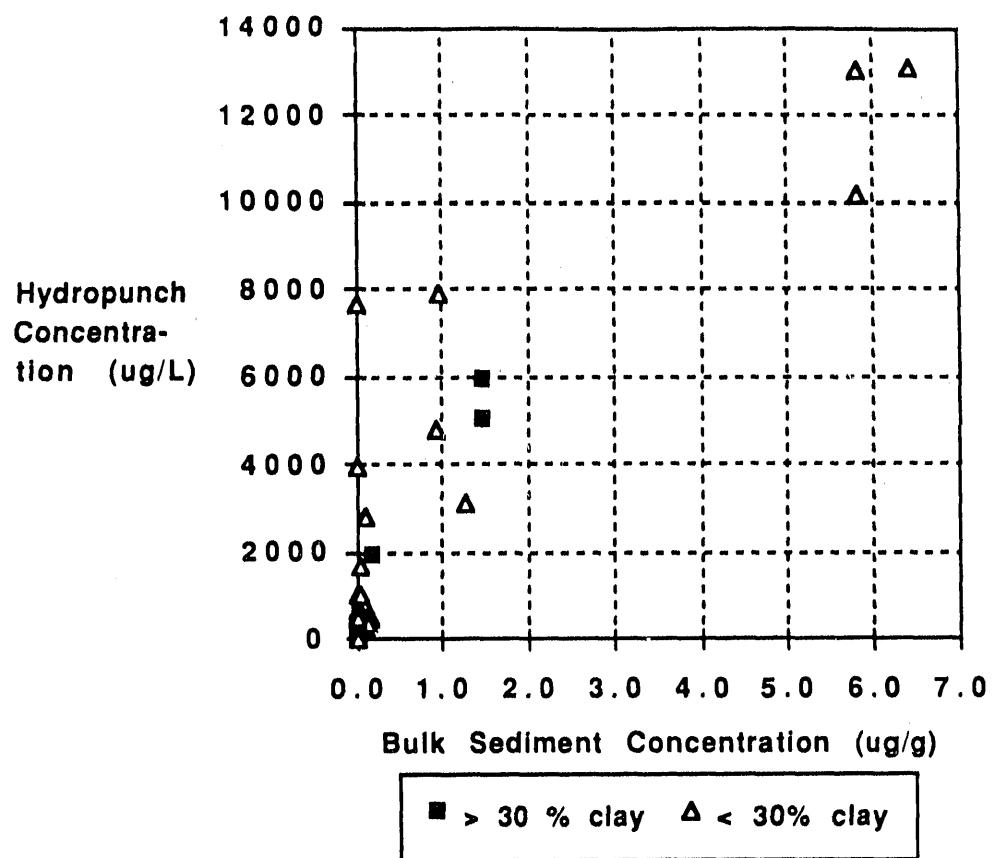


Figure 7.31 Plot of HydroPunch Concentrations vs. Bulk Sediment Concentrations

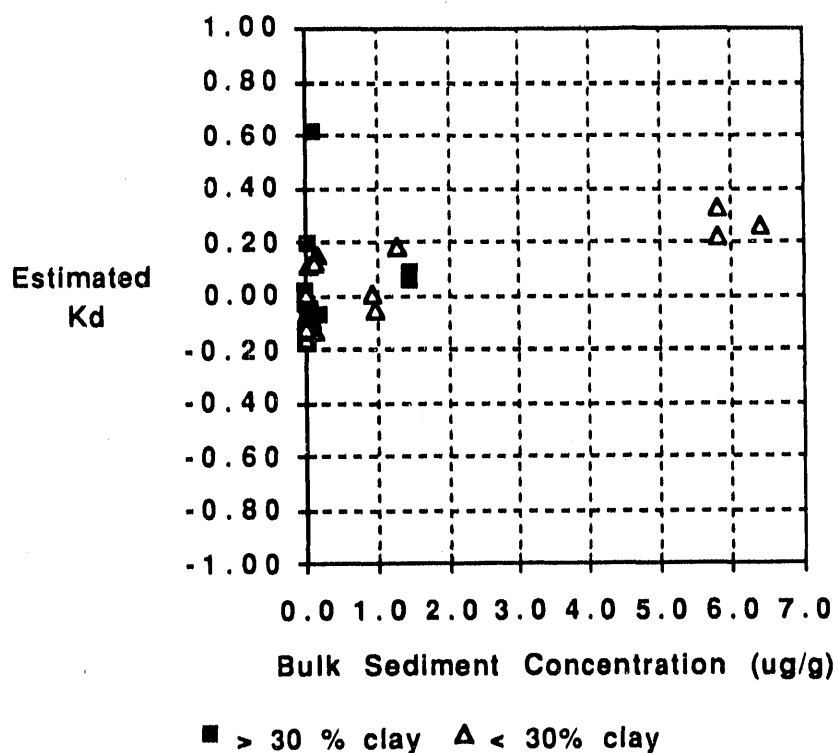


Figure 7.32 Plot of Field Estimated Kd Values vs. Bulk Sediment Concentrations

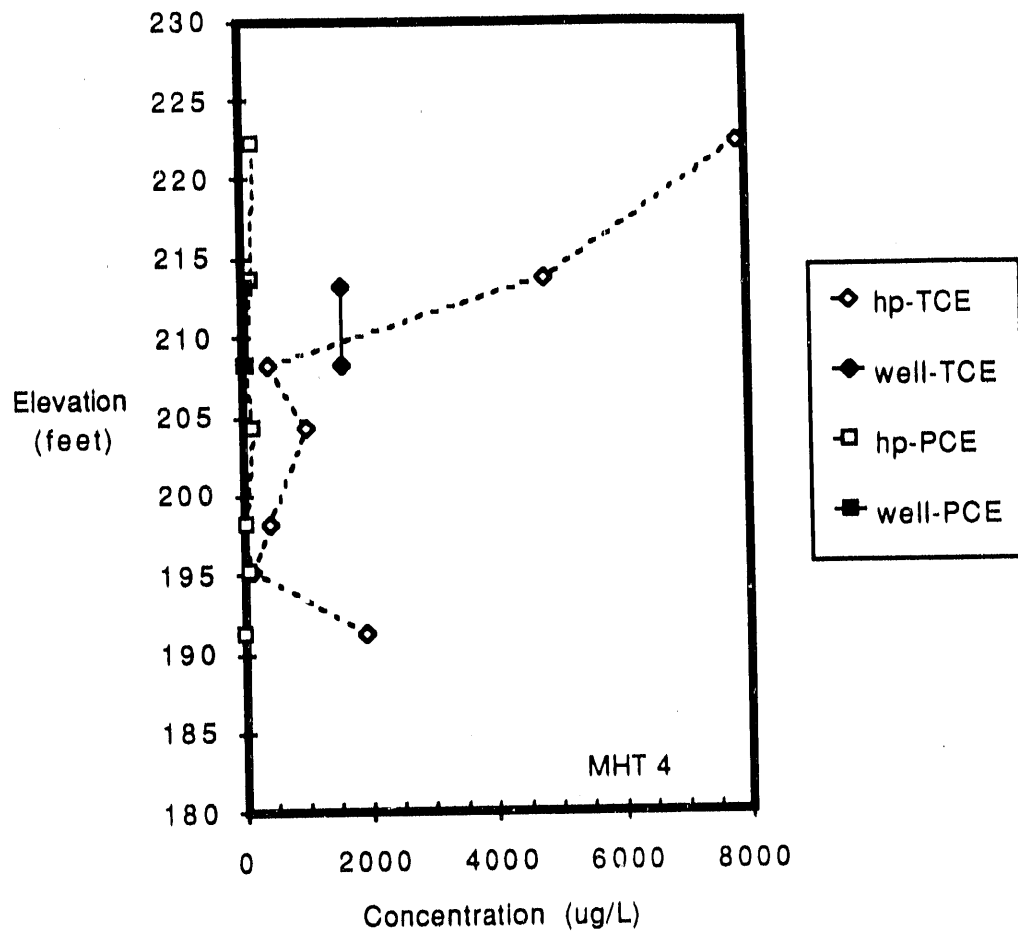


Figure 7.33 Depth Profile of HydroPunch Concentrations and Well Water Concentrations From MHT 4C

FIGURE 7.34 CHANGES IN DIRECT COUNT BY DEPTH

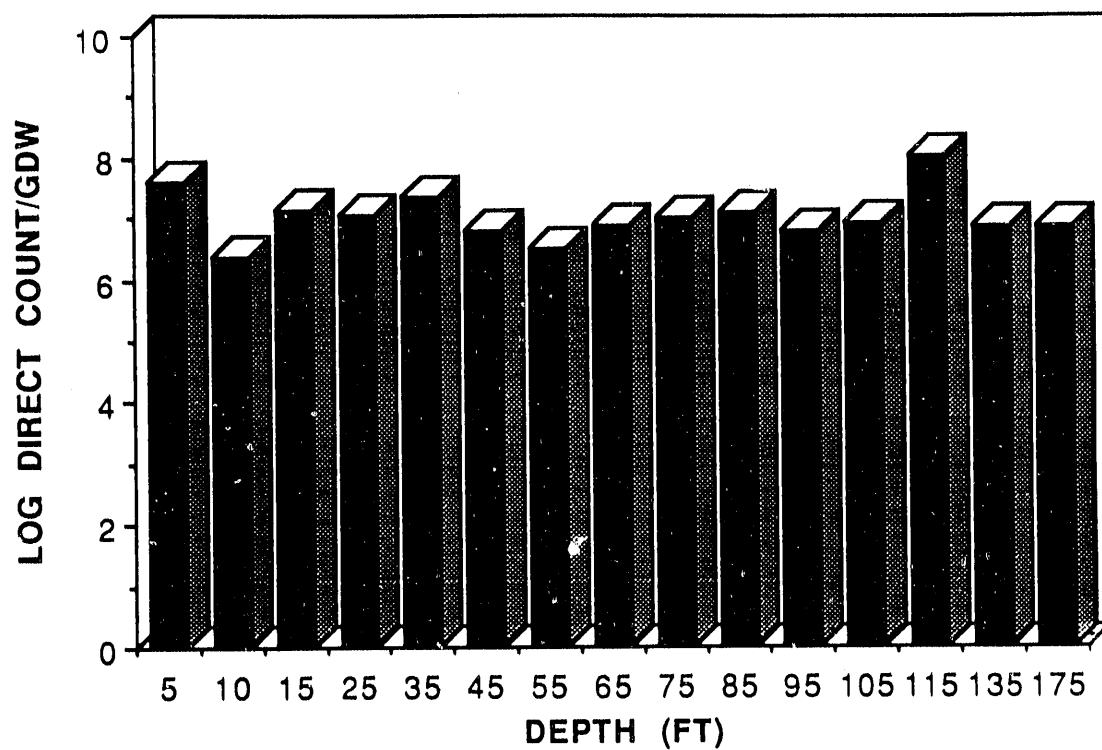


FIGURE 7.35 CHANGES IN MHT-2C PLATE COUNT BY DEPTH

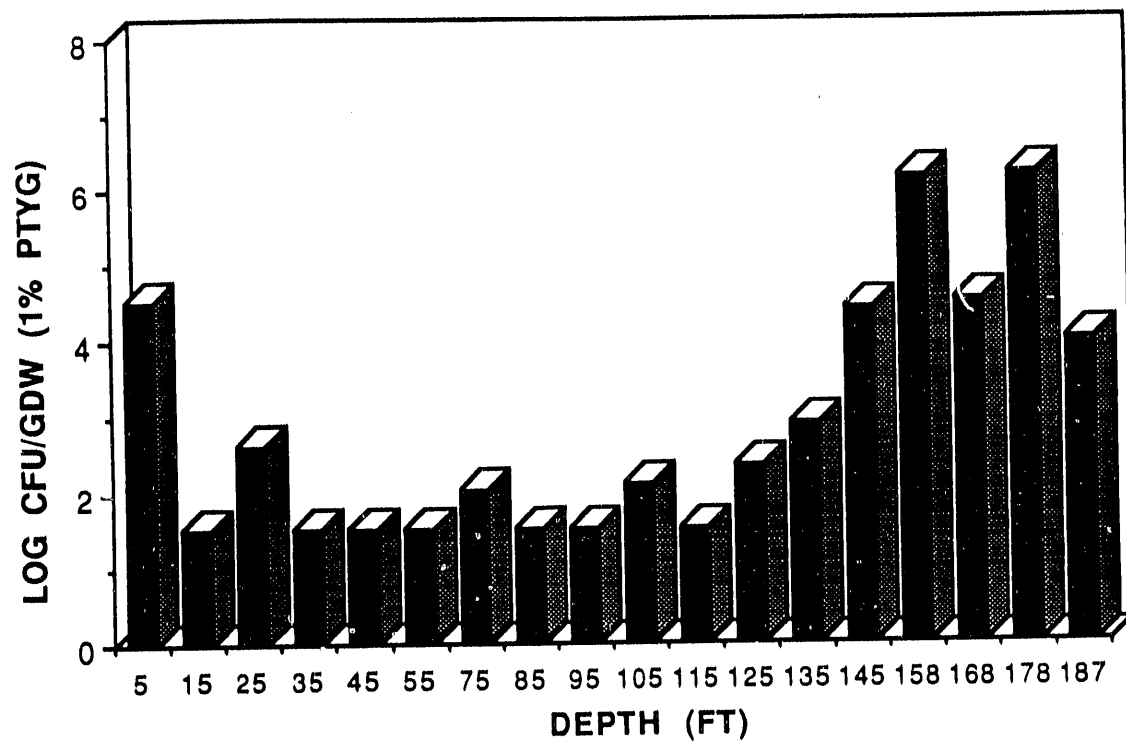


FIGURE 7.36 CHANGES IN MHT-8C PLATE COUNT BY DEPTH

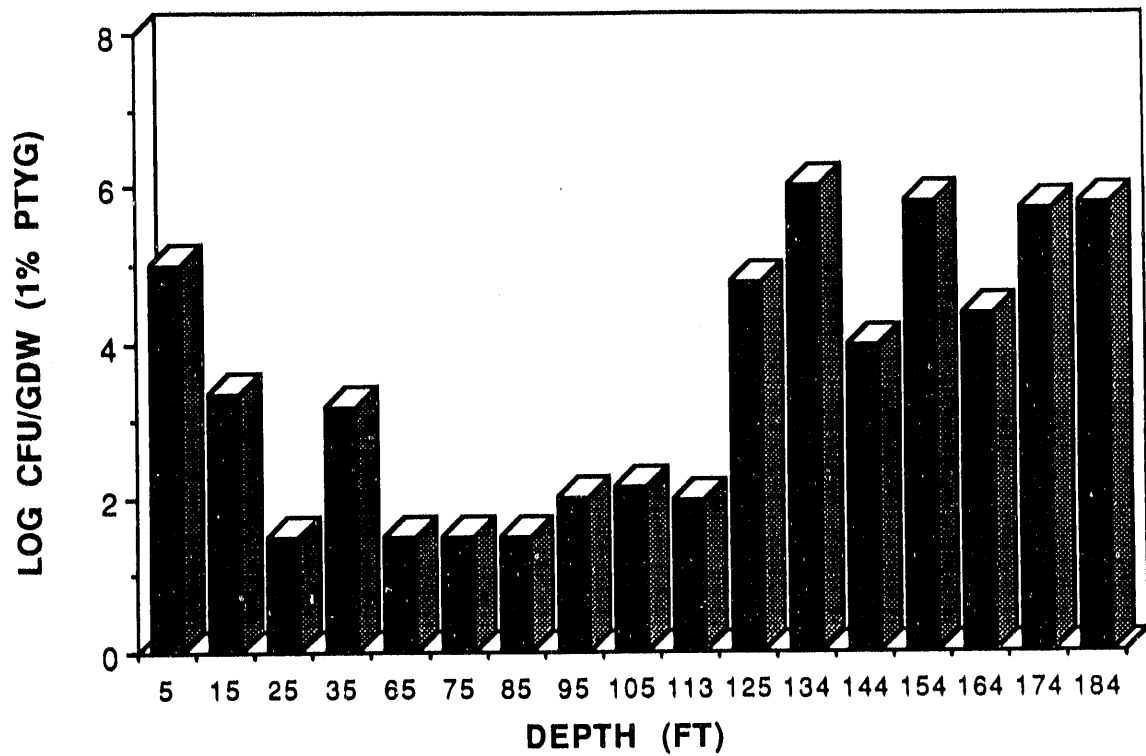


FIGURE 7.37 CHANGES IN AVERAGE 1% PTYG BY DEPTH

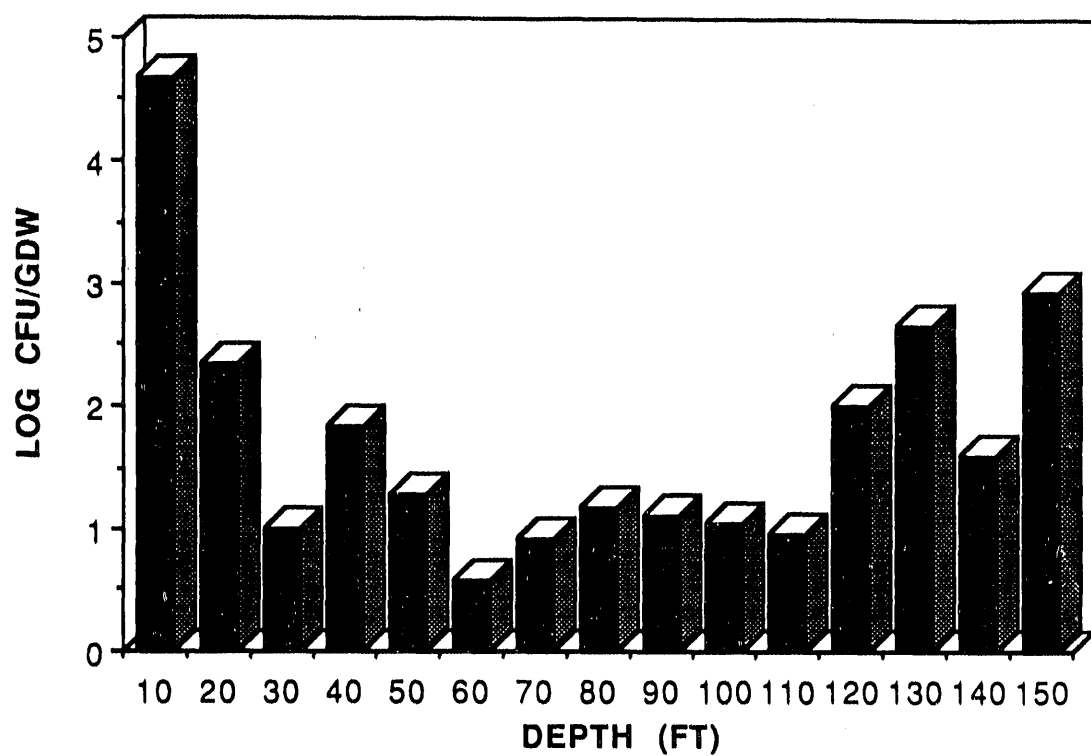


FIGURE 7.38 BACTERIA (DRILLING FLUID vs. SEDIMENT)

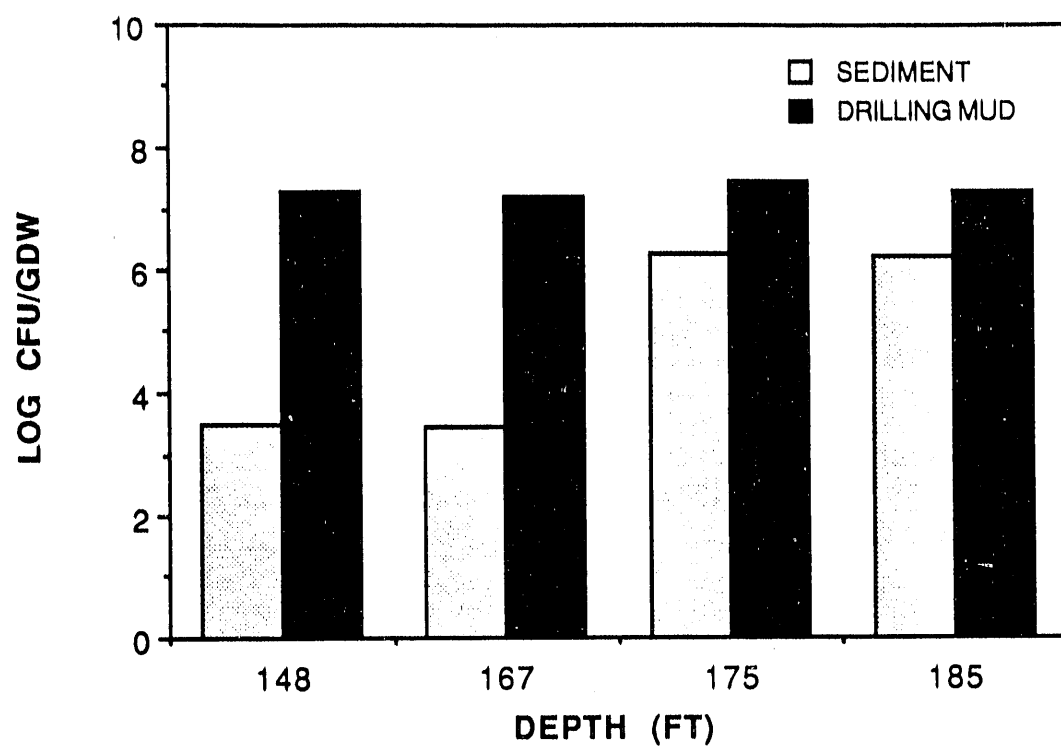


FIGURE 7.39 COMPARISON OF MHT-5C DIRECT AND PLATE COUNTS

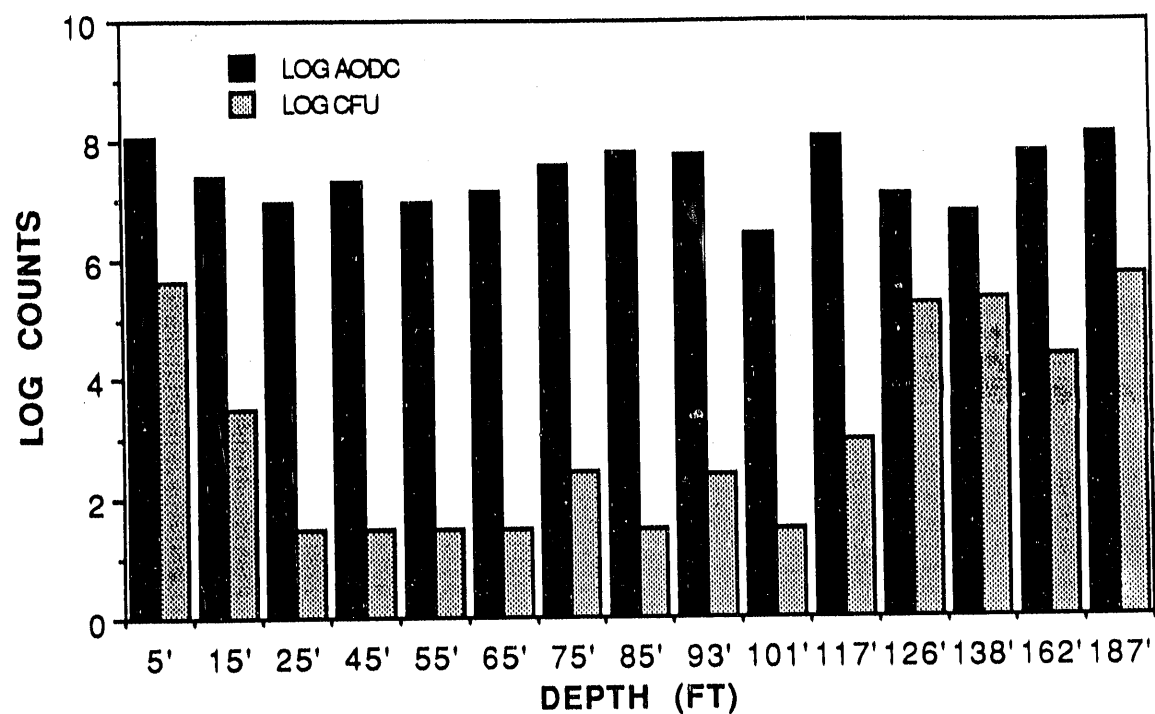


FIGURE 7.40 RATIO OF MHT-5C DIRECT COUNTS TO PLATE COUNTS

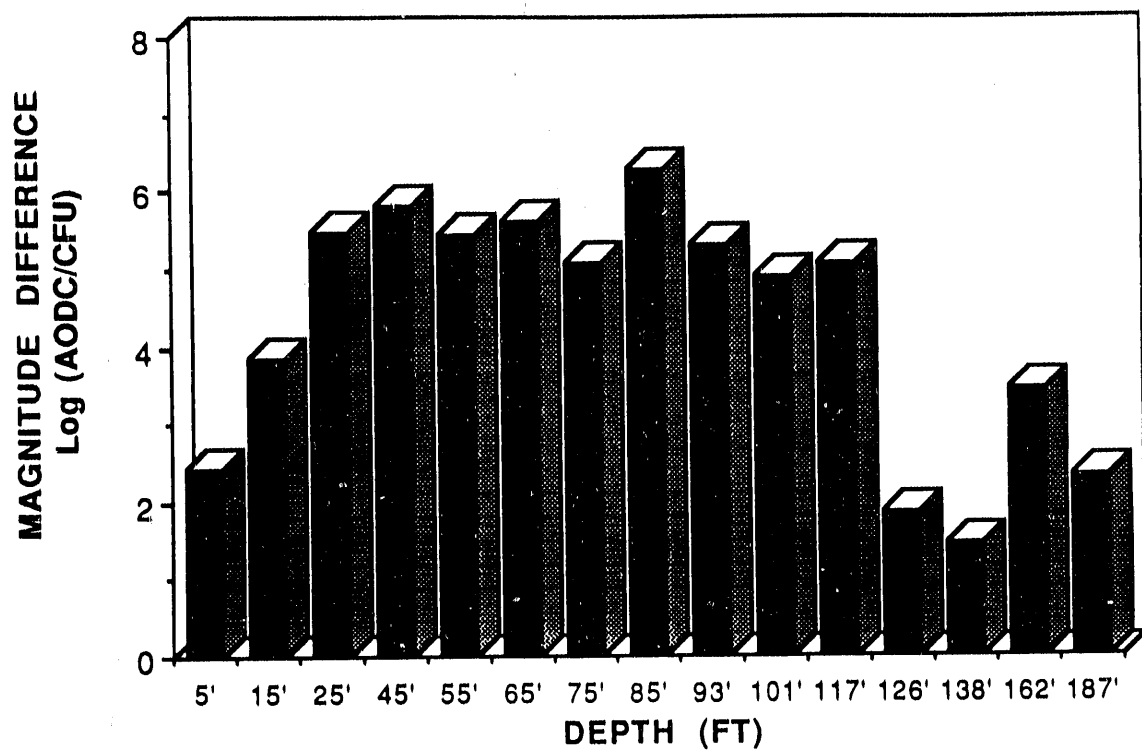


FIGURE 7.41 MHT-3C BACTERIAL DIVERSITY BY DEPTH

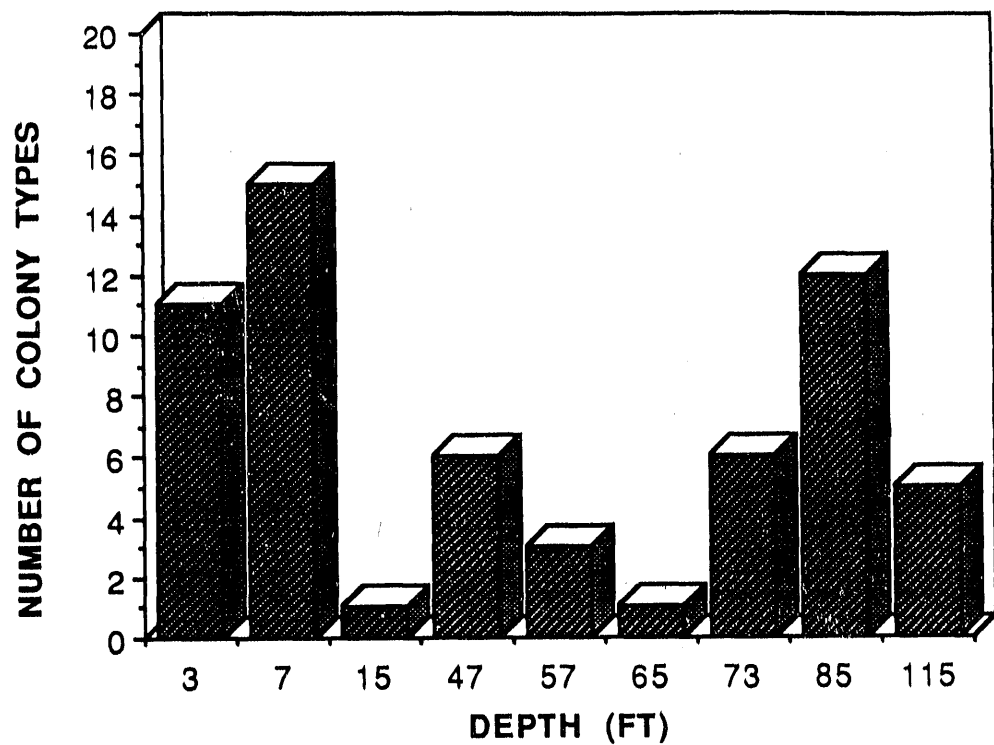


FIGURE 7.42 MHT-3C BACTERIAL DIVERSITY BY DEPTH

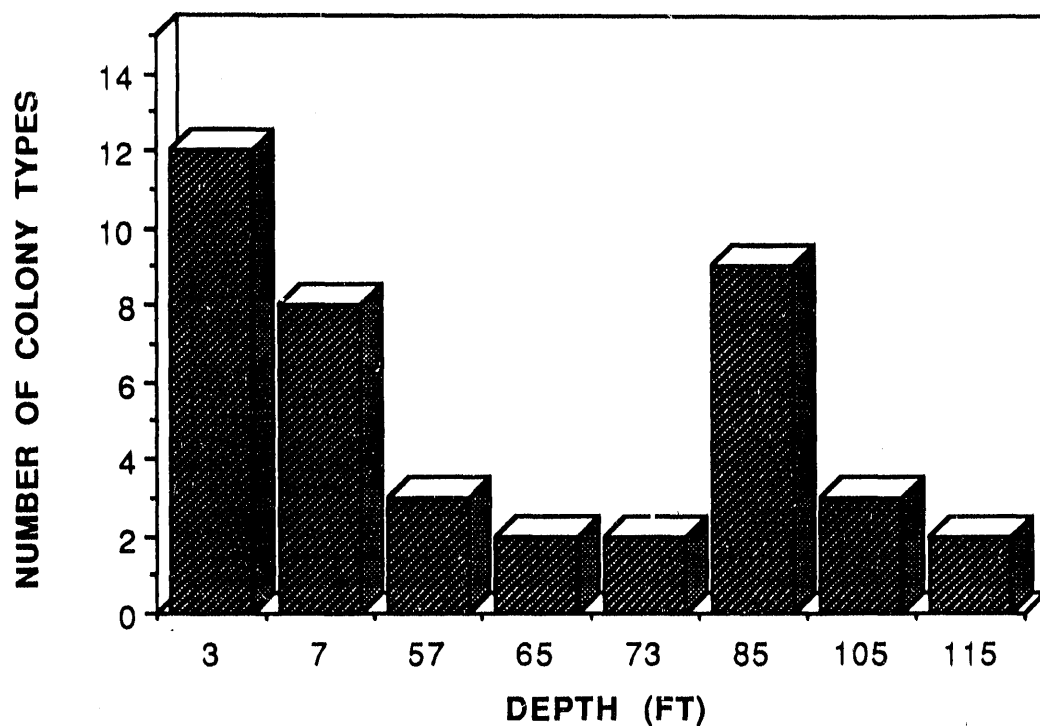
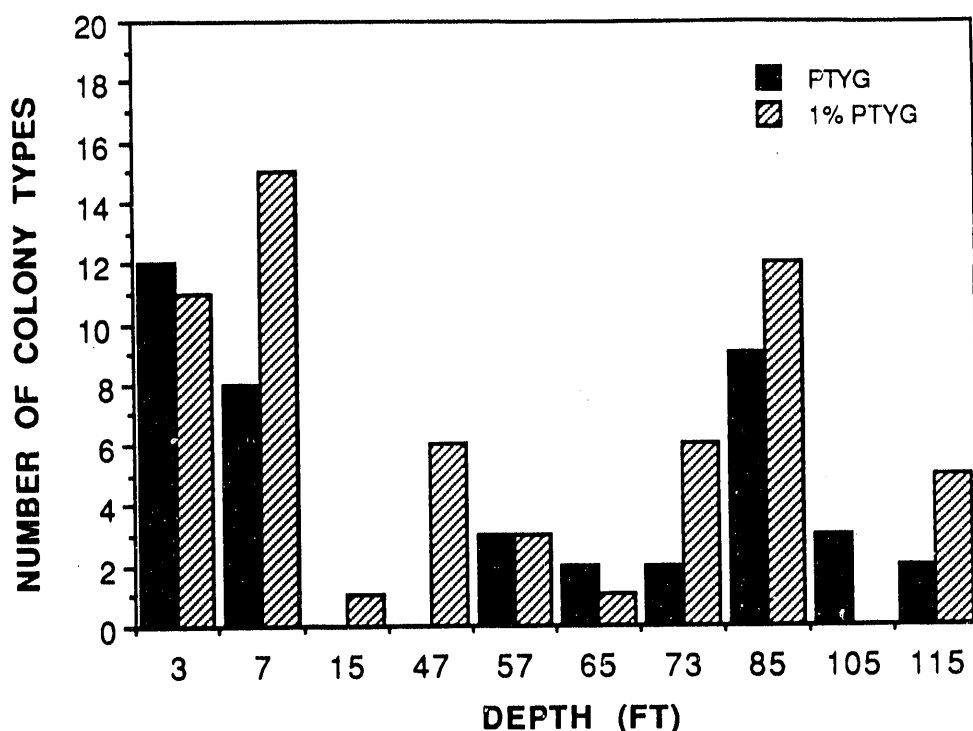
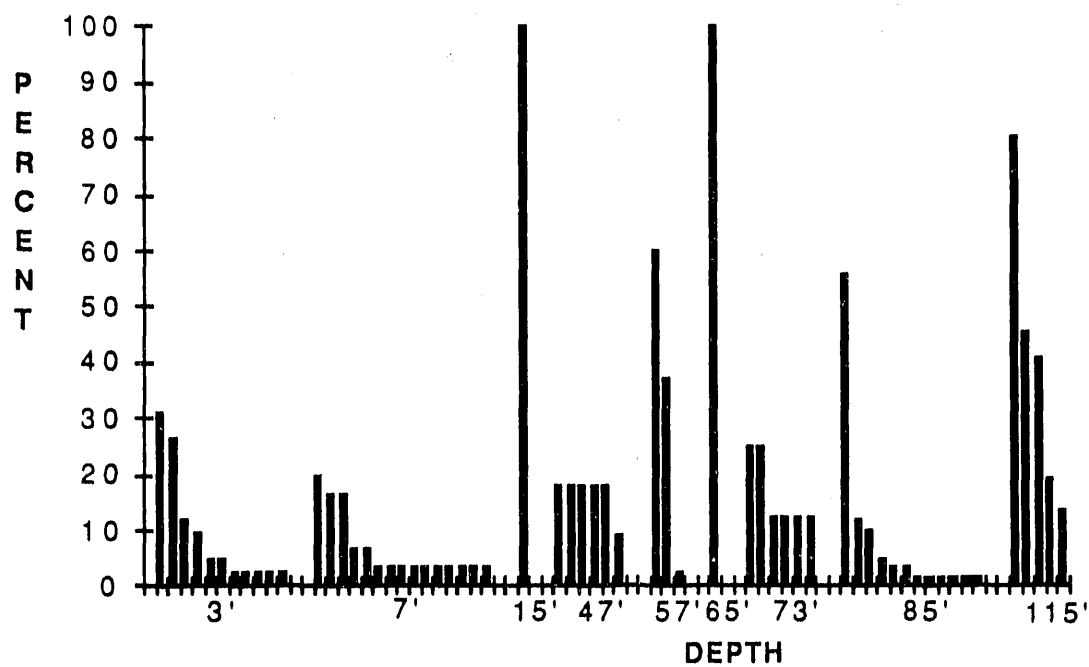


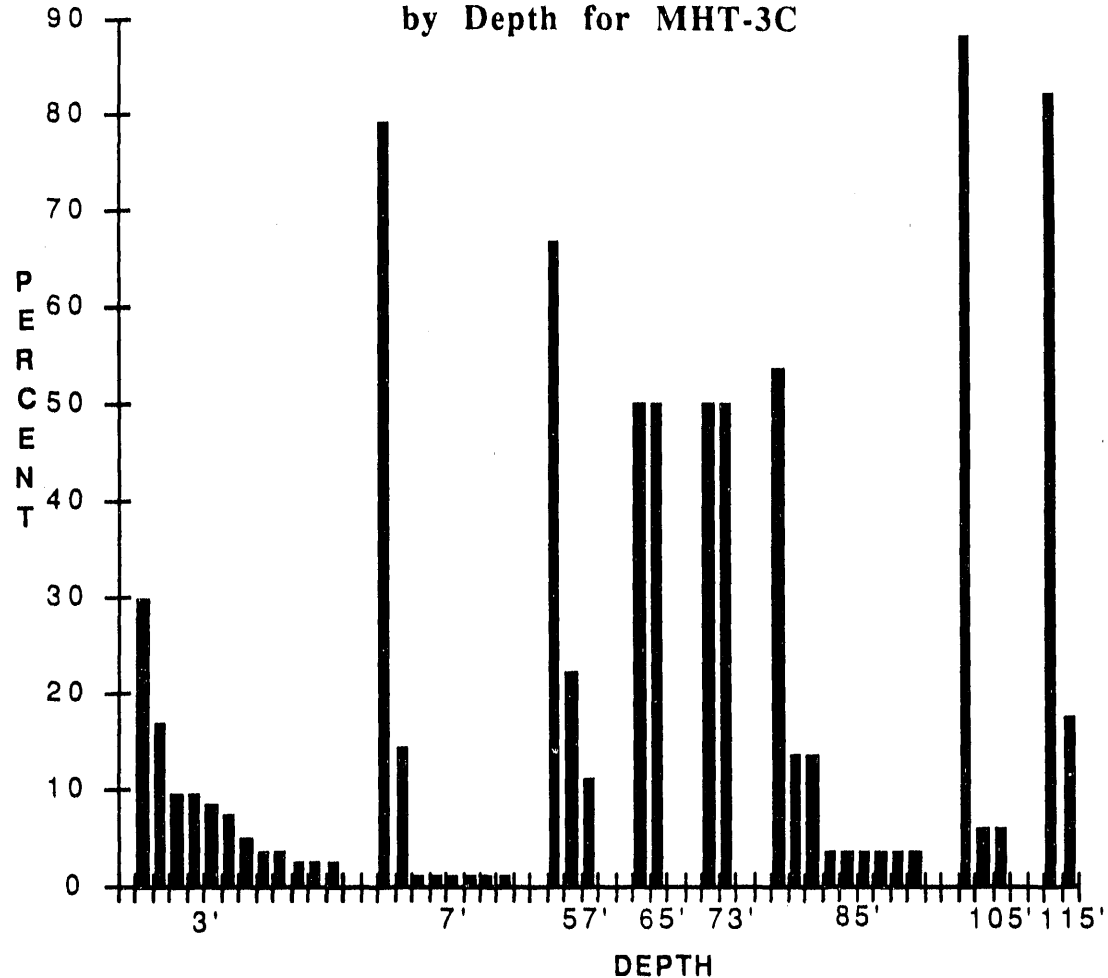
FIGURE 7.43 MHT-3C BACTERIAL DIVERSITY BY DEPTH



**FIGURE 7.44 ALLOCATION SPECIES FROM
1% PTYG TO MHT-3C COMMUNITY BY DEPTH**



**Figure 7.45 Allocation Species from PTYG to Community
by Depth for MHT-3C**



8.0 Summary

The study area is composed of layered sand, clay, and gravel deposited during the Middle to Upper Eocene in shallow marine, lagoonal, or fluvial environments. Standard geologic techniques were used to correlate sedimentary units and to establish a regional stratigraphic and hydrostratigraphic framework at the site. Clay layers in the study area are generally relatively thin and discontinuous and do not form impermeable aquitards. The upper two hundred feet of the stratigraphic sequence is of interest to this study and consists of a vadose zone, a relatively thin water table, an underlying semiconfined zone, and is bounded at the base by the top of a confined aquifer. Aquifer parameters for the site that were estimated by pump tests, calibrated models, and sieve analysis are consistent with values expected for interbedded sands silts and clays found at other locations at SRS and in Coastal Plain sediments.

Groundwater

Concentrations of volatile organic contaminants in the groundwater vary vertically and horizontally beneath the site. Concentrations of TCE and PCE measured in groundwater collected from wells in the study area range from approximately 400 to 1800 ppb for TCE and 20 to less than 200 ppb for PCE. Samples collected with the HydroPunch sampler spanned a wider range from less than detection to 13,000 ppb for TCE and less than detection to 280 ppb for PCE. The apparent discrepancy between the ranges measured between samples collected from wells and by the HydroPunch results in part from the homogenization of the water samples over the length of the screen. This comparison indicates that the HydroPunch is collecting high quality groundwater samples at discrete depths. Despite the significant operational problems, these results suggest the HydroPunch yields valuable information for plume definition. Modifications, such as the addition of an air line in applications employing mud rotary drilling, should be performed to minimize the problems encountered.

Sediments

The distribution of VOC contamination in the sediment at the site is also heterogeneous. Over 1000 sediment samples from the MHT and MHV cores were analyzed for TCE and PCE. Measured concentrations of PCE and TCE range from less than detection to 16 ppm for TCE and from less than detection to 5 ppm for PCE. Generally, the highest levels of contamination were found slightly above and within the clay rich zones. The most contaminated zone in most of the borings was found slightly above, at, or less than 15 feet below the top of the tan clay zone. The pattern produced by three dimensional modeling of the contaminants in the sediments mimics the cross section prepared from lithologic data suggesting that the distribution of contamination is controlled by lithology. Three dimensional modeling is a powerful tool for the interpretation of contaminant data. The best model for the stratified sediments at the site was prepared by gridding the log values of contaminant data using 2-D minimum tension gridding on each X/Y plane and then taking the antilog of the grid values. The three dimensional modelling shows that most of the contamination at the site is associated with the clay zone at and below the 270 foot elevation. Shallower clay zones on the west side of the site near the process sewer line at 325 feet and 300 feet are also contaminated. Additional three dimensional modeling will be done to estimate the contaminant inventory present at the site.

Comparison of the analytical results from the HydroPunch data with the sediment data indicates that significant quantities of VOC have been lost from the core in the saturated zone. The results suggest that VOC loss during sediment sampling may be more significant for the sandier samples. Sampling and analytical protocols used to collect sediments samples minimize VOC loss due to rapid sample handling and sealing in final form in the headspace vial in the field. The data suggest that VOC loss from the core may result from core drainage or infiltration of the core by uncontaminated drilling fluid.

Microbiology

Overall, the total number of organisms present at various depths at the site appear approximately equivalent to the number of organisms found in the subsurface at other parts of this country. However, the number of organisms culturable from the vadose zone is lower than that generally reported elsewhere. Diversity in this system is also relatively low. It appears that the vadose zone microbial community at this site is under severe stress. This can probably be attributed to nutrient deprivation. Phospholipid fatty acid analyses show that indeed the organisms present are in stationary growth phase or in various stages of starvation survival.

Both the fluorescent antibody analyses and the nucleic acid probe analyses suggest that microorganisms capable of degrading TCE/PCE are naturally present throughout the sediment column. TCE-degraders that utilize methane are also present throughout the sediment at the site, this is particularly important to the Phase II demonstration that will involve injection of methane with air into the subsurface. All of these organisms have the potential for growth given ample nutritional requirements.

Important specific related observations are noted below:

Direct counts (AODC) remained relatively constant throughout the sediment column, except for slight increases near the surface and the capillary fringe, and were orders of magnitude higher than the corresponding plate counts. Plate counts showed relatively high counts in the near-surface depths, but numbers declined rapidly in the vadose zone. Fluctuations in plate counts at different depths may be linked to changes in lithology or degree of saturation. Counts increased at or near the saturated zone (capillary fringe) and remained elevated throughout the aquifer.

Saturated zone samples obtained by mud rotary appeared to have disproportionately elevated counts compared to corresponding samples obtained by auguring. Drilling fluids had extremely high counts and may have contaminated samples obtained by mud rotary. No correlations were seen between counts and the concentrations of TCE or PCE.

Full-strength PTYG and 1% PTYG showed differential sensitivity in their ability to retrieve bacteria at certain depths. This suggests that different populations are dominant at different depths. In general, higher diversity was observed when using 1% PTYG than when using the full strength medium.

The communities of the near-surface, capillary fringe, and water table zones appeared to be high diversity communities (compared to the low diversity communities of the vadose zone). Fluctuations in diversity at different depths may be linked to changes in lithology. FA and NA analyses indicate that most sediment communities contain methane-oxidizers and nitrogen-transforming bacteria. PLFA analyses indicate that anaerobes and eucaryotes are present in some areas. PLFA analyses indicate that direct estimates of biomass are low and compare favorably with direct count estimates of biomass. Comparison of PLFA signature compounds shows that the microbial community for most areas are under stress or in stationary growth phase and would respond well to nutrient stimulation.

9.0 References Cited

Beard, D. C., and P. K. Weyl, 1973. **Influence of Texture on Porosity and Permeability of Unconsolidated Sands.** American Association of Petroleum Geologists Bulletin, Volume 57, pp 349-369.

Beaudoin, C.M., Schreuder, P.J., and Haselow, J.S., 1991. **A Groundwater Flow Model for the A/M Area of SRS, WSRC-RP-91-0585**, Westinghouse Savannah River Company, Aiken SC, 29808.

Bledsoe, H. W., 1984. **SRP Baseline Hydrogeologic Investigation - Phase I.** DPST-84-833, E. I. du Pont de Nemours and Company, Savannah River Laboratory, Aiken SC 29808.

Bledsoe, H. W., 1986. **SRP Baseline Hydrogeologic Investigation - Phase II.** DPST-86-674, E. I. du Pont de Nemours and Company, Savannah River Laboratory, Aiken SC 29808

Bledsoe, H. W., 1988. **SRP Baseline Hydrogeologic Investigation - Phase III.** DPST-88-627, E. I. du Pont de Nemours and Company, Savannah River Laboratory, Aiken SC 29808.

Christensen, E. J., and D. E. Gordon, 1983. **Technical Summary of Groundwater Quality Protection Program at Savannah River Plant**, DPST-83-829 volume 1, E. I. du Pont de Nemours and Company, Savannah River Laboratory, Aiken SC 29808.

DPSOP 254, Hydrogeologic Data Collection Methods, Procedures, and Specifications, Westinghouse Savannah River Company, Aiken SC 29808.

Dupont, 1986. **Hydrogeologic Conditions and Evaluation of Chemical Transport in the Vicinity of the M Area Settling Basin and Lost Lake.** CORR-86-0396. Report by S. S. Papadopoulos and Associates for E. I. du Pont de Nemours and Company, Savannah River Laboratory, Aiken SC 29808.

Folk, R. L., 1980. **Petrology of Sedimentary Rocks.** Hemphill Publishing Co, Austin TX.

Freeze, R. A., and J. A. Cherry, 1979. **Groundwater.** Prentice Hall Inc, Englewood Cliffs NJ 07632.

Kaback, D.S., B.B. Looney, J. C. Corey, L.M. Wright, III, and J. L. Steele. **Horizontal Wells for In-situ Remediation of Groundwater and Soils.** Proceedings of the Third Outdoor Action Conference, Association of Groundwater Scientists and Engineers, Las Vegas, NV, May 1989.

Looney, B. B., M. W. Grant, and C. M. King, 1987. **Estimation of Geochemical Parameters for Assessing Subsurface Transport at the Savannah River Plant.** DPST-85-904, E. I. du Pont de Nemours and Company, Savannah River Laboratory, Aiken SC 29808.

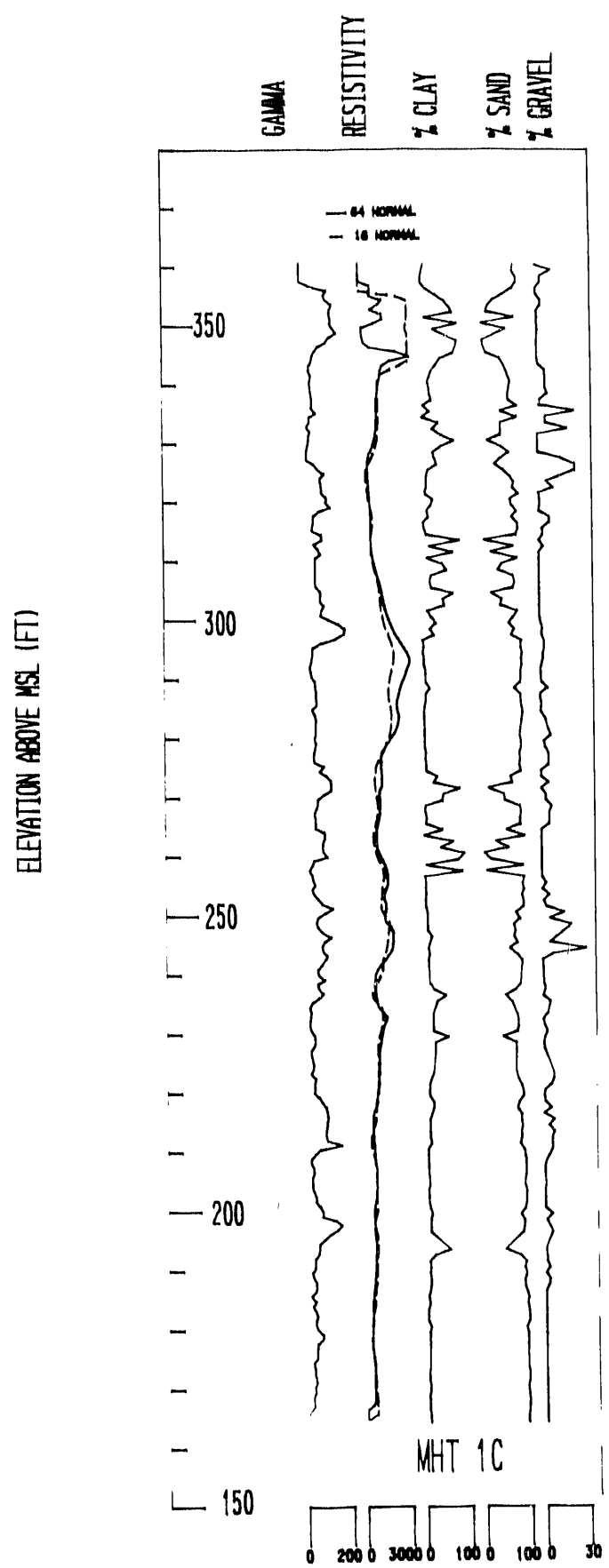
Looney, B. B., H. W. Bledsoe, V. Price Jr, J. S. Haselow, D. S. Kaback, R. L. Nichols, D. E. Stephenson, R. K. Aadland, A. L. Stieve, C. A. Eddy, and T. C. Hazen, 1990. **Recent Measurements of Groundwater Elevations in Water Bearing Zones Underlying SRS, 1988.** WSRC-TR-90-5, Westinghouse Savannah River Company, Aiken SC, 29808.

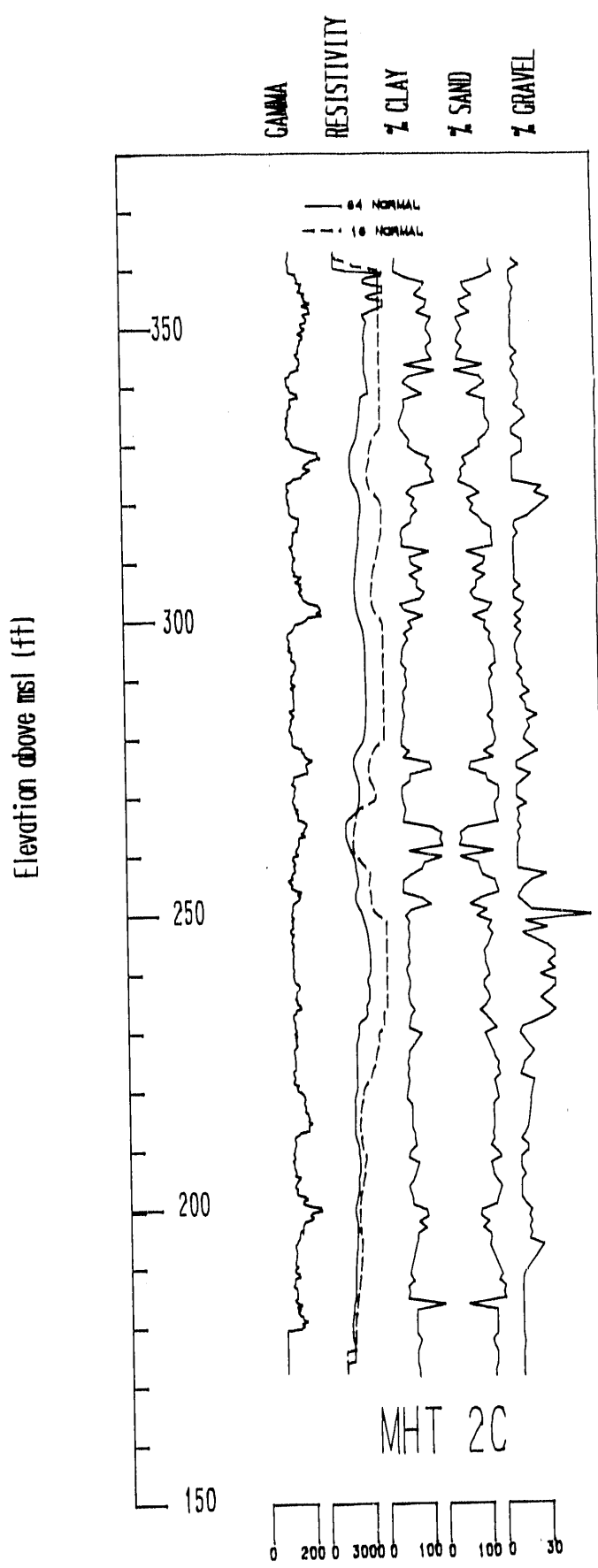
Masch, F. D., and K. J. Denny, 1966. **Grain Size Distribution and its effect on the permeability of unconsolidated sands.** Water Resources Research 2:4, pp 665-677.

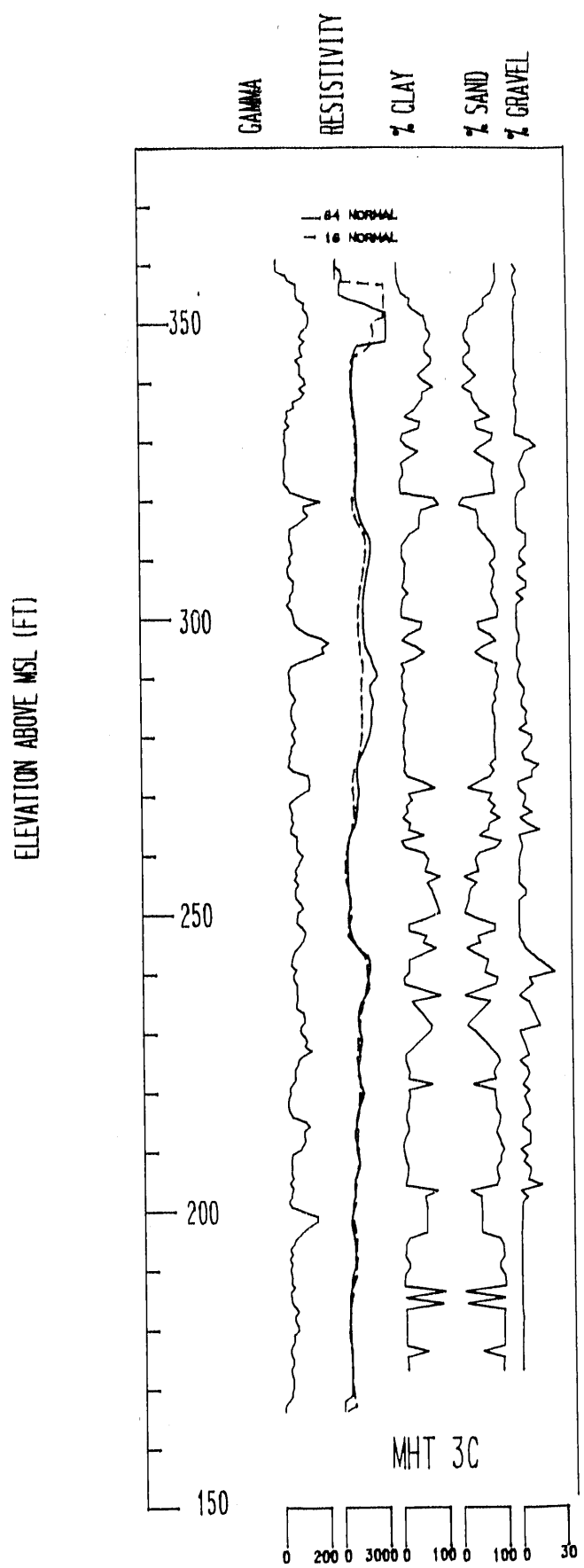
Maniatis, T.E., F. Fritsch, J. Sambrook, 1987, **Molecular Cloning: A Laboratory Manual.** Cold Spring Harbor Laboratory, Cold Spring Harbor, New York.

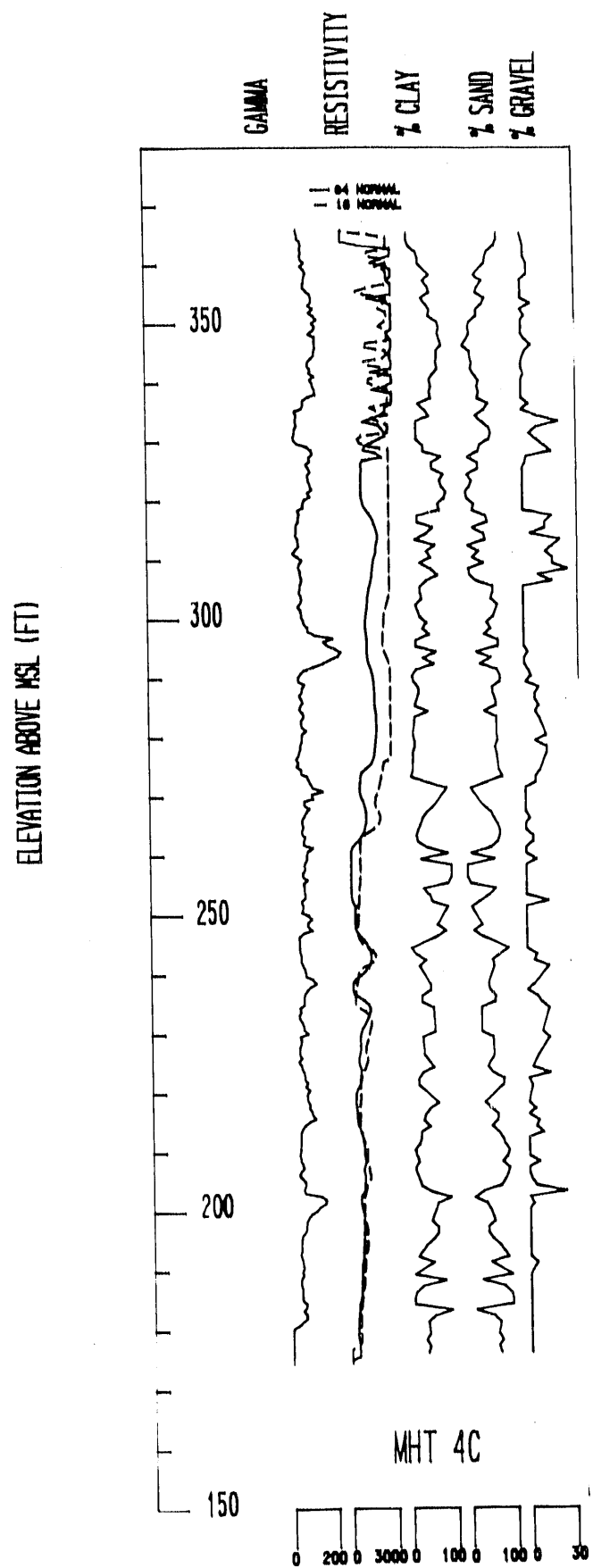
Sims, W. R., B. B. Looney and C. A. Eddy, 1991. **Evaluation of a Rapid Headspace Analysis Method for Analysis of Volatile Constituents in Soils and Sediments.** Proceedings of the Fifth Outdoor Action Conference, Association of Groundwater Scientists and Engineers, Las Vegas, NV, May 1991.

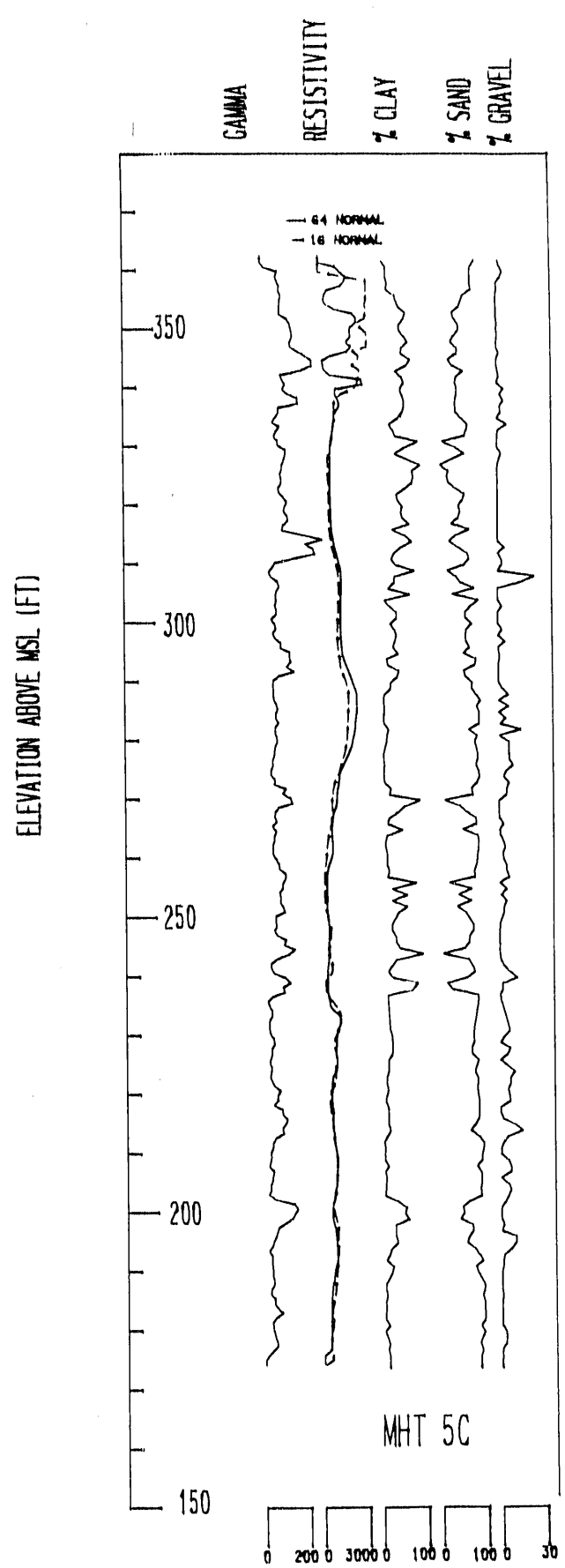
Appendix I Geophysical Logs from the MHT-C Well Series

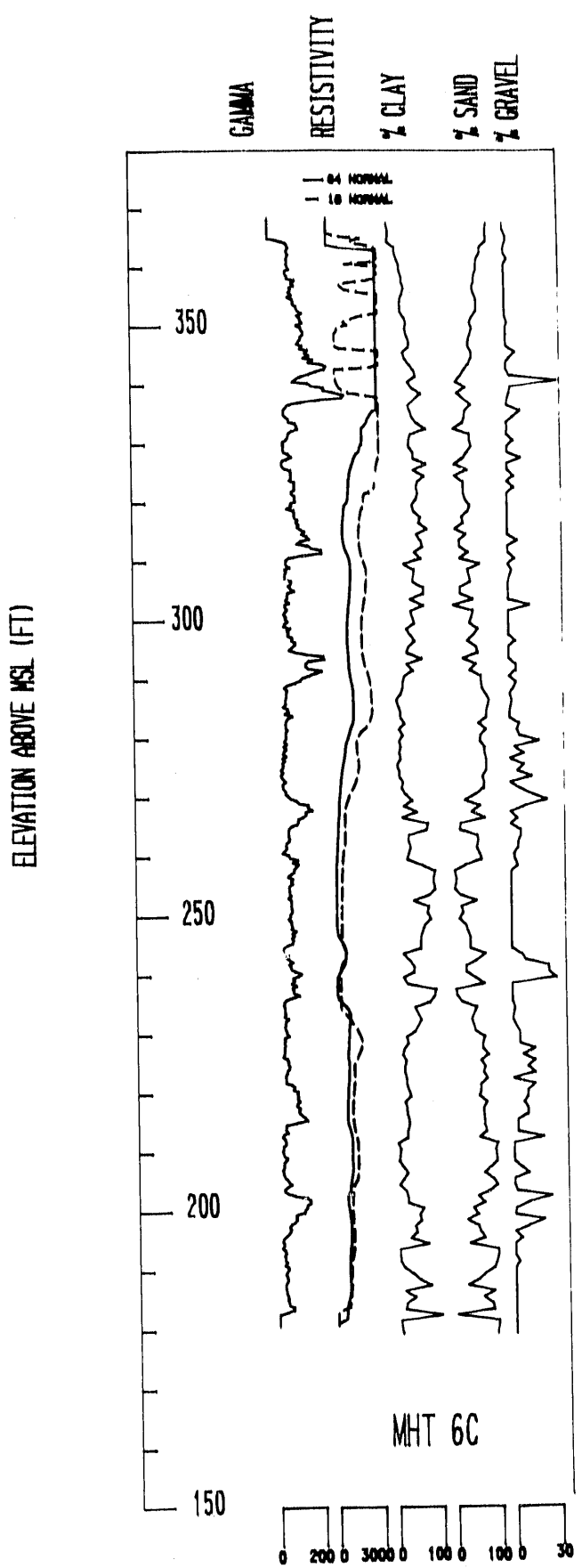


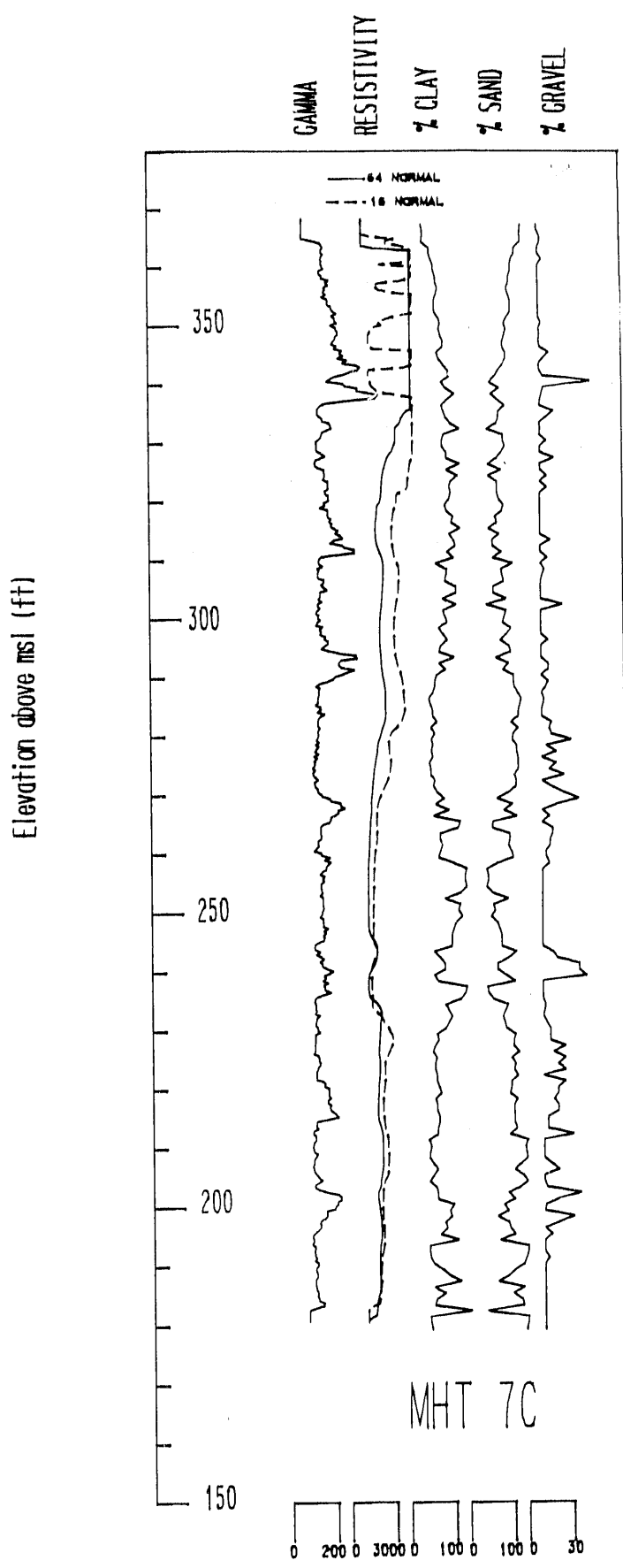


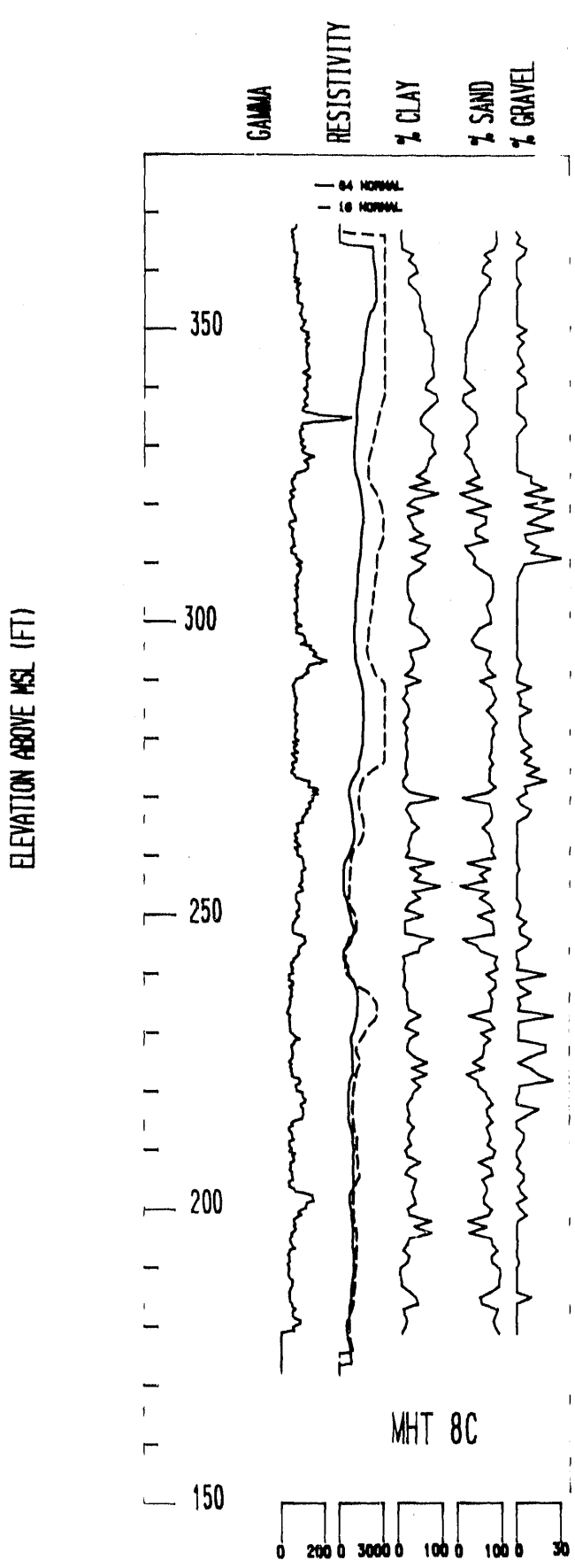


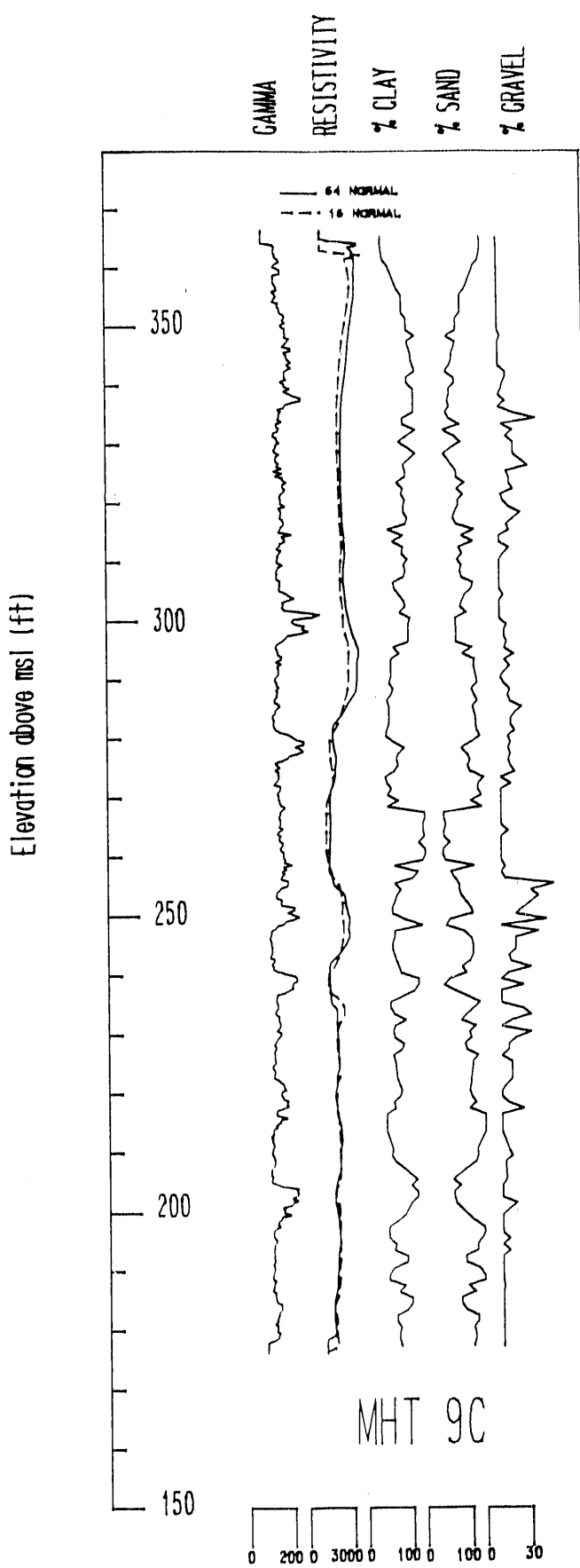


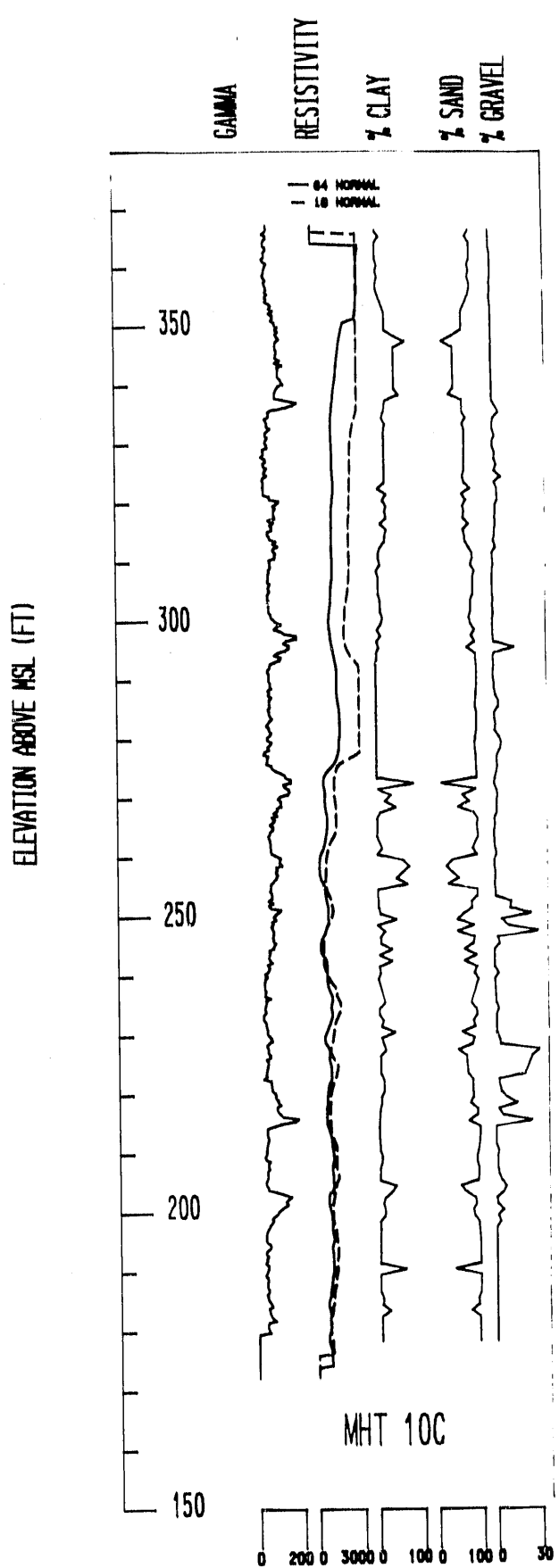












Appendix II Results from VOC Analysis of MHT and MHV Samples

WELL I.D.	DEPTH	TCE ($\mu\text{g/g}$)	PCE ($\mu\text{g/g}$)
MHT1C	3.0	< 0.002	< 0.002
MHT1C	5.0	< 0.002	< 0.002
MHT1C	9.0	< 0.002	0.004
MHT1C	17.0	0.023	0.058
MHT1C	25.0	0.312	0.565
MHT1C	29.0	0.252	0.361
MHT1C	35.0	1.082	1.434
MHT1C	37.0	1.496	3.461
MHT1C	43.0	0.139	0.375
MHT1C	53.0	1.033	0.819
MHT1C	61.5	< 0.002	0.008
MHT1C	73.0	0.109	0.216
MHT1C	83.0	0.013	0.159
MHT1C	89.0	5.755	2.333
MHT1C	93.0	0.557	0.197
MHT1C	98.0	11.491	3.391
MHT1C	105.0	< 0.002	< 0.002
MHT1C	107.0	< 0.002	< 0.002
MHT1C	113.0	0.012	< 0.002
MHT1C	118.0	1.924	0.654
MHT1C	120.0	0.126	0.024
MHT1C	128.0	0.710	0.212
MHT1C	140.0	0.050	0.005
MHT1C	159.0	0.019	0.012
MHT1C	166.0	0.027	0.014
MHT1C	176.0	0.538	0.010
MHT1C	191.0	0.361	< 0.002
MHT1C	195.0	0.018	< 0.002

WELL I.D.	DEPTH	TCE ($\mu\text{g/g}$)	PCE ($\mu\text{g/g}$)
MHT2C	5.0	< 0.002	0.010
MHT2C	15.0	0.122	0.432
MHT2C	19.0	0.243	0.715
MHT2C	25.0	0.050	0.076
MHT2C	35.0	4.948	7.028
MHT2C	45.0	0.186	0.376
MHT2C	55.0	1.838	2.340
MHT2C	65.0	< 0.002	< 0.002
MHT2C	75.0	0.008	0.005
MHT2C	80.0	< 0.002	< 0.002
MHT2C	85.0	0.014	0.022
MHT2C	90.0	0.036	0.004
MHT2C	95.0	5.718	0.819
MHT2C	99.0	11.221	0.622
MHT2C	100.0	0.010	< 0.002
MHT2C	105.0	0.229	< 0.002
MHT2C	110.0	0.960	0.008
MHT2C	115.0	0.014	0.003
MHT2C	120.0	< 0.002	< 0.002
MHT2C	125.0	0.063	0.011
MHT2C	131.0	0.046	0.010
MHT2C	133.0	0.562	0.225
MHT2C	136.0	0.493	0.177
MHT2C	139.0	0.348	0.082
MHT2C	144.0	0.131	0.041
MHT2C	145.0	0.282	0.065
MHT2C	153.0	0.214	0.007
MHT2C	158.0	0.016	< 0.002
MHT2C	163.0	0.033	0.006
MHT2C	168.0	0.057	0.011
MHT2C	178.0	0.024	< 0.002
MHT2C	183.0	0.043	< 0.002
MHT2C	187.0	7.473	< 0.002
MHT2C	190.0	1.162	< 0.002

WELL I.D.	DEPTH	TCE ($\mu\text{g/g}$)	PCE ($\mu\text{g/g}$)
MHT3C	3.0	< 0.002	< 0.002
MHT3C	7.0	< 0.002	< 0.002
MHT3C	15.0	0.007	0.014
MHT3C	25.0	0.027	0.068
MHT3C	30.0	< 0.002	0.005
MHT3C	35.0	0.013	0.044
MHT3C	47.0	< 0.002	0.002
MHT3C	55.0	0.017	0.021
MHT3C	57.0	0.085	0.097
MHT3C	65.0	0.217	0.347
MHT3C	73.0	< 0.002	< 0.002
MHT3C	85.0	0.019	0.027
MHT3C	95.0	0.144	0.186
MHT3C	100.0	0.160	0.213
MHT3C	105.0	8.021	0.656
MHT3C	115.0	0.793	0.075
MHT3C	120.0	0.183	0.025
MHT3C	126.0	1.235	0.290
MHT3C	137.0	0.043	0.005
MHT3C	147.0	0.106	0.013
MHT3C	157.0	0.008	0.004
MHT3C	166.0	0.039	0.010
MHT3C	166.0	0.024	0.004
MHT3C	177.0	0.015	< 0.002
MHT3C	187.0	5.814	< 0.002

WELL I.D.	DEPTH	TCE ($\mu\text{g/g}$)	PCE ($\mu\text{g/g}$)
MHT4C	3.0	< 0.002	< 0.002
MHT4C	5.0	< 0.002	< 0.002
MHT4C	15.0	< 0.002	< 0.002
MHT4C	25.0	< 0.002	0.005
MHT4C	35.0	0.004	0.010
MHT4C	39.0	0.513	0.900
MHT4C	47.0	0.606	0.445
MHT4C	55.0	0.083	0.083
MHT4C	65.0	0.730	0.622
MHT4C	75.0	< 0.002	< 0.002
MHT4C	85.0	< 0.002	< 0.002
MHT4C	90.0	< 0.002	< 0.002
MHT4C	95.0	11.964	4.303
MHT4C	96.0	0.916	0.208
MHT4C	103.0	0.662	0.169
MHT4C	105.0	8.202	1.295
MHT4C	108.0	10.805	0.507
MHT4C	109.0	8.472	1.813
MHT4C	115.0	3.048	0.911
MHT4C	118.0	0.106	0.012
MHT4C	125.0	0.911	0.094
MHT4C	128.0	0.043	< 0.002
MHT4C	130.0	5.502	0.303
MHT4C	134.0	0.005	< 0.002
MHT4C	138.0	0.402	0.027
MHT4C	140.0	0.062	0.003
MHT4C	142.0	0.645	0.080
MHT4C	145.0	0.971	0.027
MHT4C	152.0	1.288	0.037
MHT4C	157.0	0.077	0.005
MHT4C	162.0	0.013	0.003
MHT4C	166.0	0.084	0.008
MHT4C	171.0	0.029	0.025
MHT4C	176.0	0.190	0.004
MHT4C	181.0	0.143	0.002
MHT4C	186.0	5.293	< 0.002
MHT4C	190.0	7.812	< 0.002

WELL I.D.	DEPTH	TCE ($\mu\text{g/g}$)	PCE ($\mu\text{g/g}$)
MHT5C	5.0	< 0.002	< 0.002
MHT5C	11.0	< 0.002	< 0.002
MHT5C	15.0	< 0.002	< 0.002
MHT5C	25.0	< 0.002	< 0.002
MHT5C	33.0	0.017	0.019
MHT5C	40.0	0.009	0.008
MHT5C	45.0	0.022	0.038
MHT5C	55.0	0.086	0.091
MHT5C	65.0	0.194	0.324
MHT5C	69.0	< 0.002	0.002
MHT5C	75.0	< 0.002	< 0.002
MHT5C	85.0	0.028	0.020
MHT5C	93.0	1.081	0.521
MHT5C	101.0	0.140	0.133
MHT5C	108.0	7.235	0.515
MHT5C	111.0	8.609	0.587
MHT5C	117.0	5.775	0.985
MHT5C	119.0	4.677	0.267
MHT5C	126.0	1.002	0.063
MHT5C	138.0	0.025	0.002
MHT5C	151.0	0.014	0.003
MHT5C	162.0	0.058	0.007
MHT5C	173.0	0.002	0.002
MHT5C	185.0	0.025	< 0.002
MHT5C	187.0	3.634	< 0.002
MHT5C	189.0	11.653	< 0.002

WELL I.D.	DEPTH	TCE ($\mu\text{g/g}$)	PCE ($\mu\text{g/g}$)
MHT6C	5.0	< 0.002	< 0.002
MHT6C	15.0	< 0.002	< 0.002
MHT6C	25.0	< 0.002	< 0.002
MHT6C	36.0	< 0.002	< 0.002
MHT6C	45.0	0.006	0.018
MHT6C	55.0	0.010	0.015
MHT6C	65.0	0.028	0.025
MHT6C	75.0	0.038	0.009
MHT6C	85.0	0.010	< 0.002
MHT6C	91.0	< 0.002	< 0.002
MHT6C	95.0	< 0.002	< 0.002
MHT6C	101.0	3.108	0.027
MHT6C	103.0	16.323	2.966
MHT6C	107.0	3.443	0.608
MHT6C	111.0	8.537	0.644
MHT6C	115.0	5.121	0.155
MHT6C	121.0	1.911	0.039
MHT6C	125.0	0.215	0.005
MHT6C	131.0	9.126	0.322
MHT6C	135.0	< 0.002	< 0.002
MHT6C	137.0	0.601	0.009
MHT6C	141.0	0.156	0.007
MHT6C	145.0	0.386	0.004
MHT6C	151.0	0.313	0.004
MHT6C	155.0	1.030	0.035
MHT6C	160.0	0.170	0.007
MHT6C	165.0	< 0.002	< 0.002
MHT6C	170.0	0.036	0.034
MHT6C	175.0	0.027	0.010
MHT6C	180.0	1.475	0.026
MHT6C	181.0	2.110	0.040
MHT6C	185.0	< 0.002	< 0.002
MHT6C	187.5	< 0.002	< 0.002
MHT6C	187.5	< 0.002	< 0.002
MHT6C	187.5	0.005	< 0.002
MHT6C	188.0	1.842	< 0.002
MHT6C	189.0	0.027	< 0.002

WELL I.D.	DEPTH	TCE ($\mu\text{g/g}$)	PCE ($\mu\text{g/g}$)
MHT7C	5.0	< 0.002	< 0.002
MHT7C	15.0	< 0.002	< 0.002
MHT7C	25.0	< 0.002	< 0.002
MHT7C	35.0	< 0.002	< 0.002
MHT7C	45.0	< 0.002	< 0.002
MHT7C	55.0	< 0.002	< 0.002
MHT7C	71.0	0.017	0.011
MHT7C	75.0	0.004	< 0.002
MHT7C	85.0	< 0.002	< 0.002
MHT7C	93.0	0.992	0.172
MHT7C	105.0	0.204	< 0.002
MHT7C	115.0	0.208	0.012
MHT7C	119.0	0.032	< 0.002
MHT7C	131.0	0.009	< 0.002
MHT7C	141.0	0.015	< 0.002
MHT7C	143.0	0.004	< 0.002
MHT7C	145.0	0.011	0.004
MHT7C	155.0	0.006	< 0.002
MHT7C	177.0	0.156	< 0.002
MHT7C	179.0	1.260	< 0.002
MHT7C	181.0	0.007	< 0.002
MHT7C	189.0	0.480	< 0.002
MHT7C	191.0	0.004	< 0.002

WELL I.D.	DEPTH	TCE ($\mu\text{g/g}$)	PCE ($\mu\text{g/g}$)
MHT8C	5.0	< 0.002	< 0.002
MHT8C	15.0	< 0.002	< 0.002
MHT8C	25.0	< 0.002	< 0.002
MHT8C	35.0	< 0.002	< 0.002
MHT8C	45.0	0.010	< 0.002
MHT8C	55.0	0.095	0.012
MHT8C	65.0	0.381	0.051
MHT8C	75.0	0.633	0.064
MHT8C	85.0	0.271	0.022
MHT8C	95.0	0.101	0.006
MHT8C	105.0	< 0.002	< 0.002
MHT8C	113.0	1.250	0.004
MHT8C	124.0	3.017	0.109
MHT8C	129.0	1.160	0.017
MHT8C	134.0	0.154	0.003
MHT8C	139.0	0.196	0.002
MHT8C	144.0	0.023	0.010
MHT8C	149.0	0.360	0.027
MHT8C	154.0	0.052	< 0.002
MHT8C	159.0	0.025	< 0.002
MHT8C	164.0	0.015	0.004
MHT8C	169.0	0.125	0.004
MHT8C	174.0	0.233	< 0.002
MHT8C	179.0	< 0.002	< 0.002
MHT8C	184.0	0.267	< 0.002
MHT8C	189.0	0.148	< 0.002

WELL I.D.	DEPTH	TCE ($\mu\text{g/g}$)	PCE ($\mu\text{g/g}$)
MHT9C	5.0	< 0.002	< 0.002
MHT9C	15.0	< 0.002	< 0.002
MHT9C	25.0	< 0.002	< 0.002
MHT9C	37.0	< 0.002	< 0.002
MHT9C	45.0	0.003	< 0.002
MHT9C	55.0	< 0.002	< 0.002
MHT9C	65.0	0.005	< 0.002
MHT9C	75.0	0.005	< 0.002
MHT9C	85.0	< 0.002	< 0.002
MHT9C	89.0	0.729	0.039
MHT9C	95.0	< 0.002	< 0.002
MHT9C	101.0	0.177	< 0.002
MHT9C	105.0	0.126	< 0.002
MHT9C	107.0	< 0.002	< 0.002
MHT9C	109.0	1.528	0.093
MHT9C	115.0	0.006	< 0.002
MHT9C	130.0	0.889	0.044
MHT9C	131.0	0.256	0.011
MHT9C	133.0	0.305	0.014
MHT9C	141.0	0.017	< 0.002
MHT9C	143.0	0.012	0.006
MHT9C	145.0	0.008	0.005
MHT9C	153.0	< 0.002	< 0.002
MHT9C	155.0	< 0.002	< 0.002
MHT9C	157.0	< 0.002	< 0.002
MHT9C	165.0	0.028	< 0.002
MHT9C	167.0	0.176	0.005
MHT9C	179.0	< 0.002	< 0.002
MHT9C	181.0	0.048	< 0.002
MHT9C	189.0	1.466	< 0.002

WELL I.D.	DEPTH	TCE ($\mu\text{g/g}$)	PCE ($\mu\text{g/g}$)
MHT10C	7.0	< 0.002	< 0.002
MHT10C	15.0	< 0.002	< 0.002
MHT10C	25.0	< 0.002	< 0.002
MHT10C	35.0	< 0.002	< 0.002
MHT10C	45.0	0.012	< 0.002
MHT10C	55.0	0.042	0.005
MHT10C	65.0	0.049	< 0.002
MHT10C	75.0	0.037	< 0.002
MHT10C	87.0	< 0.002	< 0.002
MHT10C	95.0	0.390	0.026
MHT10C	105.0	0.037	< 0.002
MHT10C	111.0	2.771	0.023
MHT10C	120.0	0.027	< 0.002
MHT10C	128.0	1.971	0.034
MHT10C	131.0	0.333	< 0.002
MHT10C	141.0	0.240	0.003
MHT10C	148.0	0.016	0.012
MHT10C	157.0	0.095	< 0.002
MHT10C	167.0	0.025	0.011
MHT10C	170.0	0.117	< 0.002
MHT10C	175.0	< 0.002	< 0.002
MHT10C	180.0	0.036	< 0.002
MHT10C	185.0	0.304	< 0.002
MHT10C	190.0	0.525	< 0.002

WELL I.D.	DEPTH	TCE (µg/g)	PCE (µg/g)
MHV1	1	1.595	0.26
MHV1	19	0.015	0.028
MHV1	20	< 0.002	< 0.002
MHV1	21	0.045	0.094
MHV1	22	0.079	0.173
MHV1	22.5	0.102	0.227
MHV1	24	0.156	0.355
MHV1	26	0.097	0.218
MHV1	28	0.025	0.029
MHV1	29	0.022	0.033
MHV1	30	0.012	0.014
MHV1	31	< 0.002	< 0.002
MHV1	32	0.012	0.017
MHV1	33	0.213	0.430
MHV1	34	0.011	0.013
MHV1	35	0.054	0.089
MHV1	36	0.027	0.036
MHV1	37	0.083	0.155
MHV1	38	< 0.002	< 0.002
MHV1	39	0.227	0.508
MHV1	40	< 0.002	< 0.002
MHV1	41	0.031	0.041
MHV1	42	1.473	1.440
MHV1	43	0.063	0.075
MHV1	44	0.070	0.058
MHV1	45	< 0.002	0.002
MHV1	46	0.328	0.596
MHV1	47	0.023	0.026
MHV1	48	0.223	0.399
MHV1	49	0.944	1.201
MHV1	50	0.236	0.425
MHV1	51	0.004	0.014
MHV1	52	0.018	0.020
MHV1	53	0.011	0.013
MHV1	54	0.195	0.416
MHV1	55	0.035	0.037
MHV1	56	0.152	0.345
MHV1	57	0.006	0.009
MHV1	58	0.076	0.143
MHV1	59	0.591	0.546
MHV1	60	0.428	0.643
MHV1	62	0.021	0.012
MHV1	63	1.073	0.822
MHV1	64	< 0.002	< 0.002
MHV1	65	2.006	1.511
MHV1	66	1.739	1.606
MHV1	67	1.335	0.901
MHV1	68	1.191	0.755
MHV1	69	0.007	0.006
MHV1	70	0.044	0.027
MHV1	71	0.263	0.221

WELL I.D.	DEPTH	TCE ($\mu\text{g/g}$)	PCE ($\mu\text{g/g}$)
MHV1	72	< 0.002	< 0.002
MHV1	73	< 0.002	< 0.002
MHV1	74	< 0.002	< 0.002
MHV1	75	< 0.002	< 0.002
MHV1	76	0.056	0.047
MHV1	77	< 0.002	< 0.002
MHV1	78	< 0.002	< 0.002
MHV1	79	< 0.002	< 0.002
MHV1	80	< 0.002	< 0.002
MHV1	81	< 0.002	< 0.002
MHV1	82	< 0.002	< 0.002
MHV1	83	< 0.002	< 0.002
MHV1	84	< 0.002	< 0.002
MHV1	85	< 0.002	< 0.002
MHV1	86	< 0.002	< 0.002
MHV1	87	< 0.002	< 0.002
MHV1	88	< 0.002	< 0.002
MHV1	89	< 0.002	< 0.002
MHV1	90	< 0.002	< 0.002
MHV1	91	< 0.002	< 0.002
MHV1	92	< 0.002	< 0.002
MHV1	93	< 0.002	< 0.002
MHV1	94	11.026	4.925
MHV1	94.5	1.674	0.975
MHV1	95	1.744	0.829
MHV1	96	0.646	0.334
MHV1	97	0.311	0.095
MHV1	98	< 0.002	< 0.002
MHV1	99	< 0.002	< 0.002
MHV1	100	< 0.002	< 0.002
MHV1	101	< 0.002	< 0.002
MHV1	102	< 0.002	< 0.002
MHV1	103	5.138	0.656
MHV1	104	6.282	1.357
MHV1	105	6.701	0.824
MHV1	106	14.458	4.161
MHV1	107	8.058	0.611
MHV1	108	7.672	0.390
MHV1	109	7.450	0.878
MHV1	110	3.508	0.776
MHV1	112	7.022	2.950
MHV1	114	6.903	1.710
MHV1	115	5.870	1.554
MHV1	116	1.128	0.292
MHV1	117	1.636	0.037
MHV1	118	0.172	< 0.002
MHV1	119	1.597	0.166
MHV1	120	0.114	0.004
MHV1	121	0.358	0.029
MHV1	122	0.009	< 0.002
MHV1	123	1.456	0.108
MHV1	124	0.028	< 0.002
MHV1	125	0.441	0.015

WELL I.D.	DEPTH	TCE (µg/g)	PCE (µg/g)
MHV1	126	0.695	0.032
MHV1	127	0.959	0.100
MHV1	128	0.665	0.083
MHV1	129	0.780	0.103
MHV1	130	< 0.002	0.008

WELL I.D.	DEPTH	TCE ($\mu\text{g/g}$)	PCE ($\mu\text{g/g}$)
MHV2	15	< 0.002	< 0.002
MHV2	20	< 0.002	< 0.002
MHV2	25	< 0.002	< 0.002
MHV2	30	< 0.002	< 0.002
MHV2	35	< 0.002	< 0.002
MHV2	40	< 0.002	0.007
MHV2	40	0.084	0.092
MHV2	41	< 0.002	0.006
MHV2	41	< 0.002	0.005
MHV2	41	< 0.002	0.003
MHV2	46	0.049	0.057
MHV2	46	0.017	0.023
MHV2	46	0.025	0.032
MHV2	46	0.034	0.041
MHV2	46	0.032	0.039
MHV2	46	0.025	0.035
MHV2	46	0.014	0.023
MHV2	46	0.025	0.035
MHV2	50	0.050	0.069
MHV2	51	0.117	0.141
MHV2	51	0.321	0.444
MHV2	51	0.104	0.120
MHV2	55	0.042	0.033
MHV2	60	< 0.002	< 0.002
MHV2	60	0.074	0.099
MHV2	60	0.078	0.098
MHV2	60	0.096	0.117
MHV2	60	0.094	0.108
MHV2	60	0.131	0.158
MHV2	60	0.068	0.085
MHV2	64	0.007	0.004
MHV2	64	0.287	0.324
MHV2	64	0.125	0.125
MHV2	69	0.076	0.033
MHV2	69	0.029	0.015
MHV2	69	0.029	0.010
MHV2	75	< 0.002	< 0.002
MHV2	75	< 0.002	< 0.002
MHV2	75	< 0.002	< 0.002
MHV2	79	< 0.002	< 0.002
MHV2	79	< 0.002	< 0.002
MHV2	79	< 0.002	< 0.002
MHV2	85	< 0.002	< 0.002
MHV2	85	< 0.002	< 0.002
MHV2	85	< 0.002	< 0.002
MHV2	90	< 0.002	< 0.002
MHV2	90	< 0.002	< 0.002
MHV2	90	< 0.002	< 0.002
MHV2	95	7.151	2.105
MHV2	95	4.556	0.924
MHV2	95	6.623	1.048
MHV2	95	6.002	0.880
MHV2	95	4.562	0.782

WELL I.D.	DEPTH	TCE (µg/g)	PCE (µg/g)
MHV2	95	2.571	1.014
MHV2	100	0.223	0.064
MHV2	100	0.133	0.017
MHV2	100	0.083	0.011
MHV2	105	6.049	1.787
MHV2	105	0.273	0.090
MHV2	105	< 0.002	< 0.002
MHV2	108	9.978	1.324
MHV2	108	< 0.002	< 0.002
MHV2	110	2.626	1.246
MHV2	110	5.821	2.204
MHV2	112	3.729	0.134
MHV2	112	2.090	0.073
MHV2	115	1.790	0.621
MHV2	115	1.598	0.436
MHV2	120	1.359	0.083

WELL I.D.	DEPTH	TCE (µg/g)	PCE (µg/g)
MHV3	5	< 0.002	< 0.002
MHV3	15	< 0.002	< 0.002
MHV3	25	< 0.002	< 0.002
MHV3	33	< 0.002	0.007
MHV3	39	0.035	0.071
MHV3	45	0.056	0.169
MHV3	55	0.077	0.109
MHV3	65	0.228	0.398
MHV3	67	0.447	0.577
MHV3	67	0.404	0.493
MHV3	67	0.311	0.390
MHV3	75	1.281	0.641

WELL I.D.	DEPTH	TOE (µg/g)	PCE (µg/g)
MHV4	20	< 0.002	0.005
MHV4	20	< 0.002	0.014
MHV4	20	< 0.002	0.006
MHV4	25	< 0.002	0.629
MHV4	25	< 0.002	0.662
MHV4	25	0.004	0.673
MHV4	30	0.061	0.338
MHV4	30	0.016	0.094
MHV4	30	< 0.002	0.010
MHV4	35	0.264	0.360
MHV4	35	0.864	0.855
MHV4	35	0.339	0.456
MHV4	40	0.092	0.131
MHV4	40	< 0.002	0.006
MHV4	43	8.579	6.306
MHV4	43	5.519	5.429
MHV4	43	7.802	8.750
MHV4	45	5.577	6.504
MHV4	45	7.447	8.286
MHV4	45	5.449	5.956
MHV4	50	0.057	0.033
MHV4	50	0.026	0.018
MHV4	50	0.005	0.005
MHV4	55	1.231	0.686
MHV4	55	0.323	0.256
MHV4	55	0.389	0.361
MHV4	60	0.275	0.222
MHV4	60	0.102	0.071
MHV4	60	0.086	0.062
MHV4	65	6.996	3.441
MHV4	65	5.778	3.611
MHV4	65	7.164	3.224
MHV4	70	0.174	0.115
MHV4	70	0.227	0.162
MHV4	70	0.684	0.527
MHV4	75	0.318	0.057
MHV4	75	0.072	0.012
MHV4	75	0.160	0.034
MHV4	83	0.060	0.011
MHV4	83	0.050	0.010
MHV4	83	0.942	0.260
MHV4	85	< 0.002	< 0.002
MHV4	85	0.229	0.049
MHV4	85	0.075	0.020
MHV4	85	0.127	0.026
MHV4	90	< 0.002	< 0.002
MHV4	90	< 0.002	< 0.002
MHV4	90	< 0.002	< 0.002
MHV4	94	7.941	1.073
MHV4	94	10.961	3.258
MHV4	94	8.823	2.812
MHV4	95	8.310	0.672

WELL I.D.	DEPTH	TCE ($\mu\text{g/g}$)	PCE ($\mu\text{g/g}$)
MHV4	95	6.172	0.747
MHV4	95	2.855	0.514
MHV4	100	9.981	0.734
MHV4	100	0.052	0.005
MHV4	100	0.005	< 0.002
MHV4	105	12.191	1.101
MHV4	105	13.541	0.909
MHV4	105	14.210	1.150
MHV4	107	8.713	0.308
MHV4	107	9.110	0.288
MHV4	107	7.164	0.200
MHV4	110	1.656	0.068
MHV4	110	1.708	0.083
MHV4	110	1.831	0.031
MHV4	115	3.621	0.408
MHV4	115	6.891	0.589
MHV4	115	2.330	0.340
MHV4	120	< 0.002	< 0.002
MHV4	120	< 0.002	< 0.002
MHV4	120	< 0.002	< 0.002
MHV4	125	< 0.002	< 0.002
MHV4	125	< 0.002	< 0.002
MHV4	125	< 0.002	< 0.002
MHV4	130	0.037	< 0.002
MHV4	130	0.131	0.013
MHV4	130	0.072	0.004

WELL I.D.	DEPTH	TCE (µg/g)	PCE (µg/g)
MHV5	15	< 0.002	< 0.002
MHV5	21	< 0.002	< 0.002
MHV5	25	< 0.002	< 0.002
MHV5	27	< 0.002	< 0.002
MHV5	27	< 0.002	< 0.002
MHV5	27	< 0.002	< 0.002
MHV5	31	< 0.002	< 0.002
MHV5	31	< 0.002	< 0.002
MHV5	31	< 0.002	< 0.002
MHV5	35	< 0.002	< 0.002
MHV5	35	< 0.002	< 0.002
MHV5	35	< 0.002	< 0.002
MHV5	40	0.005	< 0.002
MHV5	40	0.021	0.009
MHV5	40	0.018	0.005
MHV5	45	< 0.002	< 0.002
MHV5	45	< 0.002	< 0.002
MHV5	45	0.022	0.008
MHV5	50	0.194	0.106
MHV5	50	0.158	0.092
MHV5	50	0.128	0.066
MHV5	55	0.567	0.216
MHV5	55	0.830	0.283
MHV5	55	0.519	0.190
MHV5	60	0.983	0.189
MHV5	60	0.360	0.079
MHV5	60	0.069	0.012
MHV5	65	1.532	0.263
MHV5	65	0.392	0.038
MHV5	65	0.374	0.042
MHV5	70	0.774	0.106
MHV5	70	0.600	0.087
MHV5	70	0.695	0.116
MHV5	75	1.639	0.256
MHV5	75	1.548	0.213
MHV5	75	1.322	0.176
MHV5	80	5.883	0.596
MHV5	80	5.114	0.582
MHV5	80	6.848	0.727
MHV5	85	0.070	0.006
MHV5	85	0.269	0.020
MHV5	85	0.037	0.003
MHV5	90	0.386	0.029
MHV5	90	0.577	0.035
MHV5	90	0.501	0.033
MHV5	91	0.070	0.004
MHV5	91	0.021	< 0.002
MHV5	91	0.041	< 0.002
MHV5	95	0.034	< 0.002
MHV5	95	0.014	< 0.002
MHV5	95	0.027	< 0.002

WELL I.D.	DEPTH	TCE (µg/g)	PCE (µg/g)
MHV5	100	1.843	0.567
MHV5	100	1.749	0.538
MHV5	100	2.301	0.621
MHV5	105	1.663	0.476
MHV5	105	1.350	0.368
MHV5	105	1.166	0.360
MHV5	110	1.509	0.375
MHV5	110	3.259	0.393
MHV5	110	3.130	0.394
MHV5	115	4.461	0.497
MHV5	115	4.646	0.587
MHV5	115	4.205	0.530
MHV5	117	4.719	0.447
MHV5	117	8.596	0.648
MHV5	117	7.974	0.466
MHV5	120	2.278	0.153
MHV5	120	8.800	0.397
MHV5	120	10.054	0.486
MHV5	125	1.348	0.087
MHV5	125	1.468	0.073
MHV5	125	1.400	0.104
MHV5	130	13.208	0.384
MHV5	130	12.608	0.355
MHV5	130	13.402	0.371

END

DATE
FILMED
5/18/92

